SILICONE SURFACE MODIFICATION WITH COLLAGEN

SILICONE SURFACE MODIFICATION WITH COLLAGEN

AND ITS BIOLOGICAL RESPONSES

By

LIHUA LIU, M.Sc.

A Thesis

Submitted to the School of Graduate Studies

In Partial Fulfillment of the Requirements

For the Degree of

Master of Science

McMaster University

MASTER OF SCIENCE (2006) McMaster University

(Chemistry) Hamilton, Ontario

TITLE: Silicone Surface Modification with Collagen and Its Biological Responses

AUTHOR: Lihua Liu, M.Sc. (Institute of Chemistry, Chinese Academy of Sciences)

SUPERVISOR: Professor Michael A. Brook

NUMBER OF PAGES: xvii, 108

Abstract

Collagen, due to its good biocompatibility and abundance in mammalian structures, has been widely applied in developing better biomaterials. There remains the need for yet more stable surfaces of biomaterials. One strategy to achieve this is improved binding to surfaces using covalent rather than physical linking. However, due to collagen's poor solubility in neutral or alkaline conditions, there are only a few papers describing covalently linked collagen so far, and they generally use acidic conditions to generate surfaces with only low collagen density. *N*-Hydroxysuccimide ester (NHS) chemistry has been widely used in covalently binding proteins, but the NHS activity and its preparation efficiency are plagued with undesired, premature hydrolysis. A two-step method was developed for making NHS functional surfaces with a non-fouling spacer, PEO. The process was more efficient and led to concentrated NHS surfaces. Collagen was successfully immobilized onto this NHS surface after optimizing the conditions for immobilization. The solubility problem was overcome by increasing the ionic strength of the solution. Abundant collagen molecules could then be immobilized on the silicone surface. ATR-FTIR was used as a diagnostic tool to prove the surface had been modified. The low water contact angle (40°) indicated the presence of collagen. XPS data showed a significant increase on the nitrogen content after tethering collagen molecules. Deep freezing ToF-SIMS displayed a decrease in the peak intensity for cationic fractions of collagen molecules when warming from -96 °C to room temperature, which suggested the surface rearrangement due to the hydrophilic character of collagen. Profilometer and tapping-mode AFM were used to investigate the surface morphology after modification.

The latter showed a high density mesh work (immobilized collagen fibers) on the collagen-modified surface. Collagen stain with Sirius Red F3B allowed us to look into the tertiary structures of covalently tethered collagen on the surface. However, it was found that only some of them were still in their native form. Interestingly, a subsequent epithelial cell culture assay showed that the cells grew very well on this collagen rich silicone surface. This suggested collagen's tertiary structure may not be necessary to support cell growth on the silicone surface covalently modified with collagen through the PEO spacer. However, further biochemical experiments are required to establish the underlying source of this observation.

Acknowledgements

First, I would like to make a grateful acknowledgement from the bottom of my heart to my supervisor, Professor Michael A. Brook, for his invaluable insight, guidance, time, patience and help on my life throughout the course of this thesis. The research experience in Dr. Brook's lab was extremely worthwhile for my future career. I would also like to thank my supervisory committee member, Professor Heather Sheardown for her helpful discussions and time. Thanks to the staff, students, and post-docs whom I had the opportunity to work with for their insightful discussions about science. I would also like to extend my gratitude to Carol Dada, Barbra DeJean, Tammy Feher, Josie Petrie, Dr. Don Hughes, Mike Malott, Karen Neumann, Brad Sheeler, Andy Duft, Steve Kornic, Steve Koprich and Professor Rana Sodhi. I appreciated the help offered by Dr. Sheardown's group and Dr. Pelton's group.

During my study in the Department of Chemistry at McMaster University, the help and friendship that my group members offered to me are invaluable. I would like to express my appreciation to Dr. Dan Chen, Dr. Ferdinand Gonzaga, Dr. Rebecca Voss, Dave Thompson, Weian Zhao, Forrest Gan, Hazem Amarne, and Lucy Ye.

Finally, I would like to thank my family: my parents, my brother, sisters, and my husband, Yu Liu, for their understanding on my busy study life, their compassion during the times of frustration, and their encouragement and support on completing my thesis. (最后, 我由衷地感谢我的父母, 哥哥姐姐, 和我的爱人刘瑜在我的学习期间给予无私的关爱, 理解, 支持和鼓励.)

In addition to those mentioned above, I would like to thank the many others that have offered help to me during my time at McMaster.

Table of Contents

List of Figures

List of Tables

List of Schemes

Abbreviations

AFM	Atomic Force Microscopy
ATR/FTIR	Attenuated Total Reflection Fourier Transform Infrared Spectroscopy
bioMEM	biological microelectromechanical systems
BPE	bovine pituitary extract
D^4	octamethylcyclotetrasiloxane
D^5	decamethylcyclopentasiloxane
DC1107	poly(methylhydrosiloxane), PHMS
DCC	dicyclohexylcarbodiimide
di-NHS	*N,N'*-disuccinimidyl carbonate
DPPC	phosphatidylcholine
ECM	extracellular matrix
EDC	ethylenedicarbodiimide
EGF	epidermal growth factor
Gly	glycine
iPA	isopropanol
KSFM	keratinocyte serum-free medium
LB	Langmuir-Blodgett
LCST	lower critical solution temperature
MPC	2-methacryloyloxyethyl phosphorylcholine
NHS	*N*-hydroxysuccinimide

PBS	Phosphate Buffered Saline
PDMS	Poly(dimethylsiloxane)
PEO	Polyethylene oxide
PEO-co-PLA	Poly(ethylene glycol)-co-poly(lactic acid)
PMMA-g-PEO	poly(ethylene glycol)
pNIPAAm	Poly(*N*-isopropylacrylamide)
PSf	polysulfone
PU	polyurethane
PVA	poly(vinyl alcohol)
PVP	polyvinylpyrrolidone
RGD	Arginine-Glycine-Aspartic acid
SAM	self-assembled monolayer
TfOH	Trifluoromethanesulfonic acid (triflic acid)
ToA	takeoff angle
ToF-SIMS	Time-of-Flight Secondary Ion Mass Spectrometry
Tris	Tris (hydroxymethyl) aminomethane Buffer
UFH	unfractionated heparins
UV-Vis	Ultraviolet-visible Spectroscopy
XPS	X-ray Photoelectron Spectroscopy (or ESCA)

CHAPTER 1 – INTRODUCTION

1.1. BIOMATERIALS

A biomaterial in surgery is a synthetic or natural material used to replace part of a living system or to function in intimate contact with living tissue. The current most acceptable definition is "a non-drug substance intended to interface with biological systems to evaluate, treat, augment or replace any tissue, organ or function of the body".[1] Artificial materials and devices were developed so that they can replace various components of the human body from as early as a century ago.[2] These materials can be used in contact with bodily fluids and tissues for prolonged periods of time, and should elicit little if any adverse reactions. There have been a wide range of applications for synthetic materials and modified natural materials in human bodies. From dental repairs to controlled drug release or total organ/joint replacement, almost every human being will be exposed to one or another biomaterial during their lifetime in order to relieve pain and/or maintain to a healthy and functional life style. The worldwide market of biomaterials has seen a consistent growth over recent years with a steady introduction of new ideas. The central objective of this field of science is to develop biomaterials with suitable properties, appropriate functionality and also biocompatibility, which ultimately determines the usability of the material in the body.

1.1.1. Biocompatibility

The earlier simplistic definition of "biocompatibility" is a material that is fully accepted by the body and not treated as foreign.[3] However, this objective is too high to be likely realized for any artificial device. There will always be contact induced reactivity in a biological environment no matter what the degree of chemical inertness of constituent parts.[4] Ratner proposed a new definition of biocompatibility in 1993: the exploitation by materials of the proteins and cells of the body to meet a specific performance goal.[4] This definition suggests the central role in biocompatibility of interfacial proteins and cellular recognition processes, which also stresses the active role (exploitation) of the biomaterial. As more and more new biomaterials are developed in various applications, the current formal definition becomes more acceptable, which is "the ability of a material to perform with an appropriate host response in a specific application".[5]

The biocompatibility of a medical implant will be influenced by a number of factors, such as the toxicity of the materials, the form and design of the implant, the skill of the implanting surgeons, the dynamics or movement of the device in situ, the resistance of the device to chemical or structural degradation, the nature of the interfacial biological reactions (biological responses), and so on. Among them, the toxicity of the materials, the biostability and the interfacial biological reactions are the primary concerns for biomaterials' exploitation. The evaluation of biological responses in the assessment of biocompatibility is considered to be a predictor for whether a biomaterial, medical device, or prosthesis will display potential harm to the patient by evaluating conditions that simulate clinical use.[6]

1.1.2. Biological responses to materials

All the biomaterials, medical devices, or prostheses to be used in humans face a cascade of events that occur when a foreign material is placed in contact with living tissue. Injury to tissues or organs first arises during the implantation process.[7] The inflammatory response (acute inflammation and chronic inflammation), wound healing response, foreign-body reaction, and ultimately fibrous encapsulation (scar formation) are followed and generally considered as parts of the tissue or cellular host responses to injury.[4] Among them, the foreign-body reaction, which is instigated by the non-specific protein adsorption on the biomaterial may persist at the tissue-implant interface for the lifetime of the implant.[8] Of course, the extent of the responses above is determined by multiple factors, such as the extent of injury, the loss of basement membrane structures, the extent of inflammation, the form and topography of the surface of the biomaterial and so on.[6] Anderson had reviewed the biological responses to materials from the perspective of the fundamental aspects of tissue responses and the *in vivo* evaluation of tissue responses in 2001.[6] To screen new materials for use in humans with the minimal delay, *in vitro* evaluation performed, followed by *in vivo* and carefully clinical trials are very valuable.[9]

1.2. CLASSIFICATIONS OF BIOMATERIALS

Many types of biomaterials have been developed, including metals (stainless steel, titanium, cobalt chrome, nitinol), ceramics and glasses (alumina, calcium phosphate, hydroxyapatite), composites, and a wide range of synthetic and natural polymers

(polymeric, composite and biological biomaterials). Metals are used widely in load bearing applications because of their high strength, ductility, and resistance to wear. Their major disadvantages are high stiffness compared to host tissues and sensitivity to corrosion; the release of metal ions which may cause allergic tissue reactions.[10,11] The range of applications for which titanium and its alloys are applicable, for example, is high because of their excellent biocompatibility. Ceramics are known for their good biocompatibility, corrosion resistance, and high compression resistance. However, they have the drawbacks of brittleness, low fracture strength, difficulty in fabrication, low mechanical reliability and lack of resilience. The drawbacks of these biomaterials have stimulated researchers and engineers to develop composite materials as an alternative choice in bioengineering applications.

Because of the diversity of needs for biomaterials' applications and usage, recent developments of synthetic and natural polymers are radically expanding the capabilities of polymeric biomaterials, especially for soft tissue applications. To minimize the foreign body reaction and promote normal wound healing, researchers have used surface modification of the existing devices and materials to reduce non-specific protein adsorption *in vivo*. Nevertheless, to help the body mend itself and regenerate new tissues that can last for the patient's lifetime, replacing the damaged tissue with a similar one that contains the appropriate tissue architecture of cells and extracellular matrix (ECM) is likely to ultimately provide the best solution. A number of approaches are being investigated aiming to improve biocompatibility of biomaterials, such as immobilization of signaling groups on surfaces, the development of synthetic materials with controlled

and tailored properties for drug and cell carriers to facilitate tissue growth, biologically inspired materials that mimic natural processes, the design of 3-D architectures to produce well-defined patterns for developing biological microelectromechanical systems (bioMEM) and tissue-engineering scaffolds.[2] In this chapter, only some representative biomaterials will be introduced.

1.2.1. Nonfouling surfaces

There are many nonfouling surfaces, such as those modified with poly(ethylene glycol), also known as poly(ethylene oxide) (PEO),[12] phospholipid surfaces, and saccharidic surfaces.[13] PEO can be attached to surfaces through covalent immobilization, adsorption or interpenetration. Researchers regard the PEO-grafted surfaces as brush polymers.[14-17] The nonfouling feature results from the water layer formed on PEO surface *in vitro* or *in vivo* and also the brush functionality, of course it depends on molecular weight and surface density of PEO.[14-17] Phospholipids have been shown to inhibit the almost instantaneous protein surface adsorption and subsequent denaturation processes, which is typically the initial event affecting practically every material used in the body: in blood contact it can lead to thrombus formation, to a significant degree.[18-20] For example, it has been reported that a small-diameter (2-mm) vascular graft prepared from a blend of 2-methacryloyloxyethyl phosphorylcholine (MPC) polymer and segmented polyurethane (PU) did not occlude for more than 8 months after implantation in a rabbit, whereas an identical, but unmodified segmented PU graft occluded within 90 minutes.[21]

1.2.2. Hydrogels

Hydrogels have attracted a lot of researchers because of their special features. They are crosslinked polymer networks with an insoluble but swellable character in aqueous media, which offers an environment resembling the highly hydrated state of natural tissues.[22] This character makes hydrogels excellent candidates for tissue scaffolds and drug delivery. The crosslinking of hydrogels can be ionic,[23,24] physical,[25] chemical,[26] or hydrogen bonded.[27] Chemically crosslinked hydrogels allowed for their chemical versatility and ease of fabrication. For instance, synthetic poly(ethylene glycol)-co-poly(lactic acid) (PEO-co-PLA), poly(vinyl alcohol) (PVA), PVA-g-PLA and natural hyaluronic acid, chondroitin sulfate both have been modified with methacrylates to form crosslinkable structures that finally form hydrogels with a wide range of different chemistries. Recently a photopolymerized hydrogel has been successful used as a depot for delivering oligonucleotides throughout the kidney.[28]

1.2.3. Smart biomaterials

Smart biomaterials refer to those materials that can respond to their local environment, such as pH, temperature and light changes. They are especially useful in drug delivery.[29] Researchers have developed pH-sensitive materials that can survive the acidic stomach environment (pH 2) and be successful delivered in the small intestine. The representative pH responsive hydrogels prepared from poly(methacrylic acid) grafted with poly(ethylene glycol) (PMMA-g-PEO) shrink at pH2 trapping the drug cargo, but swell 3-25 times at physiological pH7.4 releasing its cargo in the desired compartment.[30]

Thermally responsive biomaterials have been reviewed.[31] Their usefulness is based on their demonstration of a polymer lower critical solution temperature (LCST). Poly(*N*-isopropylacrylamide) (pNIPAAm) is one of the extensively investigated polymers because of its hydrophobicity change with temperature.[32] It has been used as a drug delivery vehicle[33] and many other applications. pNIPAAm is hydrophobic at 37 °C, and so promotes protein adsorption and then cell adhesion. When the temperature is lowered below 32 °C, it becomes hydrophilic so that it releases proteins and the adherent cells from the surface.

1.2.4. Self-assembled biomaterials

Self-assembled materials have made the realm of polymer science more attractive. The molecules can self-organize into hierarchical structures to perform a specific task. The driving force for self-assembly is the formation of weak noncovalent bonds, such as hydrogen, ionic, van der Waals bonds or hydrophobic interactions.[34] An amphiphilic phospholipid is a natural self-assembly molecule. Through mimicking this character, researchers have made some amphiphilic molecules with hydrophobic and hydrophilic segments. They can self-assemble into distinct structures, such as micelles, vesicles, and tubules with the length of tens to hundreds of nanometers. These self-assembled biomaterials have the promising use in tissue engineering for drug and cell carriers.[35]

1.2.5. Biomimetic biomaterials

Biomimetic materials are not made by living things but have compositions and properties similar to those made by living things. The hydroxyapatite coating found on many artificial hips is a sort of artificial bone that allows for easier attachment of the implant to the living bone. For normal tissues, a complex 3-D architecture is important for the mechanics and functionality of biological organisms. Synthetic materials can offer suitable mechanical properties and degradation profiles but can provide little control over cell behavior and tissue response *in vivo*. Therefore, current efforts are focusing on adding biological constituents to synthetic materials, trying to mimic the native tissue while maintaining control over the material properties. Incorporating short oligopeptides such as arginine-glycine-aspartic acid (RGD) sequence into synthetic materials is one of the examples.[36] The combination of the bioactive elements with supporting materials has very promising applications in regeneration of new tissues.[37]

1.3. SURFACE MODIFICATIONS AND CHARACTERIZATIONS

Even though more and more diverse biomaterials are being investigated and developed, the surface remains of critical importance in determining the performance of a biomaterial *in vivo* or *in vitro*. The surface chemistry and topography of a biomaterial are vital parameters that influence protein adsorption, cell interaction, and the host response.[38] However, some research has suggested that *in vivo* the foreign body reaction is independent of simple surface chemistry. Almost all materials are prone to elicit this response *in vivo*, irrespective of the surface properties.[39-41] This is thought to be attributed

to nonspecific protein adsorption.[2] As we know, some biomaterials possess non-fouling properties that render the surfaces more bio-inert. However, a biocompatible material is not necessarily bioinert. In contrast, the surfaces associated with biological recognition are effective in controlling biological responses. Thus, to address this issue, current efforts are focusing on surface modifications to control protein interaction. For example, the surface can be decorated with appropriate signaling molecules, to provide biomimetic or bio-active materials by the coupling of proteins to the surface, or by coating the surface with self-assembling peptide scaffolds to lend bioactivity and/or cell attachment-compatible 3-D matrix. Different approaches to functionalize biomaterials exist, and they are described below.

A large variety of measurements is used for the characterization of biomaterials either for bulk (deep surface to microns) or surface analysis. Fourier Transform Infrared Spectroscopy (FTIR), for example, is a good tool for bulk analysis. The real 'surface' analysis methods include, X-ray Photoelectron Spectroscopy (XPS or ESCA), Secondary Ion Mass Spectrometry (SIMS), and Atomic Force Microscope (AFM) etc.[42] Sheardown has reviewed the most frequently used surface analysis methods in detail.[43]

1.3.1. Chemical grafting modification

There is a strong initiative currently under way to develop methods of chemically immobilizing biomimetic or bioactive molecules for enhancing the biocompatibility of a biomaterial. Heparin, an important anticoagulant, has been directly bound to the surface by insertion of either functional groups or spacer arms to minimize thrombus formation

on artificial surfaces,[44,45] but the activity of heparin was significantly decreased after binding compared with raw heparin.[46]

In addition, increasing the surface hydrophilicity by chemical modification is also a useful method for improving blood compatibility. Various polymers have been successfully modified with PEO, following which the surfaces better prevent plasma protein adsorption, platelet adhesion, and thrombus formation as mentioned in previous sections. Similarly, hydrophilic polysulfone (PSf) membranes, after being covalently conjugated with polyvinylpyrrolidone (PVP) on the surface, were found to give lower protein adsorption from a plasma solution than PSf membranes. This is also attributed to the hydrophilicity of the PVP–PSf surface.[47] Recently, a novel non-thrombogenic biomaterial was designed and synthesized by modifying the surface of cellulose with zwitterionic monomers including ammonium sulfonates, phosphates and carboxylates. The zwitterionic structure of the molecules is considered to be favorable to the maintenance of normal conformation of protein and its assembly.[48]

1.3.2. Physical adsorption

Unlike chemical modification, physical adsorption is generally a simple process to perform and no toxic monomer residues or toxic by-products are present. However, its use is confounded by a lack of stability. PEO surfaces, after blending with some other polymers such as poly(ether urethane), showed ideal blood testing results.[49] Amiji also reported that physically adsorbed poly(ethylene oxide)/poly(propylene oxide)/poly(ethylene oxide) triblock copolymers (Pluronics) on biomaterials surfaces can

prevent fibrinogen adsorption, platelet adhesion and activation.[50] The ability of Pluronics to prevent adhesion and activation was considered to be mainly dependent on the number of propylene oxide residues by the authors, rather than the number of ethylene oxide residues. However, the presence of at least 19 ethylene oxide residues in the hydrophilic poly(ethylene oxide) chains was sufficient to repel fibrinogen and platelets by the mechanism of steric repulsion.

1.3.3. Ozone-induced grafting technology

Ozone-induced grafting technology has been widely used in polymer science due to its ease of handling.[51] Flat polymer surfaces, or even small-diameter vascular grafts, can be exposed to ozone gas leading to the formation of peroxides on the surface, which can be used as initiators for vinyl monomer polymerization. It was reported that a silicone surface was successful modified with 2-methacryloyloxyethyl phosphorylcholine (MPC) through this inexpensive ozone-induced grafting technology, which led to improved hemocompatibility.[52] The blood compatibility of polysulfone (PSf) membrane was also reported to be improved, using this method, with the conjugation of chitosan and heparin.[53]

1.3.4. Plasma deposition

In recent years, plasma deposition has been widely used to modify surfaces. During this process, it has been shown that the bulk physical properties of a biomaterial are not affected. It also offers an easy way to modify the surface with a wide variety of

chemicals that can not be polymerized by conventional synthetic approaches. Therefore, the method can introduce different specific functional groups on the substrate surface. Researchers have shown that by plasma deposition with appropriate gases the blood compatibility of vascular grafts, derived from these surfaces, was improved.[54,55] However, it is also well known that the long term stability of the plasma-treated surface is a big issue[56] and complex chemical reactions can occur in the plasma phase and on the surface of the biomaterial, which makes it hard to predict the biocompatibility-linking surface chemistry.

1.3.5. Langmuir-Blodgett (LB)-deposition

LB-deposition has long been a focal point of research for some groups, in that it is capable of preparing highly ordered, uniform monomolecular films with precise control.[57] LB films of suitable materials are ideal model systems for biological membranes. As shown in Figure 1.1, Langmuir-Blodgett films that self-assemble on a water surface are built up at a constant surface pressure, and multilayers on surfaces are formed by a process of successive deposition of individual Langmuir monolayers. Of the presently known techniques for the nanofabrication of ultra-thin films, the LB technique is unique in its ability to control the density of each layer. However, the deposition process is based on physical adhesion, so the endurance of the resulting film is a concern and the range of applications that can be considered will be limited compared to the chemically self-assembled film. As an example, researchers have made surface bound films, such as

phosphatidylcholine (DPPC) and cholesterol, via this technique and compared for their hemocompatibility.[56]

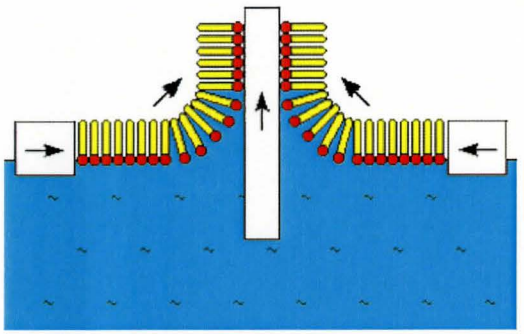

Figure 1.1 Deposition of a Langmuir-Blodgett film from a floating Langmuir monolayer

1.3.6. Self-assembly technology

Self-assembly/deposition has aroused much interest because, with it, surface properties can be obtained in a controlled manner. The surface layer can be modified at the molecular level and the surface can be highly ordered and orientated. Whitesides has made alkanethiolates self-assembled monolayer (SAM) on gold and palladium successfully.[58] Some efforts have been focusing developing SAM to achieve hemocompatibility. However, a variety of different cellular responses occurred. Tegoulia's research group has prepared SAMs of alkylsiloxanes supported on polydimethylsiloxane (PDMS) via the linker alkyltricholorosiloxanes to construct the inner lumen of tubes, and found that different terminal groups on alkyltrichlorosilanes led to different blood compatibilities.[59] This promising technique allows scientists to choose the chemical composition of the monolayer, and thus the surface properties likely.

1.4. THE FUTURE OF BIOMATERIALS

For current biomaterials, the link-up between the micro and macroscopic scale is still poorly understood and the relationships between chemical structure of biomaterials and cell-biomaterial interactions remain to be established. Once fundamental rules are developed, rational design of new biomaterials can be tailored for a specific use. Tissue engineering and regenerative medicine will likely change the face of biomaterials and ultimately revolutionize medical implants; at the same time tissue engineering needs biomaterials. The need for synthetic biomaterials will not decrease through this century as researchers once predicted. More and more biomaterials capable of interacting specifically with predetermined cell types, and not being recognized by other cell types, need to be developed. This specificity can be possibly generated by first producing a non-adhesive surface and then attaching specific biologically active ligands.[60]

1.5. THESIS OBJECTIVES

Proteins are present in all body fluids and are present in most culture media. Proteins are a primary source of information for biological recognition. Cell adhesion, both in the body and on synthetic substrates, is mediated by protein interactions with cell-surface receptors.

Chemical surface modifications should provide intrinsic advantages, including offering a stable biointerface, ease of fabrication, and diversity of the surface for various applications. However, not everything can be easily immobilized. Some special proteins

or signal molecules require special conditions or methods to be effectively tethered to surfaces.

Collagen is the major connective tissue protein in animals, accounting for about 25% of the total body protein of vertebrates. As a natural biomaterial, it has been found to be useful in more and more applications. Our interest was to investigate methods to covalently bind collagen to one of the most used polymer materials in soft tissue implants, silicone, and to study and better understand its biological responses. Collagen is known to be a giant protein and, as will be discussed in Chapter 3, only several papers so far prepared covalently linked collagen surfaces, and only with low efficiency. Our objectives were to develop strategies to prepare stable silicone surfaces modified with collagen via chemical immobilization, while maintaining the collagen activity. PEO was selected as a spacer to link collagen to the silicone surface. Developing beneficial biological responses of the collagen surfaces was one of the main objectives of the study.

1.6. REFERENCES

(1) Williams, D. F. *Williams Dictionary of Biomaterials*; LUP, 1999.

(2) Ratner, B. D.; Bryant, S. J. *Annu rev biomed eng* **2004**, *6*, 41-75.

(3) Hench, L. L.; Ethridge, E. C. *Biomaterials: an interfacial approach*; Academic Press: New York, 1982.

(4) Ratner, B. D. *J Biomed Mater Res* **1993**, *27*, 837-50.

(5) Vadgama, P. *Annul Rep Prog Chem, Sect C: Phys Chem* **2005**, *101*, 14-52.

(6) Anderson, J. M. *Annu Rev Mater Res* **2001**, *31*, 81-110.

(7) Anderson, J. M. *Cardiovasc Pathol* **1993**, *2*, 33-41.

(8) Chambers, T. J.; Spector, W. G. *Immunobiology* **1982**, *161*, 283-9.

(9) Gibbons, D. F. *Annu Rev Biophys Bioeng* **1975**, *4*, 367-75.

(10) Azevedo, C. R. F. *Eng Fail Anal* **2003**, *10*, 255-263.

(11) Schmalz, G.; Garhammer, P. *Dent Mater* **2002**, *18*, 396-406.

(12) Nuzzo, R. G. *Nat Mater* **2003**, *2*, 207-8.

(13) Holland, N. B.; Qiu, Y.; Ruegsegger, M.; Marchant, R. E. *Nature* **1998**, *392*, 799-801.

(14) Heuberger, M.; Drobek, T.; Voros, J. *Langmuir* **2004**, *20*, 9445-8.

(15) Lee, J. H.; Ju, Y. M.; Lee, W. K.; Park, K. D.; Kim, Y. H. *J Biomed Mater Res* **1998**, *40*, 314-23.

(16) McGurk, S. L.; Green, R. J.; Sanders, G. H. W.; Davies, M. C.; Roberts, C. J.; Tendler, S. J. B.; Williams, P. M. *Langmuir* **1999**, *15*, 5136-5140.

(17) Morra, M. *J Biomater Sci Polym Ed* **2000**, *11*, 547-69.

(18) Ishihara, K.; Fujita, H.; Yoneyama, T.; Iwasaki, Y. *J Biomater Sci, Polym Ed* **2000**, *11*, 1183-1195.

(19) Ishihara, K.; Fukumoto, K.; Iwasaki, Y.; Nakabayashi, N. *Biomaterials* **1999**, *20*, 1553-1559.

(20) Ishihara, K.; Fukumoto, K.; Iwasaki, Y.; Nakabayashi, N. *Biomaterials* **1999**, *20*, 1545-1551.

(21) Yoneyama, T.; Ito, M.; Sugihara, K.; Ishihara, K.; Nakabayashi, N. *Artif Organs* **2000**, *24*, 23-8.

(22) Wang, D.; Ratcliffe, A.; Elisseeff, J. H.; U.S. Pat Appl Publ 170663, **2004**, 28pp.

(23) Senuma, Y.; Lowe, C.; Zweifel, Y.; Hilborn, J. G.; Marison, I. *Biotechnol Bioeng* **2000**, *67*, 616-22.

(24) Novikova, L. N.; Mosahebi, A.; Wiberg, M.; Terenghi, G.; Kellerth, J. O.; Novikov, L. N. *J Biomed Mater Res A* **2006**, *77*, 242-52.

(25) Kim, M. R.; Park, T. G. *J Control Release* **2002**, *80*, 69-77.

(26) Andreopoulos, F. M.; Beckman, E. J.; Russell, A. J. *Biomaterials* **1998**, *19*, 1343-52.

(27) Xing, B.; Yu, C. W.; Chow, K. H.; Ho, P. L.; Fu, D.; Xu, B. *J Am Chem Soc* **2002**, *124*, 14846-7.

(28) Ramakumar, S.; Phull, H.; Purves, T.; Funk, J.; Copeland, D.; Ulreich, J. B.; Lai, L. W.; Lien, Y. H. *J Urol* **2005**, *174*, 1133-6.

(29) Hoffman, A. S.; Stayton, P. S.; Press, O.; Murthy, N.; Lackey, C. A.; Cheung, C.; Black, F.; Campbell, J.; Fausto, N.; Kyriakides, T. R.; Bornstein, P. *Polym Adv Technol* **2002**, *13*, 992-999.

(30) Kim, B.; La Flamme, K.; Peppas, N. A. *J Appl Polym Sci* **2003**, *89*, 1606-1613.

(31) Jeong, B.; Kim, S. W.; Bae, Y. H. *Adv Drug Deliv Rev* **2002**, *54*, 37-51.

(32) Chilkoti, A.; Dreher, M. R.; Meyer, D. E. *Adv Drug Deliv Rev* **2002**, *54*, 1093-111.

(33) Sershen, S.; West, J. *Adv Drug Deliv Rev* **2002**, *54*, 1225-35.

(34) Zhang, S. *Biotechnol Adv* **2002**, *20*, 321-39.

(35) Kisiday, J.; Jin, M.; Kurz, B.; Hung, H.; Semino, C.; Zhang, S.; Grodzinsky, A. J. *Proc Natl Acad Sci U S A* **2002**, *99*, 9996-10001.

(36) Shin, H.; Jo, S.; Mikos, A. G. *Biomaterials* **2003**, *24*, 4353-64.

(37) Wakisaka, S.; Atsumi, Y.; Youn, S. H.; Maeda, T. *Arch histol cytol* **2000**, *63*, 91-113.

(38) Aldenhoff, Y. B.; Blezer, R.; Lindhout, T.; Koole, L. H. *Biomaterials* **1997**, *18*, 167-72.

(39) Behling, C. A.; Spector, M. *J Biomed Mater Res* **1986**, *20*, 653-66.

(40) Piglowski, J.; Gancarz, I.; Staniszewska-Kus, J.; Paluch, D.; Szymonowicz, M.; Konieczny, A. *Biomaterials* **1994**, *15*, 909-16.

(41) Deligianni, D. D.; Katsala, N.; Ladas, S.; Sotiropoulou, D.; Amedee, J.; Missirlis, Y. F. *Biomaterials* **2001**, *22*, 1241-51.

(42) Ratner, B. D. *Cardiovasc Pathol* **1993**, *2*, 87S-100S.

(43) Merrett, K.; Cornelius, R. M.; McClung, W. G.; Unsworth, L. D.; Sheardown, H. *J Biomater Sci, Polym Ed* **2002**, *13*, 593-621.

(44) Chen, H.; Brook, M. A.; Sheardown, H. D.; Chen, Y.; Klenkler, B. *Bioconjug Chem* **2006**, *17*, 21-8.

(45) Chen, H.; Chen, Y.; Sheardown, H.; Brook, M. A. *Biomaterials* **2005**, *26*, 7418-24.

(46) Weber, N.; Wendel, H. P.; Ziemer, G. *Biomaterials* **2002**, *23*, 429-39.

(47) Higuchi, A.; Shirano, K.; Harashima, M.; Yoon, B. O.; Hara, M.; Hattori, M.; Imamura, K. *Biomaterials* **2002**, *23*, 2659-66.

(48) Zhang, J.; Yuan, J.; Yuan, Y.; Shen, J.; Lin, S. *Colloids Surf,B: Biointerfaces* **2003**, *30*, 249-257.

(49) Wang, D. A.; Ji, J.; Gao, C. Y.; Yu, G. H.; Feng, L. X. *Biomaterials* **2001**, *22*, 1549-62.

(50) Amiji, M.; Park, K. *Biomaterials* **1992**, *13*, 682-92.

(51) Zhou, J.; Yuan, J.; Zang, X.; Shen, J.; Lin, S. *Colloids Surf, B: Biointerfaces* **2005**, *41*, 55-62.

(52) Xu, J.; Yuan, Y.; Shan, B.; Shen, J.; Lin, S. *Colloids Surf, B: Biointerfaces* **2003**, *30*, 215-223.

(53) Yang, M. C.; Lin, W. C. *Polym Adv Technol* **2003**, *14*, 103-113.

(54) Lin, J. C.; Cooper, S. L. *Biomaterials* **1995**, *16*, 1017-23.

(55) Yeh, Y. S.; Iriyama, Y.; Matsuzawa, Y.; Hanson, S. R.; Yasuda, H. *J Biomed Mater Res* **1988**, *22*, 795-818.

(56) Lee, Y.-L.; Chen, C.-Y. *Appl Surf Sci* **2003**, *207*, 51-62.

(57) Peterson, I. R. *J Phys D: Appl Phys* **1990**, *23*, 379-95.

(58) Love, J. C.; Wolfe, D. B.; Chabinyc, M. L.; Paul, K. E.; Whitesides, G. M. *J Am Chem Soca* **2002**, *124*, 1576-1577.

(59) Silver, J. H.; Lin, J. C.; Lim, F.; Tegoulia, V. A.; Chaudhury, M. K.; Cooper, S. L. *Biomaterials* **1999**, *20*, 1533-43.

(60) Hubbell, J. A.; Massia, S. P.; Desai, N. P.; Drumheller, P. D. *Biotechnology (N Y)* **1991**, *9*, 568-72.

CHAPTER 2 – THE STRATEGIES FOR PREPARATION OF NHS-MODIFIED SURFACE

2.1. INTRODUCTION

There have been many ways designed to prepare protein bound surfaces, including blending,[1] or surface coating[2] of polymers with biological active proteins. In addition to physical coating, functional groups[2] that can react with proteins can be grafted onto the polymer's surface. Typically, two strategies are used for this purpose. Either carbodiimides[3] are used to facilitate amide formation, or activated esters are used to bind protein-based amine groups. For example, Grainger's group has prepared NHS-PEO-siloxane monolayer on gold surfaces to which proteins can be covalently tethered.[4] Brook's group has made *N*-succinimidyl carbonate modified PEO surfaces using hydrosilylation onto silicone elastomers.[5]

The current goals are to make more concentrated NHS surfaces, and to do so more efficiently. One of the challenges is the stability of the activated ester surface. Because NHS groups hydrolyze fairly readily, they can be hydrolyzed before or after being tethered on the surface. For these surfaces to be usefully applied, the efficiency and reproducibility of surface grafting must be controlled. Grainger's group demonstrated that hydrolysis was a problem with DNA modified microarrays and developed a method to regenerate NHS-reactive surfaces using organic solvents with dicyclohexylcarbodiimide (DCC), under aqueous conditions using

ethylenedicarbodiimide (EDC).[6] Although the process was time consuming, the improvement in surface grafting was significant.

Our objective was to develop strategies for making high density, NHS-tethered silicone surfaces in a more efficient manner, with good reproducibility, and subsequently demonstrate that the surfaces can be converted into effective biomaterials. We report below our efforts to improve the preparation of NHS-modified silicone surfaces, and demonstrate their efficacy by binding heparin to them.

2.2. EXPERIMENTAL SECTION

2.2.1. Materials

A polydimethylsiloxane (PDMS) film was prepared using the Sylgard 184 Silicone elastomer Kit (Dow Corning Corporation, Silicone elastomer: Silicone elastomer Curing agent = 10:1). Dow Corning 1107 (poly(methylhydrosiloxane) and poly(ethylene glycol monoallylether)(Polyglycol 550, Clariant, Mw 550g/mol) (PEO 550), which were obtained as gifts and used as received. Polydimethylsiloxane, trimethylsiloxane terminated (Mw~6000) was obtained from United Chemical Technologies, Inc. Triethylamine, 99% (Anachemia) was dried with molecular sieves before use. Trifluoromethanesulfonic acid (98%), anhydrous hexanes, anhydrous acetonitrile, anhydrous toluene, and anhydrous diethylene glycol dimethyl ether (diglyme), toluidine blue (Basic Blue 17; C. I. 52040), and *n*-hexane were purchased from Sigma-Aldrich Chemical Co. and used as received. Tris(hydroxymethyl)aminoethane (Bishop Canada Inc.), NaCl (Bishop Canada Inc.) and heparin activity reagent kit (Hepanorm) were used

as received. Absolute methanol (J. T. Baker, 'Photrex'® Reagent), di(*N*-hydroxysuccinimidyl) carbonate (Fluka), platinum-divinyltetramethyl-disiloxane complex in xylene (2.1-2.4% Pt, Gelest) (Karstedt's Pt catalyst), acetonitrile (reagent grade, Caledon), 2-propanol (reagent, Caledon) and acetone (ACS) were also used as received. Water used was purified by treating in a reverse osmosis unit followed by a Millipore unit (18 mΩ resistivity).

2.2.2. Instrumentation

2.2.2.1. Attenuated Total Reflection Fourier Transform Infrared (ATR-FTIR)

The FTIR spectra (16 scans at 4 cm^{-1} resolution) of the surfaces prepared as described below were obtained using a Bio-Rad (Cambridge, MA) FTS-40 IR spectrometer with a fixed 45° angle attenuated total reflectance (ATR, ZnSe) cell attachment under N_2 purge. Thus, the samples were placed on an ATR cell and the FTIR scans were obtained. The background was run when no sample was placed in the ATR cell. The imaging data were analyzed with WinIR Pro software (Bio-Rad) and excel software.

2.2.2.2. Nuclear Magnetic Resonance (^{1}H- NMR)

^{1}H- NMR spectra were obtained on a 200MHz Bruker NMR.

2.2.2.3. Surface Profilometer

Surface roughnesses were obtained using a Veeco WYKO NT1100 Optical Profiling System (Mode: VSI, Objective 50X, FOV 2.0X).

2.2.2.4. Atomic Force Microscopy (AFM)

Tapping mode AFM measurements were performed with a NanoScope IIIa with multi-mode. Etched silicon probes (Digital Instruments), with cantilever lengths of 116μm and resonance frequencies of about 270 kHz, were used. A sharp tip having a radius of 10nm was selected for this study. Images were recorded with a slow scan rate (0.5 Hz).

2.2.2.5. X-ray Photoelectron Spectroscopy (XPS)

The XPS measurements were performed on a Leybold (Specs) MAX 200 XPS system utilizing a monochromatic Al Kα X-ray source operating at 15 kV and 20 mA. The spot size used in all experiments was 2x4 mm^2. Survey scans were performed from 0 to 1000 eV. The low resolution and C1s high-resolution analyses were performed with a scan width of 20eV. Angle-dependent XPS data were collected at takeoff angles (ToA) of 20°, and 90° to allow the analysis of compositions from 2nm to 10nm depth. The ToA was defined as the angle between the surface normal and the axis of the analyzer lens system.[4] Specslab (specs Gmbh, Berlin) was used to perform the spectral fitting on the spectra.

2.2.3. Preparation of Si-H Surfaces

Sylgard 184, a 2 part platinum cured silicone, was allowed to cure into a film about 0.5mm thick in a Petri dish. Round polydimethylsiloxane (PDMS) disks with diameters of ¼ inch or 3/8 (0.375) inch were punched from the film before use. To a vial containing 5 mL absolute methanol and 3mL poly(methylhydrosiloxane) (DC1107) was added 30 PDMS disks (either size) and 50 μL trifluoromethanesulfonic acid (TfOH). After being vigorously shaken for 30 min at room temperature, the disks were rinsed thoroughly with dry methanol and hexane to remove TfOH and unreacted DC1107, and then promptly blown dry with nitrogen followed by further drying under vacuum for 2 hours. The presence of the SiH at the interface was shown by FTIR (cm^{-1}, neat): 2167 (Si-H). Isopropanol (iPA) was an alternative solvent used for making the Si-H surface, and led to a much more intense Si-H peak in the IR. However, the disks became brittle and a little bit cloudy after the process. Therefore, all the studies of Si-H materials described below were based on the recipe using methanol as the solvent.

The effect of reaction time on the Si-H surface was also investigated by varying the reaction duration from 1 to 35 min (1, 5, 10, 15, 20, 25, 30, 35 min). Different concentrations of TfOH (5μL, 25μL, 50μL and 125μL in 8mL of methanol and DC1107 mixture) were also used to study its effect on making Si-H surface. In the studies of the roles of the acid TfOH and DC1107, the silicone oil polydimethylsiloxane or methanol was added instead of the same volume of DC1107. The optimum conditions are discussed in the text.

2.2.4. Making NHS Surface

2.2.4.1. By direct hydrosilylation with Allyl-PEO-NHS

2.2.4.1.1. Synthesis of Allyl-PEO-NHS (α-Allyl-ω-N-succinimidyl carbonate-poly(ethylene oxide))

The procedure for synthesis of allyl-PEO-NHS was based on previous work with some refinement.[7] To a solution of poly(ethylene oxide) poly(ethylene glycol) monoallylether (2.0 g, 4.0 mmol) and triethylamine (1.62 g, 16 mmol) in CH_3CN (10 mL) was added *N,N'*-disuccinimidyl carbonate (di-NHS) (4.1 g, 16 mmol). The mixture was allowed to stir at room temperature over 10 h under N_2 and then left to stand for 1h. Three layers were obtained: a top dark red liquid layer, a middle yellowish liquid layer and a bottom pale solid layer. It was found afterwards by ^{1}H-NMR that the top dark red layer contained only a little desired product; most of it was in the middle yellowish layer and the bottom layer. Therefore, the top layer was removed with a glass pipette to another flask and the solvent was removed in vacuo. The residue was partially dissolved in anhydrous toluene (the undissolved part was very sticky and made the separation of the product difficult, which was also one of the reasons why the final yield was low). The toluene (with some product in it) was then removed to a collection flask. The residue was washed 3 times with toluene (20 mL). All the toluene washings were combined in the collection flask. The middle yellowish layer and the bottom solid layer (the excess di-NHS and *N*-hydroxy succinimide salt) were filtered using a Hirsh funnel. Both the reaction flask and the precipitate in the Hirsh funnel were washed with anhydrous toluene 3 times (20 mL). All the toluene solution was combined to the previous collection flask.

The solution was allowed to stand overnight in the freezer. A pale brown precipitate was filtered off and the residue was dissolved in anhydrous toluene (25 mL) and the solution was again cooled below 0 °C again. This procedure was repeated 3 times. 20 mL dry toluene was added to the residue and a small amount of *n*-hexanes was dropped in until the solution became a little cloudy, then the solution was cooled down to 0 °C overnight. The pale brown precipitate was filtered off again. This procedure was repeated 3 or 4 times. The whole purification procedure took about one week. The resultant compound was yellow oil (yield 80%). FTIR (cm^{-1}, neat): 1743 (NC=O), 1789 (OC=O). ^1H NMR (200.2 MHz, $CDCl_3$): δ2.78 (s, 4H, $O=CCH_2CH_2C=O$), 3.57 (bs, 40H, PEO's OCH_2), 3.72 (bs, 2H, $OCH_2CH_2OC=O$), 3.95 (d, 2H, *J*=5.6Hz, $CH_2=CHCH_2O$), 4.39 (m, 2H, $OCH_2CH_2OC=O$), 5.20 (m, 2H, $CH_2=CHCH_2O$), 5.82 (m, 1H, $CH_2=CHCH_2O$) ppm. Toluene was chosen as the solvent for the following reasons: it is a good solvent for allyl-PEO-NHS; the allyl-PEO-NHS is stable in toluene; the by product only slightly dissolves in toluene. The *n*-hexanes were used to remove the remaining traces of by product even though traces of the product were removed as well. The resulted product was sealed well and stored at 4 °C. The reaction yields over time were also recorded by running the reaction in a NMR tube from 5min to 10h and the allyl-PEO was almost completely converted to allyl-PEO-NHS after 10h (see Figure 2.9).

2.2.4.1.2. Hydrosilylation with Allyl-PEO-NHS

The Si-H disks were immersed and stirred in a mixture of allyl-PEO-NHS 0.6g and diglyme (1:4) (Total 3mL) with one drop of Karstedt's Pt catalyst at 50 °C under

nitrogen overnight. The resulting disks were thoroughly washed with dry acetone and blow dried with nitrogen followed by further drying in vacuo. The modified surfaces were stored at 4 °C in a dry condition. FTIR (cm^{-1}, neat): 1743 (N-C=O), 1789 (O-C=O), 2893-2920 (CH_2 stretching from PEO ($O-CH_2CH_2$) chain). The Si-H band at 2167 cm^{-1} disappeared after hydrosilylation with allyl-PEO-NHS.

2.2.4.2. Reaction of Allyl-PEO Surface with *N,N'*-Disuccinimidyl Carbonate

2.2.4.2.1. Hydrosilylation with Allyl-PEO-OH

The Si-H disks were immersed and stirred in a mixture of allyl-PEO 550 (2g) and diglyme (2:5) (Total 7mL) with one drop of Karstedt's Pt catalyst at room temperature. Reaction time was varied from 1h to 10h. The resulting disks were thoroughly washed with dry acetone and blow dried with nitrogen followed by further drying in vacuo. FTIR (cm^{-1}, neat): 2893-2920 (CH_2 stretching from PEO. The Si-H band at 2167 cm^{-1} disappeared after hydrosilylation with PEO 550.

2.2.4.2.2. PEO-OH Surface Reaction with N,N'-Disuccinimidyl Carbonate

To a mixture of di(*N*-hydroxysuccinimidyl) carbonate (400 mg, 1.56 mmol) and Et_3N (200 mg, 1.98 mmol) of anhydrous acetonitrile (6 mL) were added 30 PEO-modified disks. The mixture was stirred or shaken from 2 to 20 h (just to make sure the disks not to overlap tightly). The resulting surfaces were thoroughly washed with acetonitrile and dry acetone, and then blown dry under nitrogen. It was found that 2 h was

enough time for this reaction. The same result was achieved with direct hydrosilylation using allyl-PEO-NHS but much more efficiency and reproducibility were obtained (it took about one week for the synthesis and purification of allyl-PEO-NHS. Moreover, allyl-PEO-NHS very easily adsorbs water and the NHS group hydrolyzes before hydrosilylation, which makes the NHS-tethering result on the surface by this approach inconsistent).

2.2.5. Heparin Binding to NHS-modified Surface

2.2.5.1. Calibration Curve of Heparin Content

A series of heparin standard solutions with concentrations varying from 0 to 20μg/mL were prepared by diluting a stock solution according to the final concentrations (0.08, 0.16, 0.32, 0.64, 0.8 and 1.6 mg/mL, respectively). The stock solution was obtained by dissolving 10 mg heparin in an aqueous 0.2 wt% NaCl solution.[8]

Toluidine blue (50mg) was dissolved in 1mL of 0.01N HCl solution, in which 0.2 wt% NaCl had been previously dissolved. Then the solution was diluted to give 0.005mg/mL toluidine blue solution. 1.0 mL of this solution was added to a 5mL tube, and then 0.1 mL of the above heparin standard solution was added. The mixed solution was vortexed by a Vortex mixer for 30s. 1mL of *n*-hexane was then added and vigorously mixed for 30 s. Phase separation occurred over 5min. The heparin-toluidine blue complex was extracted into the upper, transparent organic layer. After the organic layer was removed, the absorbance of the aqueous layer at 631nm was measured on a Beckman DU640UV/VIS spectrophotometer, the empty cuvette as a blank. A linear standard calibration curve was

obtained by measuring absorbance at 631 nm versus concentration of heparin in the aqueous NaCl solution.

2.2.5.2. Preparation of Heparin-modified Surface

The heparin-modified surface was made following literature procedures.[5] The NHS-tethered surfaces were immersed in phosphate buffered saline (PBS, pH 8.0) containing the heparin (10mg/mL) for 6 h. Surfaces were incubated in and rinsed with PBS three times (10 min, 2mL, each time) and then dried under vacuum.

2.2.5.3. Heparin Density of the Surface

For each experiment, 0.1 mL of 0.2% NaCl solution and 1.0 mL of 0.005 mg/mL (0.0005%) toluidine blue solution were mixed in a 5 mL polypropylene test tube. The heparin-modified surfaces with 0.77cm^2 area were immersed in the solution and vortexed for 30s. Then 1 mL *n*-hexane was added and the mixture was well shaken. The mixture was allowed to phase-separate for 5 min after removal of the surfaces. Similarly, the upper organic layer was removed and the absorbance of the aqueous layer at 631nm was investigated on a Beckman DU640 UV/VIS spectrophotometer, the empty cuvette as the blank. The density of total heparin immobilized on the surfaces was calculated from the above calibration curve. For each surface, the heparin density was expressed in mass per unit surface area. Average heparin density: 0.68μg/cm^2.

2.2.5.4. Heparin Activity Measurement

The heparin activity standard curve was obtained by running a Hepanorm reagent kit, which is kit of calibration plasmas for assays of unfractionated heparin (UFH) using the anti-Factor Xa method. The heparin-modified surfaces were regarded as non-volume entities since they were removed after the reaction. The remaining solution was tested the same way as the standard samples. The average heparin activity of 0.3442IU/mL (0.657mg/mL) was obtained and 96.7% of activity was remained after immobilization.

2.3. *RESULTS*

2.3.1. Preparation of Si-H Surfaces

Unlike most organic polymers, silicones undergo ring-opening polymerization reversibly. That means with acid or base a linear silicone can undergo depolymerization, forming small cyclics (such as octamethylcyclotetrasiloxane (D_4) and decamethylcyclopentasiloxane (D_5))[9] or oligomers, and repolymerization based on an equilibrium. If these reactions are performed in the presence of a second silicone, it is possible to metathesize the groups such that constituents of each polymer exchange. In the case of a dimethylsilicone elastomer, the acid catalyzed equilibration with $(MeHSiO)_n$ led to silicone surfaces enriched with Si-H groups (See Scheme 2.1, Scheme 2.2).

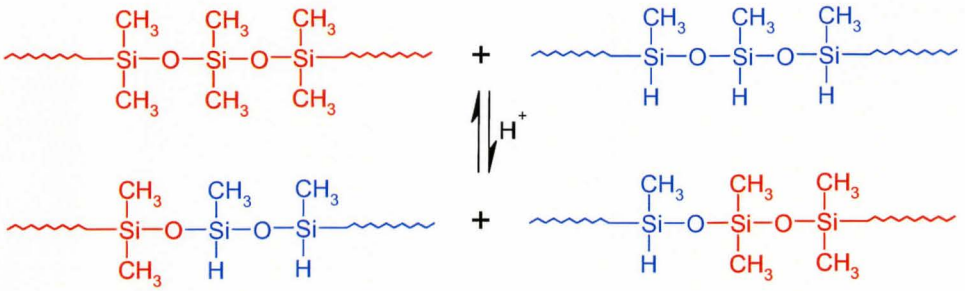

Scheme 2.1 Acid catalyzed equilibration reaction of polydimethylsiloxane and poly(methylhydrosiloxane)

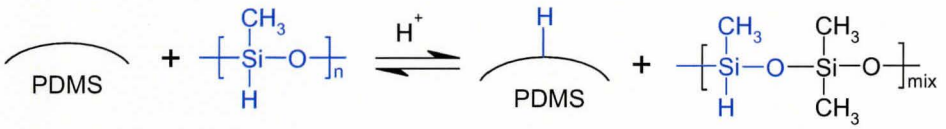

Scheme 2.2 Acid catalyzed equilibration reaction of crosslinked PDMS surface and poly(methylhydrosiloxane)

2.3.1.1. Effect of Solvents on the Si-H Preparation

The efficiency of the redistribution reaction is dependent on the solvents used. In the case of methanol, a relatively poor solvent for silicones, the exchange reactions primarily take place at the external elastomer surface. However, this reaction can be somewhat difficult to control because the fluid methylhydrosilicone is not properly soluble in methanol and the reaction is done as a dispersion.

Isopropanol (IPA) was used as the alternate solvent to try to get a homogeneous solution. It is a much better solvent for silicones, and dissolved both TfOH and DC1107. The IR spectrum of the elastomer after modification (Figure 2.1) showed a huge Si-H band at 2167 cm^{-1}. Exposure to base led to the formation – visible to the naked eye – of hydrogen bubbles. Thus, the reaction is inherently more efficient. However, problems accompanied this change. First, because iPA swelled the surface to some extent,

especially when the contact time was long the substrate surface was not very flat; the surface became brittle.

To rationalize the reaction conditions and subsequent surface properties, an investigation on the effect of different contact times and concentrations of TfOH was undertaken in methanol.

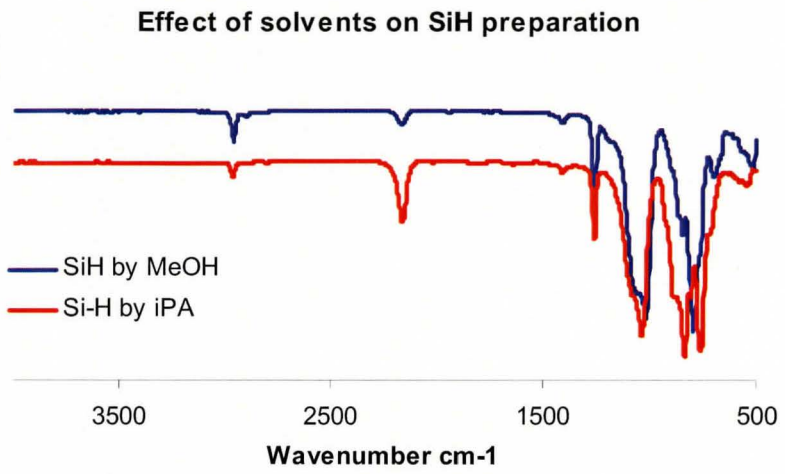

Figure 2.1 FTIR spectra of the Si-H surfaces using methanol and isopropanol (iPA) as the solvent respectively

2.3.1.2. Effect of reaction duration on the Si-H preparation

To optimize the reaction durations, a time course of contact for making Si-H was performed. From Figure 2.2, it can be seen that the relatively intensive band for Si-H was reached at 30 minutes and above.

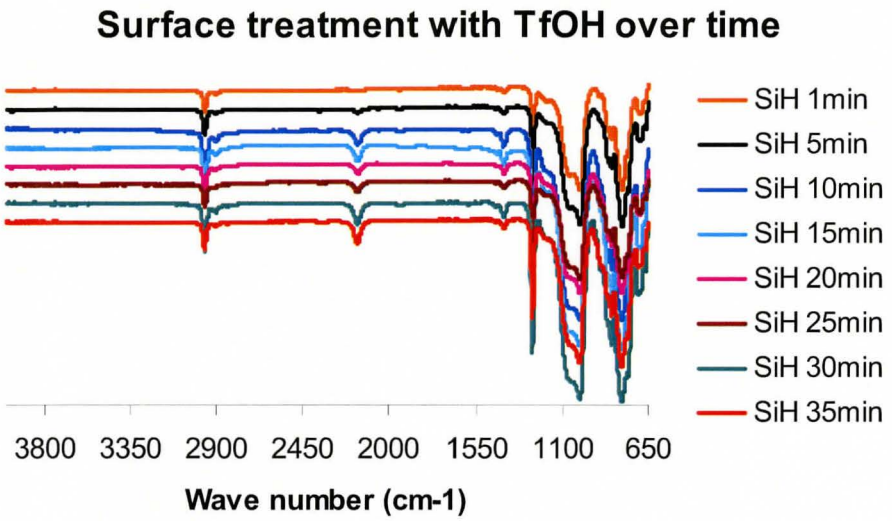

Figure 2.2 FTIR spectra of the Si-H surfaces over various reaction durations from 1 to 35 minutes

2.3.1.3. Effect of concentration of TfOH on the Si-H preparation

To investigate the influence of TfOH concentration on the Si-H preparation, various concentrations of TfOH were used in this depolymerization-copolymerization process. The surface/acid contact time was controlled at 30 minutes. It was found that, as Figure 2.3 shows, when 0.06% TfOH was used, a relatively small peak for Si-H was obtained. 0.3% and 0.6% TfOH gave similar results, a medium strong Si-H peak. However, further increasing the concentration of TfOH to 1.6% gave a huge SiH peak.

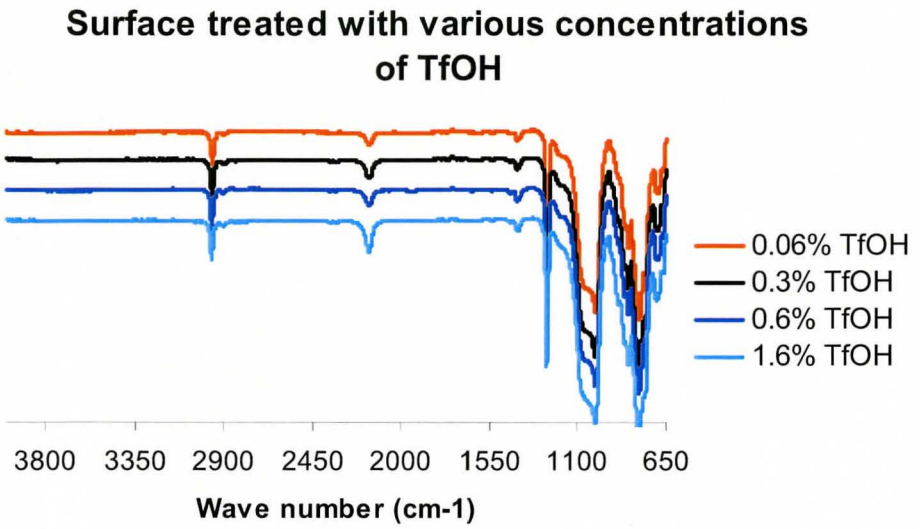

Figure 2.3 FTIR spectra of Si-H surfaces using different concentrations of TfOH varied from 0.06% to 1.6% for 30 minutes

2.3.2. Investigations on the Si-H surface roughness

The surface roughness of these systems was obtained using an optical profilometer.

2.3.2.1. Effect of contact time on the Si-H surface roughness

The surface roughness was studied as a function of contact time in order to show its effect on the surface 'insult'. 0.6% TfOH was used in all the reactions within the time course. Longer contact time may lead to more erosion. As displayed in Figure 2.4, the surface roughness was increased with the increasing time of contact with TfOH and DC1107 in methanol. On contact for longer times, more erosion or more polymerization will occur.

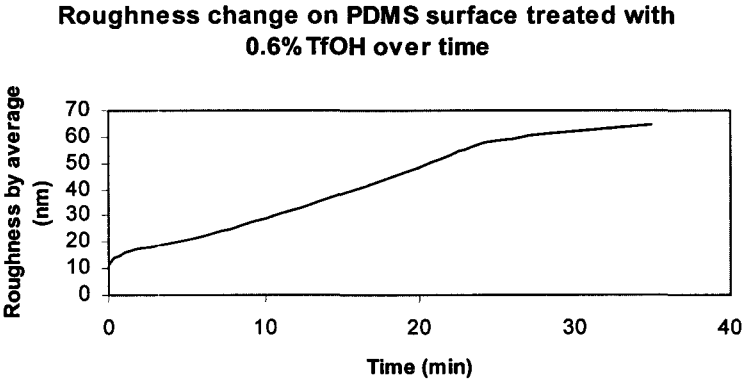

Figure 2.4 SiH Surface roughness variations with different reaction durations from 0 to 35 minutes

2.3.2.2. Effect of TfOH concentration on the Si-H surface roughness

The roughness of the Si-H surfaces only slightly increased with the increase of TfOH concentration as it's shown in Figure 2.5. It may suggest that more TfOH used lead to rougher surface but not with significant change when the same contact time was used.

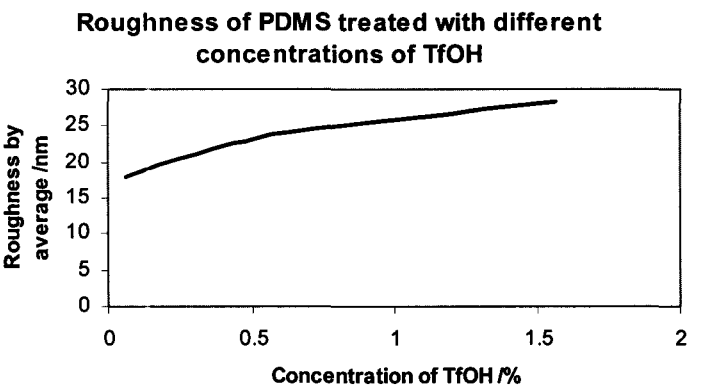

Figure 2.5 Si-H Surface roughness variations upon treatment with various concentrations of TfOH for 30 minutes (with DC1107)

2.3.2.3. The roles of TfOH and DC1107 in varying the Si-H surface roughness

From the above results it can be seen that the Si-H surface roughness increased more or less with the increase of both contact time and the TfOH concentration. It was of interest to know if the acid TfOH alone aroused the erosion on the surface or either or both DC1107 (poly(methylhydrosiloxane)) played a role. Therefore, further studies without added DC1107, or using a non-functional polydimethylsiloxane (silicone oil) instead of DC1107, were undertaken. From Figures 2.6 and 2.7 it can be seen that very little variation on the surface roughness was obtained when the surfaces were treated with only TfOH (without DC1107) regardless of increasing the contact time or the TfOH concentration. When silicone oil was added instead of DC1107, a similar result was obtained (Figure 2.8). Namely, both the surface treated only with TfOH in methanol and the surface treated with TfOH and silicone oil in methanol showed no obvious change on the roughness of PDMS film. Only the one with DC1107 added showed significant change on the surface roughness. The possible reason is that after erosion a second surface layer was built up on the Si-H surface layer in the presence of trace of water.

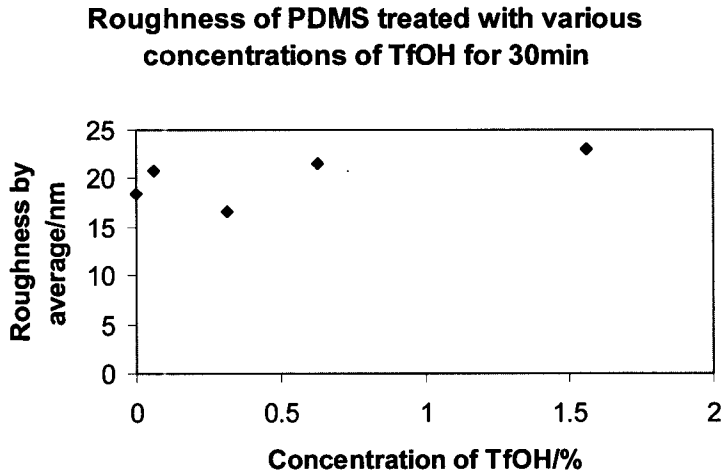

Figure 2.6 PDMS surface roughness change when treated with various concentrations of TfOH varied from 0 to 1.6% (no DC1107 in the solution)

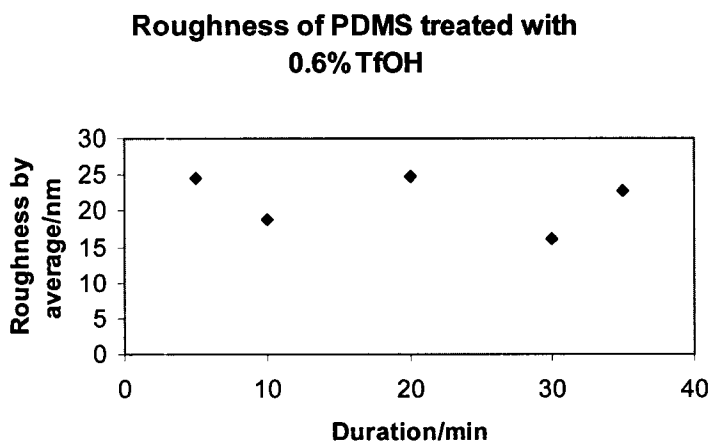

Figure 2.7 PDMS surface roughness change when treated with 0.6% TfOH for different durations varied from 0 to 35 minutes (no DC1107 in the solution)

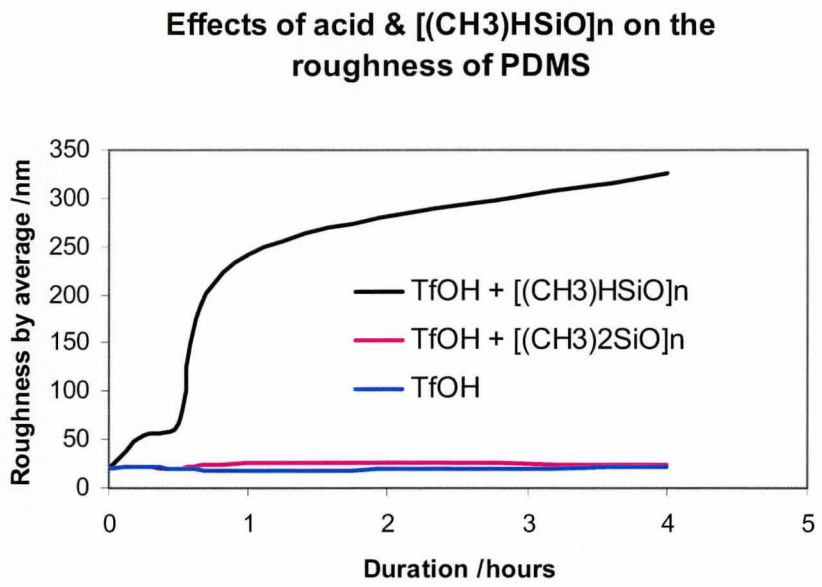

Figure 2.8 Real factors affecting the surface roughness (not TfOH itself, but with DC1107)

2.3.3. Preparation of NHS-tethered silicone surface

The studies above demonstrated that changes in surface morphology can be induced by the polymerization of DC1107 on the PDMS elastomer surface. This functional surface served as the key intermediate in the preparation of activated ester surfaces. Two different approaches were taken. In the first, a single step was used to introduce NHS-capped PEO onto the silicone surfaces. In the second approach, PEO with a free OH group was hydrosilylated onto the silicone surface and then, in a second step, the OH group was converted into an NHS group.

2.3.3.1. By direct hydrosilylation with allyl-PEO-NHS

2.3.3.1.1. Synthesis of allyl-PEO-NHS

The method used for synthesis of allyl-PEO-NHS has been previously used by our group[7] (Scheme 2.3) but the yield was not very high (60%). Side reactions (Scheme 2.4) may be one of the reasons. Purification is another issue.

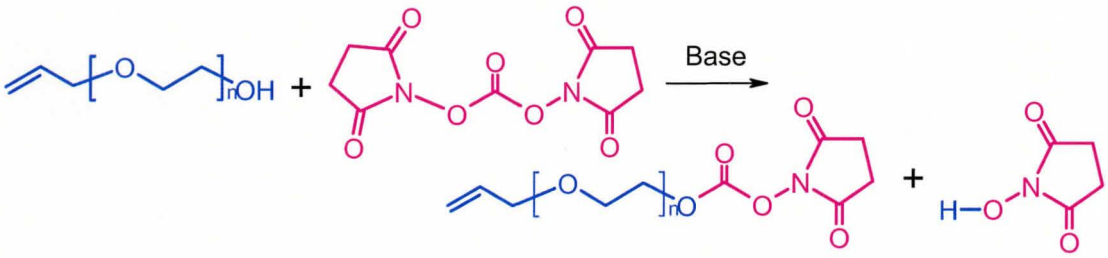

Scheme 2.3 Synthesis of allyl-PEO-NHS

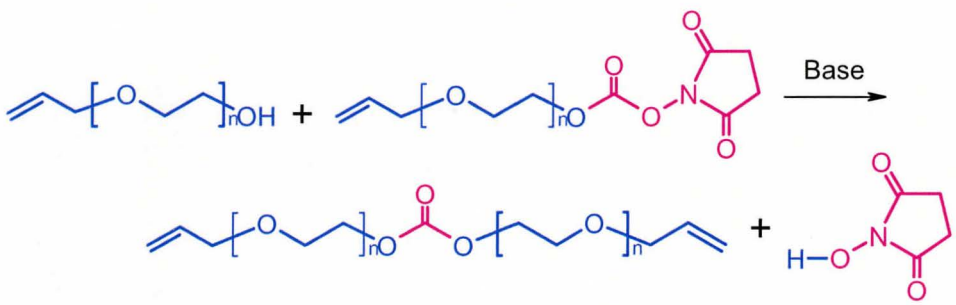

Scheme 2.4 Side reaction for synthesis of allyl-PEO-NHS

To investigate the relationship between the conversion and the reaction duration, a reaction in an NMR tube using acetonitrile-d_3 as the solvent was performed. The yield over time was calculated based on the integration of hydrogens following the ^{1}H-NMR assignment (Scheme 2.5). Figure 2.9 shows that the reaction started very rapidly right after mixing, and the conversion reached almost 100% after about 10h: most of the PEO

had been converted to allyl-PEO-NHS. The isolated yield was relatively low, which may be a consequence of the purification process. The byproduct was very sticky and relatively insoluble in toluene. Our new purification procedure leads to two layers: the byproduct-rich but product-poor layer (the top dark red layer) and the product-rich but byproduct-poor layers (the middle yellowish layer and the bottom solid layer). By separate purification of the two parts, the loss of the product ally-PEO-NHS can be significantly lowered. Our final yield was optimized at reach 80%.

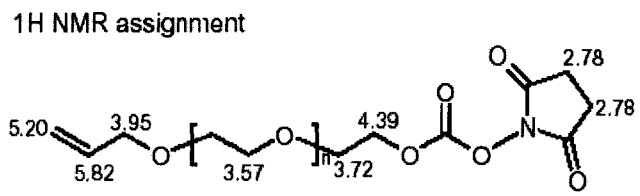

Scheme 2.5 ^{1}H NMR assignment of the protons on allyl-PEO-NHS

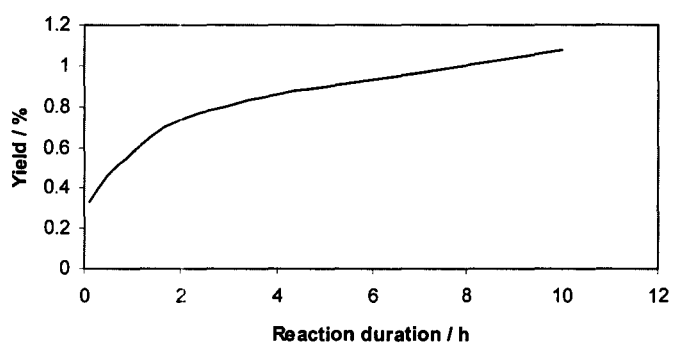

Figure 2.9 The conversion of allyl-PEO-NHS over time at room temperature using acetonitrile as the solvent

2.3.3.1.2. Direct hydrosilylation with allyl-PEO-NHS

In order to obtain an activated silicone surface, SiH surfaces were direct hydrosilyzed with ally-PEO-NHS as Scheme 2.6 showed. The NHS was successful tethered onto silicone surfaces but the results were inconsistent time after time due to the easy hydrolysis of ally-PEO-NHS. This is exacerbated by the hydroscopicity of PEO. Thus, while the process to create NHS functional surfaces is effective, reproducibility wasn't as high as desired and the stability of the surface to hydrolysis was limited.

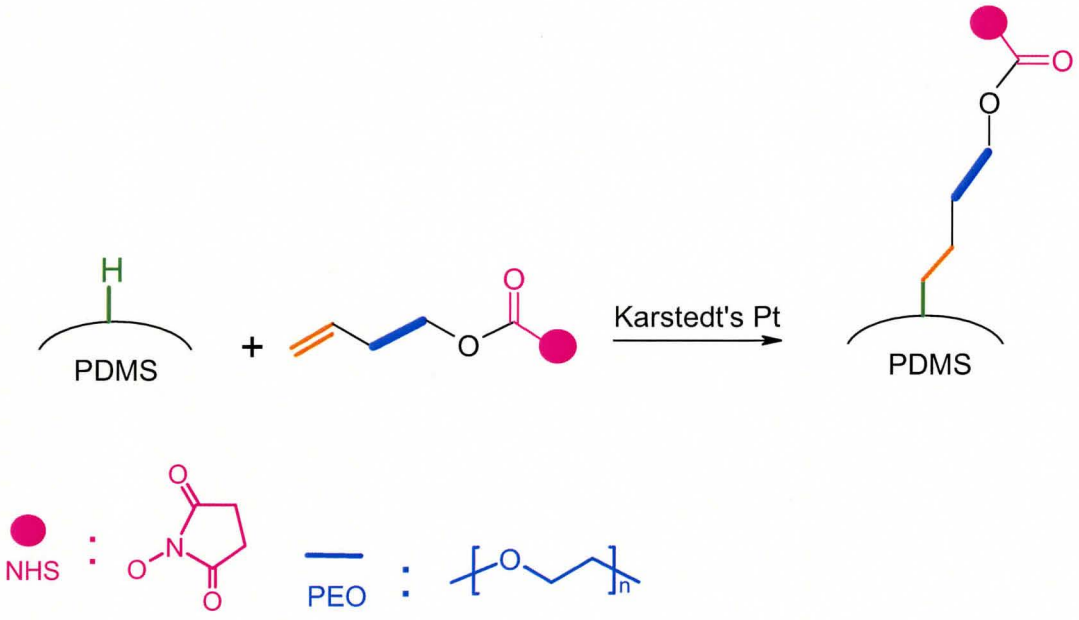

Scheme 2.6 Hydrosilylation of SiH surface with allyl-PEO-NHS

2.3.3.2. Hydrosilylation with allyl-PEO-OH followed by reaction with di-NHS

The FTIR spectra of surfaces from every modification step were shown in Figure 2.10.

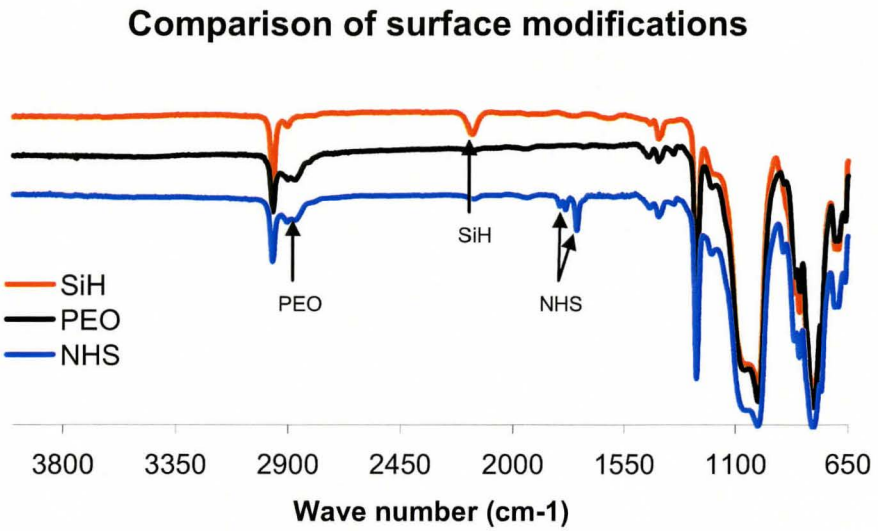

Figure 2.10 FTIR spectra of the PDMS surfaces after different modification

2.3.3.2.1. Hydrosilylation with allyl-PEO-OH

The efficiency of a reaction sequence usually correlates to the number of steps involved. It was thus anticipated that a direct process would be more efficient. As noted above, this hypothesis is challenged by the relatively facile hydrolysis of the NHS groups even after being tethered to the surface. Grainger has similarly noted this problem on DNA microarrays.[4,6,10] To find a more efficient and reproducible route to NHS surfaces, an alternative strategy was developed that involved two steps, the first of which was hydrosilylation with allyl-PEO as showed in Scheme 2.7 and the second involved reacting the PEO-tethered surface with di-NHS carbonyl. This second process can be done immediately prior to grafting of other biological species to the surface.

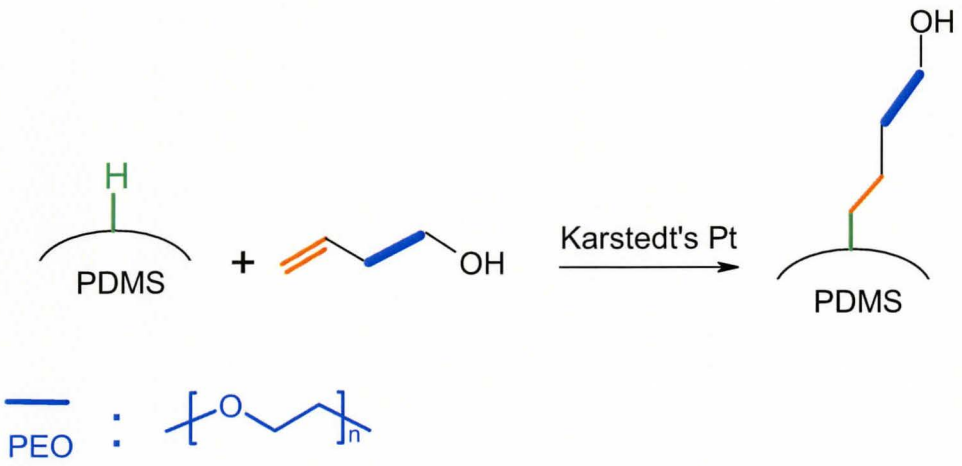

Scheme 2.7 Hydrosilylation of SiH surface with allyl-PEO-OH

These two reactions were optimized. The effective hydrosilylation time was first investigated by running the reaction time from 1h, 2h and 10h. It was shown in Figure 2.11 that there was little difference after 1 hour reaction time: therefore, 2 h was used for all subsequent reactions to allow for sufficient hydrosilylation.

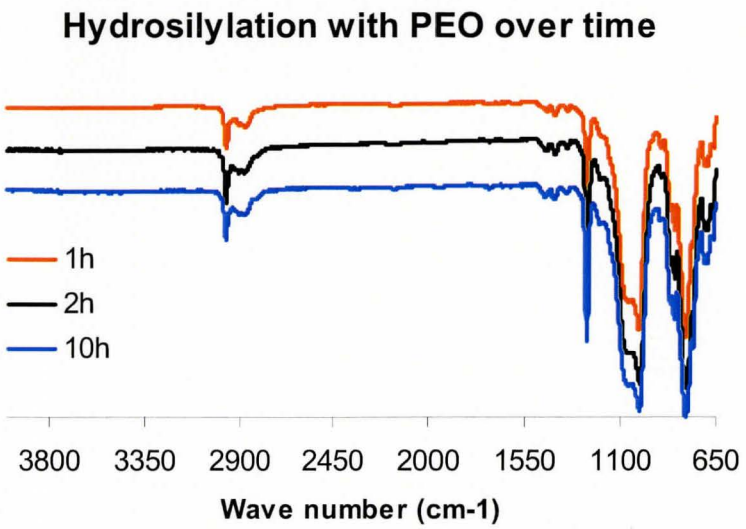

Figure 2.11 FTIR spectra of the PEO-surfaces made by hydrosilylation with allyl-PEO-OH over time varied from 1h to 10h

2.3.3.2.2. Reaction of PEO-tethered surfaces with di-NHS

The reaction of PEO-tethered surfaces with di-NHS was optimized according to Scheme 2.8. The reaction was performed for 2h, 5h and 20h, respectively. There was little obvious difference in the efficiency of the reactions based on the FTIR spectra (Figure 2.12). Therefore, 2h was carried out for this reaction to tether the NHS groups on the surfaces. Using a two step process resulted in the use of much less di-NHS carbonyl, and led to higher reaction yields. The two step process is a much more economical way considering the costliness of di-NHS and the consumption of time. More importantly l, there is no need to worry about the synthesis (relatively low yield), purification (long period), and shelf life (hydrolysis before hydrosilylation) of the critical compound used in the single step process, allyl-PEO-NHS.

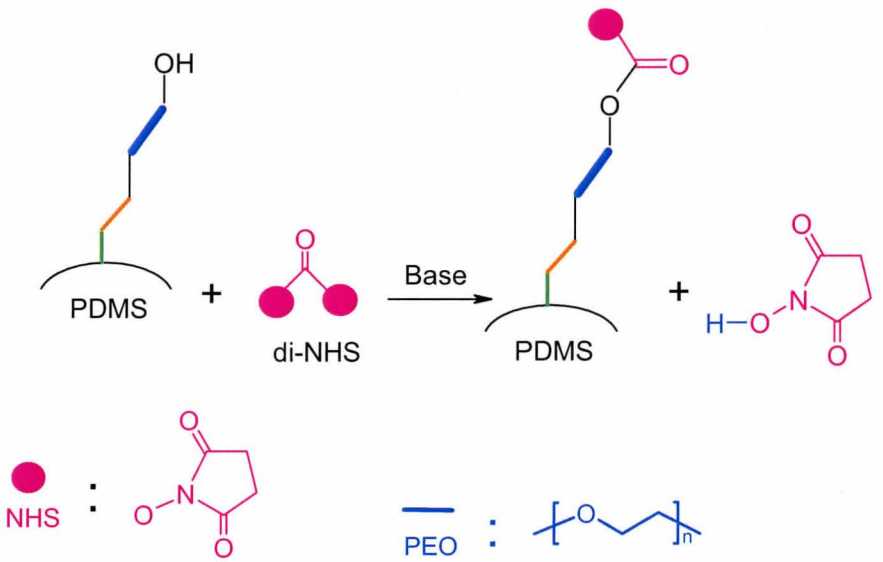

Scheme 2.8 Reaction for tethering NHS group on the PEO-grafted PDMS surface

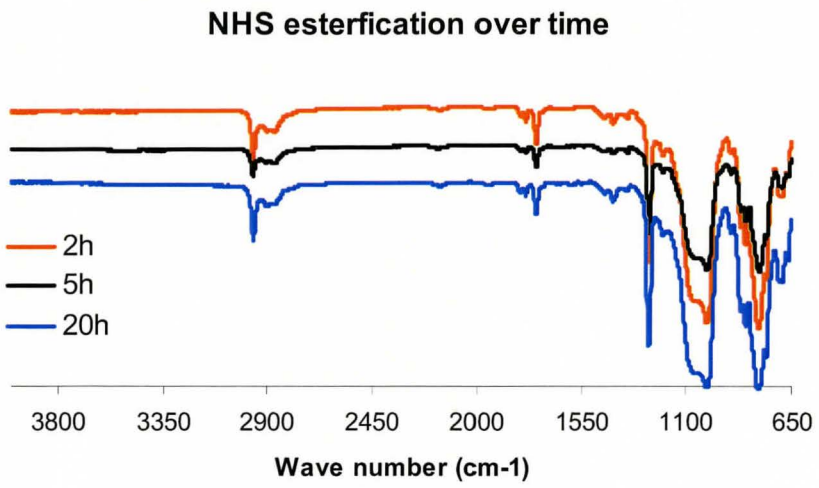

Figure 2.12 FTIR-spectra of the NHS-surface produced from the reaction of PEO-surface and di-NHS at various reaction times (from 2h to 20h)

2.3.4. Surface morphology

2.3.4.1. Profilometer

The roughness of the surfaces was observed using an optical profilometer. Representative pictures of the different surfaces are shown below (Figure 2.13). There were some variations from surface to surface even for those prepared by the same method. However, there was generally an increase in surface roughness after modification with PEO/NHS. As previously described, the silicone surface roughness was initially increased after erosion and/or polymerization with TfOH and DC1107. After hydrosilylation using allyl-PEO-OH, a new surface layer was built up and the graft density and loci of grafting may be affected by the morphology of the Si-H surface layer. Subsequently, the PEO surface layer may further determine the morphology of the third layer, NHS layer, which can lead to and even rougher surface.

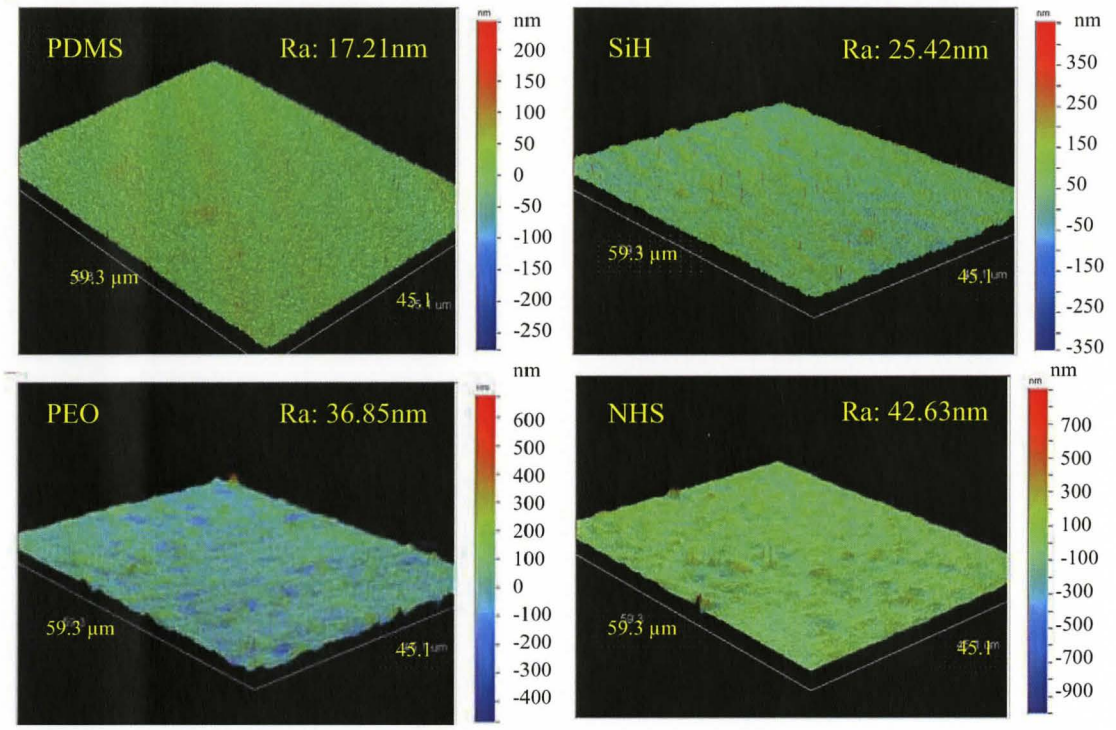

Figure 2.13 Pictures of PDMS, SiH, PEO and NHS surfaces taken with the optical profilometer (Note: Ra stands for the roughness by average)

2.3.4.2. Tapping Mode-Atomic Force Microscope (AFM)

Although AFM shares essential features with the profilometer, the tapping-mode AFM has become increasingly important because it can image surface structure on the nanometer scale.[11,12] Our silicone surfaces before and after modifications were also investigated by tapping mode-AFM. Both phase and height images are shown in Figure 2.14. From the height images, it can be seen that there were some protuberances on all the surfaces (the bright dots), including the one before modification, but the latter one displayed much less of them, which may be due to the surface defects. The phase images gave us more useful information is this case in that the topology of the surfaces can be

clearly seen. The intact silicone surface was fairly flat except some defects. The Si-H surface showed some dark areas, which may be caused by acid erosion, and some bright regions as well, where a second layer of Si-H polymerization in the presence of trace of water likely occurred. The presence of plenty of beads packed on the NHS surface suggested the surface morphology was significantly changed after tethering of NHS groups. These chancges can be also regarded as a clue that the NHS groups were attached onto the silicone surfaces.

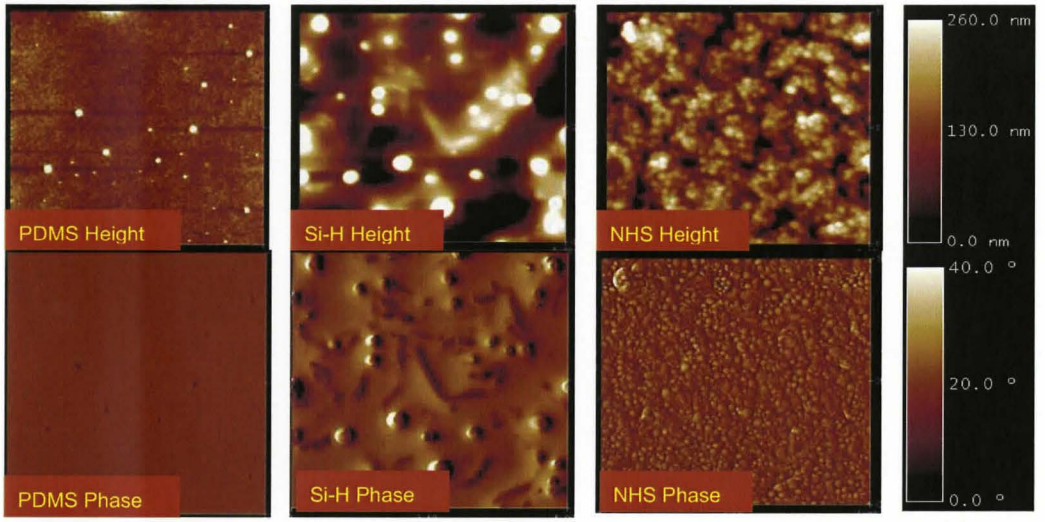

Figure 2.14 Tapping mode-AFM images of PDMS, SiH and NHS surfaces (5μm x 5μm)

2.3.4.3. X-ray Photoelectron Spectroscopy (XPS)

XPS has been shown to be a very useful tool for surface investigation at depths from 2nm to 10nm.[13,14] The XPS study was performed at take-off angles (ToA) 20° and 90° to investigate the surface composition. The following data are all at ToA 90° because there may be surface rearrangement in air or vacuum condition for hydrophilic surfaces. Table 2.1 listed the low resolution C(1s) content and also O(1s), Si(2p), N(1s) contents of

the surfaces before and after modification. As expected, the Si content was significantly decreased after modification with PEO and NHS. The carbon content was only slightly increased after tethering PEO, but the carbon content at 286.2eV (C-O)[7,15,16] in the high resolution spectrum was increased, which demonstrated the presence of PEO on the PEO and NHS surfaces. Nitrogen only appeared on the NHS surfaces, which indicated NHS was grafted onto the surface.

Table 2.1 XPS data for surface compositions

Surface	C (1s) Atom%					O (1s) Atom%	Si (2p) Atom%	N (1s) Atom%
	Total	284.4eV	286.2eV	288.4eV	288.8eV			
PDMS	48.0	41.8	4.7	1.5	0	25.7	26.2	0
SiH	42.5	36.8	4.5	1.3	0	30.9	26.6	0
PEO	48.6	26.2	19.0	1.6	0.6	25.6	16.3	0
NHS	53.1	22.0	28.3	0.7	2.7	30.3	15	1.6

The high resolution C1s spectra of the surfaces, as in Figure 2.15, allowed us to assign the different carbons based on their binding energies. There was no obvious difference between the PDMS and the Si-H surface spectra, which is reasonable since there was no obvious change in the carbon environment. The spectra of all the surfaces showed a huge peak at 284.5eV, which was assigned to the methyl carbons (C-H) attached to silicons in PDMS.[14] The dramatic peak at 286.2eV, corresponding to C-O species, appeared in the spectra of the PEO and NHS surfaces, which provided evidence of PEO being tethered on the silicone surface.[7,15,16] The carbons with binding energy of

288.8eV in the spectrum of the NHS surfaces were assigned to those of carbons in O-C=O. The carbons with binding energy of 287.8eV assigned to O=C-N species were not differentiated from O-C=O due to their similar concentration and close positions in the spectrum for NHS surfaces.[17]

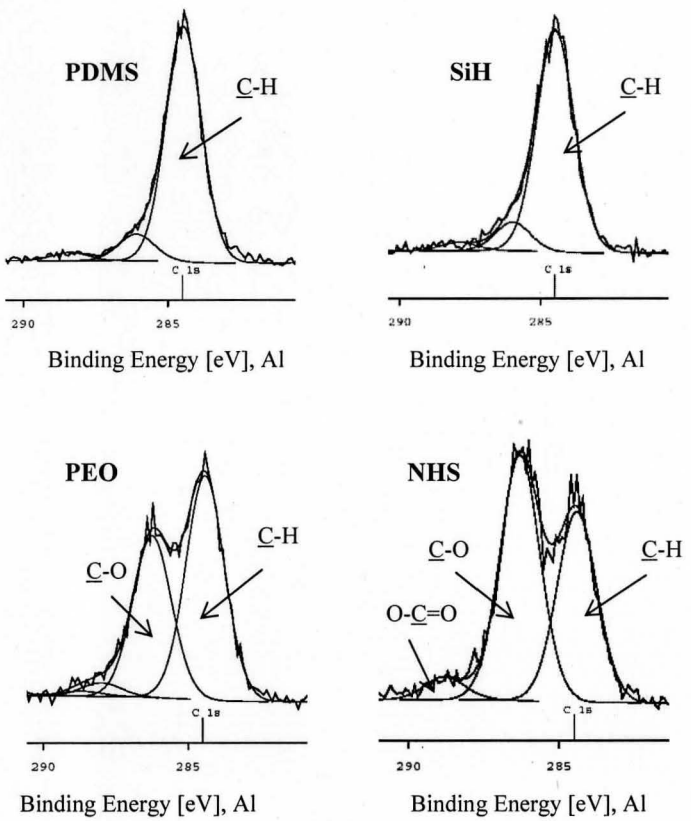

Figure 2.15 High resolution C1s XPS spectra of the PDMS surfaces (intact PDMS, modified with SiH, PEO, and NHS, respectively)

2.3.5. The functionality of the NHS-modified surface – Testing with Heparin

Heparin is an anticoagulant. It is used to decrease the clotting ability of the blood and to help prevent harmful clots from forming in the blood vessels.[18] Heparin will not

dissolve blood clots that have already formed, but it may prevent the clots from becoming larger and causing more serious problems.[19] It is often used as a treatment for certain blood vessel, heart, and lung conditions. Heparin is also used to prevent blood clotting during open-heart surgery, bypass surgery, and dialysis.[20] We therefore tethered heparin to the NHS modified surfaces.

In order to investigate if the heparin on the surface was still active and the heparin density and activity on the surface were examined. The density of the total heparin immobilized on the heparin-tethered surfaces was measured by a colorimetric method. Toluidine blue is a metachromatic dye, which can bind to heparin to form a heparin-dye complex.[21] Upon binding to heparin, the absorbance maximum of the dilute aqueous toluidine blue solution is shifted from 631nm to about 550nm, The decrease in absorbance at 631nm is dependant on the concentrations of the dye and the heparin in the solution. Therefore, the concentration of heparin can be determined by monitoring the solution absorbance at 631nm. A Hepanorm reagent kit was used to give the heparin activity standard curve (see supplementary materials) by Anti-Factor Xa method using UV/vis spectrophotometer. The absorption at 405nm of the surface contained solution was measured. The calibration curves for measuring heparin density and activity were both shown in the supplementary materials. A high heparin density of 6.83μg/cm*cm and the activity of 0.3442 IU/mL were obtained. These results demonstrate that the NHS-surface has very strong binding ability to heparin.

The study of the heparin activity on silicone surfaces provided insight on the interactions between this protein and the surface and the effects of the surface on this

protein. The method used in this study was also helpful on my following research on the collagen modified surfaces.

2.4. DISCUSSION

2.4.1. Surface Chemistry

Acids are known to be able to erode silicone surface by catalysis of the silicone equilibration reaction (depolymerization-polymerization). During this process, cyclic silicones D_4 and D_5 will be formed.[9] In the presence of a second silicone, copolymerization may occur, which makes the incorporation of functional groups on the silicone surface possible. Different solvents may have different effects on the erosion process when the second functional silicone is added, since only the reaction on the surface (not inside) is desired. The contact time with acid and the concentration of acid may influence the reaction extent on the surface. As expected, the nature of the solvents did affect the reactions on the surface. The good solvent, iPA, for silicones may help the acid erosion inside the surface by swelling the surface to some extent. Even though a much more intense Si-H band was obtained in the ATR-FTIR, the accompanying brittle surface due to the disruption of the bulk is not desirable. The poor solvent methanol instead led to much less opportunity for interior erosion, of course, it is also a consequence of contact time and acid concentration. Generally, longer contact times and more concentrated TfOH solutions allowed more reaction. In another words, the Si-H on the surface with more concentrated with time and TfOH concentrations. Interestingly, without adding the Si-H functional silicone, the roughness of the eroded surfaces saw no

apparent changes as a function of contact time and acid concentration. This indicated that in the presence of the functional silicone a second surface layer may be formed on the eroded surface. This may result from traces of water in the reaction system, which leads to reaction with some of the Si-H groups, generating Si-OH; further crosslinking of Si-OH forms Si-O-Si linkages. Therefore, an uneven double layer may be built up, making the surface rougher.

2.4.2. Strategies for Surface Modification

Two different strategies for making NHS surfaces were compared. The first one involved the synthesis of allyl-PEO-NHS and the direct hydrosilylation with allyl-PEO-NHS on the Si-H surfaces, while the second one used the reaction between di-NHS carbonyl and the hydrosilylated Si-H surfaces with allyl-PEO-OH. Both strategies for making NHS-tethered surfaces worked, but the former one using allyl-PEO-NHS had poor reproducibility and efficiency. First, the synthesis and purification of allyl-PEO-NHS took more than one week. Second, the di-NHS carbonyl is an expensive compound, and an excess, at least 4 molar equivalents when compared to allyl-PEO-OH, had to be used to minimize formation of the PEO dimer by-product. The purification steps further decreased the final yield. Moreover, this product has a high affinity for water because of the hydrophilic PEO attached, which makes the hydrosilylation less efficient: the product can easily hydrolyze before the hydrosilylation step. The newly developed method was more efficient on all counts: less time and much less di-NHS were necessary to achieve improved synthetic yields. Although the second method involves two steps, it is actually

more efficient. Quantities of of PEO-modified silicone surfaces can be prepared by hydrosilylation and stored: there is no need to worry about hydrolysis. When an NHS-modified surface is needed, it can be obtained in 2 or 3h. Most importantly, a higher density of NHS groups on the surface was obtained by this strategy based on the ATR-FTIR spectra (the spectra obtained from the first method was not listed in the thesis, it is just less intense than that from the second one).

To ensure that the NHS surface remained reactive to further reaction, heparin was tethered to the surface. The heparin density and activity suggested the NHS-modified surface is an efficient support for silicone biomaterials.

The surface morphology examined by profilometer and tapping-mode AFM indicated the surface became rougher and rougher after modifications as expected, which provides indirect evidence that multilayers may be built up on the surface. The XPS data further supported this, due to the presence of nitrogen on the NHS surface, and the appearance and the high intensity of the peak for C-O in the high resolution binging energy spectra of C(1s) for both PEO and NHS surfaces.

2.5. CONCLUSION

Surface roughness can be induced by the acid catalyzed reaction of a PDMS elastomer surface with poly(methylhydrosiloxane). It is possible that the increase in roughness is a consequence of further polymerization of the Si-H groups on the eroded surface, rather than erosion inside of the surface. Two strategies for modifying silicone surfaces with NHS groups were used. The one step method for making NHS-surfaces was

subject to hydrolysis on storage. A more effective route to NHS surfaces, which are active towards heparin binding, is to activate OH groups on the surface just before reaction with diNHS. The process uses the expensive NHS groups more efficiently and leads to a higher surface density of NHS.

2.6. REFERENCES

(1) Aprahamian, M.; Lambert, A.; Balboni, G.; Lefebvre, F.; Schmitthaeusler, R.; Damge, C.; Rabaud, M. *J Biomed Mater Res* **1987**, *21*, 965-77.

(2) Shimizu, Y.; Abe, R.; Teramatsu, T.; Okamura, S.; Hino, T. *Biomater Med Devices Artif Organs* **1977**, *5*, 49-66.

(3) Olde Damink, L. H.; Dijkstra, P. J.; van Luyn, M. J.; van Wachem, P. B.; Nieuwenhuis, P.; Feijen, J. *Biomaterials* **1996**, *17*, 765-73.

(4) Xia, N.; Hu, Y.; Grainger, D. W.; Castner, D. G. *Langmuir* **2002**, *18*, 3255-3262.

(5) Chen, H.; Chen, Y.; Sheardown, H.; Brook, M. A. *Biomaterials* **2005**, *26*, 7418-24.

(6) Gong, P.; Grainger, D. W. *Surf Sci* **2004**, *570*, 67-77.

(7) Chen, H.; Brook, M. A.; Sheardown, H. D.; Chen, Y.; Klenkler, B. *Bioconjug Chem* **2006**, *17*, 21-8.

(8) Laemmel, E.; Penhoat, J.; Warocquier-Clerout, R.; Sigot-Luizard, M. F. *J Biomed Mater Res* **1998**, *39*, 446-52.

(9) Brook, M. A. *Silicon in Organic, Organometallic, and Polymer Chemistry*; Wiley: New York, 2000.

(10) Gong, P.; Grainger, D. W. *Biomed Sci Instrum* **2004**, *40*, 18-23.

(11) Radmacher, M.; Tillamnn, R. W.; Fritz, M.; Gaub, H. E. *Science* **1992**, *257*, 1900-5.

(12) Wang, L. *Appl Physics Lett* **1998**, *73*, 3781-3783.

(13) Chang, M. C.; Tanaka, J. *Biomaterials* **2002**, *23*, 3879-3885.

(14) Beamson, G.; Briggs, D. *High resolution XPS of organic polymers: the Scienta ESCA300 database*; Wiley: Chichester, 1992.

(15) Chen, H.; Brook, M. A.; Sheardown, H. *Biomaterials* **2004**, *25*, 2273-82.

(16) Chen, H.; Zhang, Z.; Chen, Y.; Brook, M. A.; Sheardown, H. *Biomaterials* **2005**, *26*, 2391-9.

(17) Cheng, Z.; Teoh, S. H. *Biomaterials* **2004**, *25*, 1991-2001.

(18) Bjork, I.; Lindahl, U. *Mol Cell Biochem* **1982**, *48*, 161-82.

(19) Folkman, J.; Langer, R.; Linhardt, R. J.; Haudenschild, C.; Taylor, S. *Science* **1983**, *221*, 719-25.

(20) Cesaretti, M.; Luppi, E.; Maccari, F.; Volpi, N. *Glycobiology* **2004**, *14*, 1275-84.

(21) Ander, B.; Karlsson, A.; Ohrlund, A. *J Chromatogr A* **2001**, *917*, 105-10.

CHAPTER 3 – SURFACE MODIFICATION WITH COLLAGEN BY COVALENTLY BONDING AND ITS BIOLOGICAL PROPERTIES[1]

3.1. INTRODUCTION

3.1.1. Properties and Applications of Collagen

Collagen proteins are comprised of polypeptide chains (α-chains) that form a unique triple-helix structure. Each α-chain has a repeating amino acid structure of Gly-X-Y, where Gly is glycine and X-Y can be any amino acid pairing, though most often are proline and hydroxyproline.[1] In biological systems, collagen fibers provide the major mechanical support for cell attachment, thus developing the shape and form of tissues.[1] Collagen, one of the main proteins of the extracellular matrix, has received considerable interest because of its potential for use, in several types of morphologies, in various medical applications.[2] Collagenous materials developed for applications in dermatology, orthopedics, or oral surgery, have been applied in tissue engineering, for instance.[3]

Even though collagen itself can be an efficacious biocompatible material, it has certain limitations. For example, it may not have sufficient mechanical strength for certain applications. By contrast, synthetic polymers often have enough mechanical strength, but poor biocompatibility. Therefore, materials obtained by the combination of collagen and synthetic polymers may prove useful in the biomedical field by providing

[1] I would like to thank Diana Morarescu of Dr. Heather Sheardown's group, Chemical Engineering, McMaster University, for performing the cell culture assays and the collagen staining. Otherwise, all the experimental work and the preparation of this document were completed by me.

both the biocompatibility and better mechanical strength. Collagen has been employed as a modifier of synthetic biomaterials by blending,[4-7] surface coating,[8,9] copolymerization by photo-irradiation in the presence of vinyl monomers,[10] and as a reagent covalently grafted via crosslinkers.[11] The properties of collagen grafted polymer materials and their interactions in biological tissues are not well understood.

3.1.2. Silicone Surfaces

Silicone (PDMS) elastomers have been used extensively in medical implants and biomedical devices due to their good blood compatibility,[12-14] low toxicity,[14-16] and good thermal stability.[17,18] These optically transparent elastomers have water-repellency, low electrical conductivity[19,20] and are very easy to fabricate into complex structures,[21] which makes this material attractive for use in studies of material science and cell biology.[22-24]

3.1.3. The Need for an Easily Prepared, Stable Combination of Silicone Surface and Collagen

It is generally accepted that covalent immobilization is superior for generating stable collagen coatings when compared to physical adsorption. Müller et al. have developed a method for covalent immobilization of collagen on stainless steel using a combination of the silane-coupling agent aminopropyl triethoxysilane and the linker molecule *N,N'*-disulphosuccinimidyl suberate, which was performed in acetic acid.[25] The covalent immobilization of collagen on silicone surface has also been reported.[26-28] Okada and his colleague grafted collagen through covalent bonding, at pH3, between the amino groups of collagen and carboxyl groups that were introduced to the silicone

surface by plasma-induced graft polymerization of acrylic acid.[26,28] However, it is well known that the functional groups on plasma treated surfaces are very unstable and they need to be modified quickly, which makes the subsequent reactions less reproducible. The covalent bonding of collagen to epoxy-activated silicone surfaces was studied by Wallace and colleagues at pH7-8, but only low levels of surface epoxy functionalization was achieved.[27]

A more efficient way to covalently bind collagen to silicone could be the use of NHS ester chemistry through a heterobifunctional polyethylene glycol (PEO) spacer. This method has been used for other proteins or DNA immobilization.[29-31] Our objectives were to develop analogous strategies to covalently immobilize collagen molecules onto silicone surfaces, which would be easier and more efficient than reported methods. At the same time, these studies would provide the opportunity to investigate the parameters affecting the collagen-grafting reaction and study the biological response to this biomaterial via in vitro cell culture.

3.1.4. Difficulties and Our Strategies

It is well known that hydrophobic surfaces tend to adsorb large amounts of proteins compared to hydrophilic ones, due to the hydrophobic effect. When proteins contact the hydrophobic surface, the hydrophobic amino acid residues become exposed to the surface through rearrangement, and then bind there: the proteins denature.[32] There could be many ways or chemistries to immobilize proteins on the hydrophobic silicone surface covalently, but once bound, they become denatured. An insulating spacer was

used as it was expected to supply a water layer between the protein layer and the silicone surface so that a biologically active protein bound surface may be obtained. A mild crosslinker like NHS may help retain the activity of proteins.[33] When doing NHS-ester chemistry for immobilization of proteins, the amine groups on the protein are expected to have stronger nucleophilicity in neutral or basic conditions than in acidic conditions. The best reaction conditions for the immobilization of proteins are thought to require soluble proteins. However, collagen is distinct from other proteins due to its unique triple-helical structure comprising three polypeptide chains (α-chains), which makes it only partly soluble in acid, conditions under which the amine groups are not nucleophilic. On the other hand, under alkaline conditions, where the nitrogens are more nucleophilic, collagen precipitates from solution. Additionally, under more alkaline conditions, hydrolysis of the NHS groups will compete with amide formation. Attempting to increase the amount of dissolved collagen by diluting the solution isn't helpful, because water is a competing nucleophile. Our goal was to overcome these difficulties and make the NHS-ester chemistry work for collagen. Our strategy was to increase the pH of the collagen solution, while making the collagen as concentrated as possible to do the reaction with as many active amine groups as possible.

There are more than 20 genetically distinct collagens existing in animal tissues. Type I collagen is the major component of bovine and human collagen and it is found throughout the body except in cartilaginous tissues. Therefore, collagen type I was selected as our modifying material.

3.2. EXPERIMENTAL SECTION

3.2.1. Materials and Methods

3.2.1.1. Materials

Collagen (bovine corneum, 97% type I, ~3% type III, collagen (~3mg/mL) in pH2 HCl) was a gift from Inamed Corp. The method for preparing *N*-hydroxysucccinimide ester (NHS) surfaces was described elsewhere (Chapter 2.2.4.2). The Membra-CEL dialysis tubing (MWCO 14KD, Serva Electrophoresis, Germany) was boiled for half an hour before use. All water used was purified by treatment in a reverse osmosis unit followed by a Millipore unit (18 mΩ resistivity).

3.2.1.2. Instrumentation

3.2.1.2.1. Attenuated Total Reflection Fourier Transform Infrared (ATR/FTIR)

The IR spectra (16 scans at 4 cm^{-1} resolution) of the PDMS surfaces modified with collagen were obtained using a Fourier transform IR spectroscopy (Bio-Rad, FTS-40 using a fixed 45° angle attenuated total reflectance (ATR, ZnSe) cell attachment. Thus, the collagen modified silicone samples were placed on an ATR cell and the FTIR scans were obtained. The background was run when no sample was placed in the ATR cell.

3.2.1.2.2. Water Contact Angle

The wettability by water of PDMS surfaces modified with collagen and those modified with polyethylene glycol (PEO) followed by NHS modification (the surfaces

before modification with collagen) were determined using KRŰSS (USA) drop shape analysis system DSA 10 at temperature 20 °C. The instrument was equipped with a flat-tipped needle with 0.525mm outside diameter. Water contact angles were measured at ambient humidity using the sessile drop method. Three approximate 0.02 ml water drops were measured on each surface. The data was collected as a function of wetting time for the surfaces. Captive bubble contact angles of the surfaces were measured using Ramé Hart NRL C.A. goniometer (Mountain Lakes, NJ). Three to five 0.02 mL air bubbles were measured on each surface. The data for captive bubble contact angles were obtained by taking the average of three to five samples on each surface.[31]

3.2.1.2.3. X-ray Photoelectron Spectroscopy (XPS)

The XPS measurements were performed on a Leybold (Specs) MAX 200 XPS system utilizing a monochromatic Al Kα X-ray source operating at 15 kV and 20 mA. The spot size used in all experiments was 2x4 mm^2. Survey scans were performed from 0 to 1000 eV. The low resolution and C1s high-resolution analyses were performed with a scan width of 20eV. Angle-dependent XPS data were collected at takeoff angles (ToA) of 20°, and 90° to allow the analysis of compositions from 2nm to 9nm depth. The ToA was defined as the angle between the surface normal and the axis of the analyzer lens system[31]. Specslab (specs Gmbh, Berlin) was used to perform the spectral fitting on the spectra.

3.2.1.2.4. Time-of-Flight Secondary Ion Mass Spectrometry (TOF-SIMS)

ToF-SIMS experiments were carried out on a ToF-SIMS IV (ION-TOF GmbH, Műnster, Germany) using a 'deep freezing' technique, equipped with a heating and cooling stage to analyze the wet surfaces. Surfaces were pre-incubated in water to allow for hydration. The wet surfaces were put in a copper probe (14 x 16 x 4 mm^2) with a central well and mounted in the heating-cooling stage. The copper probe was tightly screwed to allow good heat transfer. After the transfer chamber was thoroughly purged with N_2, the specimens were frozen using liquid N_2 to ~-130 °C and then vacuum was applied. The temperature was held at ~-120 °C, when the specimens were transferred to the analysis chamber. The spectra were obtained with the Ga source (25keV), which was operated in a high mass resolution mode. The acquisition time was set at 20s and the spectra were acquired over an area of 100x100μm^2. The surfaces were warmed up in 5 °C increments until the surfaces were lyophilized (as indicated by the disappearance of water clusters in the positive ion spectrum). The sample position was then moved in order that the beam touched an undamaged area. Both the positive and negative spectra were recorded at -96 °C followed by recording at room temperature when warmed up. The spectra were obtained at 100 scans over and area of 500 x 500 μm^2.

3.2.1.2.5. Profilometer

The roughness of the surfaces modified with collagen was measured using a Veeco WYKO NT1100 Optical Profiling System (Mode: VSI, Objective 50X, FOV 2.0X).

3.2.1.2.6. Atomic Force Microscope (AFM)

Tapping mode AFM measurements were performed with a NanoScope IIIa with multi-mode. The etched silicon probes (Digital Instruments), with cantilever lengths of 116μm and resonance frequencies of about 270 kHz, were used. A sharp tip having a radius 10 nm, was selected for this study. Images were recorded with a slow scan rate (0.5 Hz).

3.2.1.2.7. Microscope

The pictures of cell culture were taken by a ZEISS Axiovert 200 microscope at 20X using AxioVision 3.1 program.

3.2.1.3. Preparation of Polydimethylsiloxane (PDMS) Surfaces Modified with Collagen

The PDMS surfaces modified with collagen were prepared via the active *N*-hydroxysucccinimide ester reaction with the amine groups of collagen. The sensitivity of the reaction to pH was examined at pH2, 4, 5.5, 6.6, 7, 7.4, 8 and pH9, ionic strengths ranging from 50mM to 200mM, and at collagen concentrations ranging from 3mg/mL to 0.3mg/mL (3mg/mL, 1.5mg/mL, 1mg/mL, 0.75mg/mL, 0.5mg/mL, and 0.3mg/mL).

The most concentrated collagen solutions (3mg/mL) at pH7.4 and pH8.0 were obtained by dialysis with 100-fold buffer of the target pH for 2h. The exact concentration was not measured since the volume didn't change a lot after dialysis. The less concentrated collagen solutions (below 3mg/mL) were achieved by diluting the original collagen solution using the buffers of target pHs with the same ionic molarity (KCl buffer at pH2, potassium hydrogen phthalate buffers at pH4 and pH5.5, phosphate buffered

saline (PBS) at pH6.6, 7.0, 7.4, 8.0, and pH9.0). The reaction was allowed to proceed overnight. Each surface was then thoroughly washed with diluted HCl (~pH 4.0) 3-4 times (5 mL) followed by washing with Milli-Q water 3-4 times (5 mL), and then blown dry with nitrogen for testing by Attenuated Total Reflection Fourier Transform Infrared (ATR/FTIR). After the reaction, the surfaces were quenched with excess of tris(hydroxymethyl) aminomethane Buffer (Tris buffer) (pH 8) overnight to remove all the remaining NHS groups and washed with Milli-Q water 3-4 times (5 mL). The surfaces were blown dry with nitrogen followed by vacuum. The collagen covalently bound surfaces were stored at 4 °C. ATR/FTIR (neat, cm^{-1}): 1668 (amide I, C=O stretch), 1556 (amide II, C-N stretch, N-H bend combination)[34].

3.2.1.4. *In vitro* Cell Culture Assay

An immortalized human corneal epithelial cell line was provided by Dr. May Griffith's lab at the University of Ottawa. Corneal epithelial cells were cultured using keratinocyte serum-free medium (KSFM) with epidermal growth factor (EGF) and bovine pituitary extract (BPE) supplements (Gibco, No. 17005-042). Disinfection was provided by adding 10μL/mL penicillin/streptomycin (Gibco, No. 15140-122) and 1μL/mL gentamicin (Gibco, No. 15710-064) supplements. The surfaces modified with collagen were incubated in KSFM supplemented with penicillin/streptomycin and gentamicin for 24 h. The surfaces were then rinsed twice with the medium. The cells ($1x10^4$ cells in 40μL of medium, counted using a hemocytometer) were seeded on the surfaces followed by adding 250μL of medium 15 to 20 minutes after seeding. The

medium was changed every 2 to 3 days during the experiments. Corneal epithelial cells reached confluence by 4 to 5 days.

3.2.1.5. Collagen Staining with Sirius Red Dye

The method used below is related to that used by Doyle.[35] Sirius red dye solution was prepared by dissolving 1g of Sirius red F3B (Direct Red 80) (Raymond A. Lamb, London, UK) in 100mL saturated aqueous picric acid (HD supplies, Hemel Hempstead, UK). Collagen solutions were prepared by dilution with 0.5M acetic acid. To determine the binding of the dye to collagen, 250 μL of the 1% Sirius Red in picric acid solution was added to the wells of a 48 well Multiscreen®, filtration plate (0.45 μm pore size Millipore, Watford, UK) followed by 750 μL collagen solution at concentrations 0~1.5mg/ml in 0.5 M acetic acid. The plate was then sealed and agitated at room temperature for 30 min. The solution was vacuum aspirated and the precipitate was washed 3 times (200 μL) with 0.05 M acetic acid. The precipitate was resuspended in 250 μL 0.5 M NaOH for 30 min with agitation. Aliquots of the solution were transferred to a 96 well plate and the absorbance at 540 nm was determined using a Bio-Rad 550 Microplate reader. Calculated using the collagen stain calibration curve (Figure s3), the average collagen density of 1.0 $\mu g/mm^2$ on the surface was obtained.

3.3. RESULTS

As described in Chapter 2, NHS-surfaces were prepared by the hydrosilylation of a silicone elastomer bearing an Si-H rich surface, with allyl terminated poly(ethylene

oxide), followed by the reaction with *N,N'*-disuccinimidyl carbonate. The resulting polymer surface has NHS groups, and an insulating PEO layer that protects the protein from contact with the silicones.

Many attempts were made to graft the collagen onto these surfaces using a variety of different conditions, as shall be discussed below. One of the challenges of this work was the development of a suite of techniques that would report the presence of collagen on the surface. These included infrared, which shows the presence of newly formed amide bonds, staining techniques and contact angle goniometry. An overview is presented, followed by the details of the specific experiments.

ATR-FTIR is particularly diagnostic in demonstrating the presence of covalent linkages at the surface. Three signals are particularly important: at 1668 and 1556 cm^{-1}, grafted collagen; at 1743 and 1789 cm^{-1}, the surface bound NHS ester, and at 1668 cm^{-1}, the amide. Figure 3.1 shows ATR-FTIR spectra of the pre-modification and post-modification collagen surfaces. After chemical modification with collagen, the C=O bands for NHS at 1743 cm^{-1} (N-C=O) and 1789 cm^{-1} (O-C=O)[36] almost disappeared. New bands appeared at 1668 cm^{-1} and 1556 cm^{-1}, which are attributed to amide I (C=O stretch) and amide II (C-N stretch, N-H bend combination) in collagen respectively.[34] When the modified surfaces were quenched with 50mM tris buffer (pH8.0) overnight, all NHS bands disappeared.

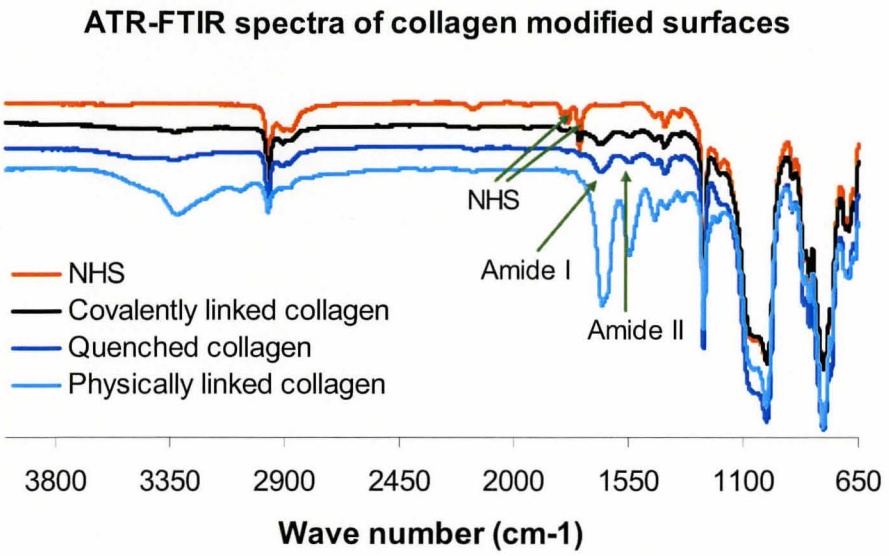

Figure 3.1 'Quenched collagen' stands for the modified PDMS surface with collagen being quenched afterwards with tris buffer (pH8.0) to get rid of the unreacted NHS groups. 'Physically linked collagen' was obtained by spreading a layer of collagen solution on top of poly(ethylene glycol) (PEO) modified PDMS surface followed by evaporating the water on the surface.

3.3.1. Collagen Solubility

As mentioned previously, collagen is usually soluble only in acidic solutions. When the basicity of the solution was increased in our experiment, collagen started precipitating at pH 5.5 (the solution became opaque and partly gelated). This phenomenon continued when the pH was further increased to pH9 using concentrated NaOH. When the opaque solution was diluted with up to 10-fold 50mM PBS, it became clearer, but still contained some precipitated collagen.

3.3.2. Effects of pH, Ionic Strength and Concentration of the Collagen Solution on Amide Formation

It was assumed that the optimum yield for collagen grafting would occur with soluble collagen, but unfortunately it was insoluble under conditions of maximum nucleophilicity, alkaline conditions. Although it was recognized these were no optimal conditions, we nevertheless attempted the experiments. Somewhat surprisingly, even with the problems of two phase reactions, some collagen did bind to the surface at higher pH. To get better results for improving the yield of amide formation, the reaction between the active *N*-hydroxysuccinimide-ester (NHS ester) and the amine groups of collagen was carried out under a variety of conditions, in particular pH, buffer concentration, and total ionic strength. Each is considered in turn.

3.3.2.1. pH Functionality

The NHS ester acylation reaction with collagen was carried out under different pH conditions ranging from pH2 to pH9 according to Scheme 3.1.

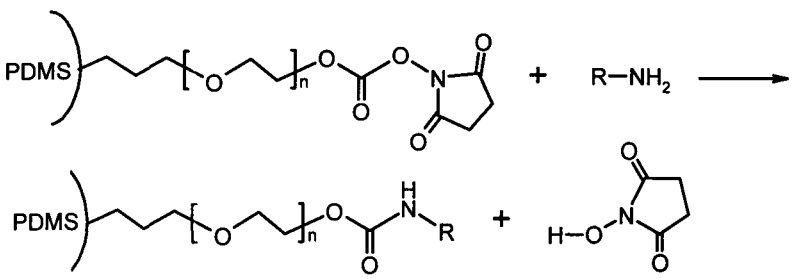

Scheme 3.1 Acylation of NHS-modified PDMS surface with collagen (R-NH_2 represents the amines groups on the collagen chain ends or its sides)

The NHS surfaces were first incubated overnight in the 3mg/mL collagen solution at various pHs adjusted using concentrated NaOH without adding a buffer. Unfortunately,

no reaction was observed by ATR-FTIR. The reacted solution was rechecked thereafter for the pH. It was found that the pH was no longer the original pH as initially adjusted for solutions at pH7 and above. The pH decreased to below 7.

There are two possible origins for the poor binding performance; the poor solubility of collagen, the other is the observed pH change. It was found afterwards that the collagen solution adjusted with NaOH solution couldn't achieve equilibrium even after 5 hours (the pH kept decreasing), which might be associated with the slow titration of some internal acid groups in collagen molecules. The presence of CO_2 could be another factor that led to pH change.[37]

In order to avoid the variability in pH, the collagen solution was diluted with the same volume of 50mM buffers at various pH and the results are shown in Figure 3.2.

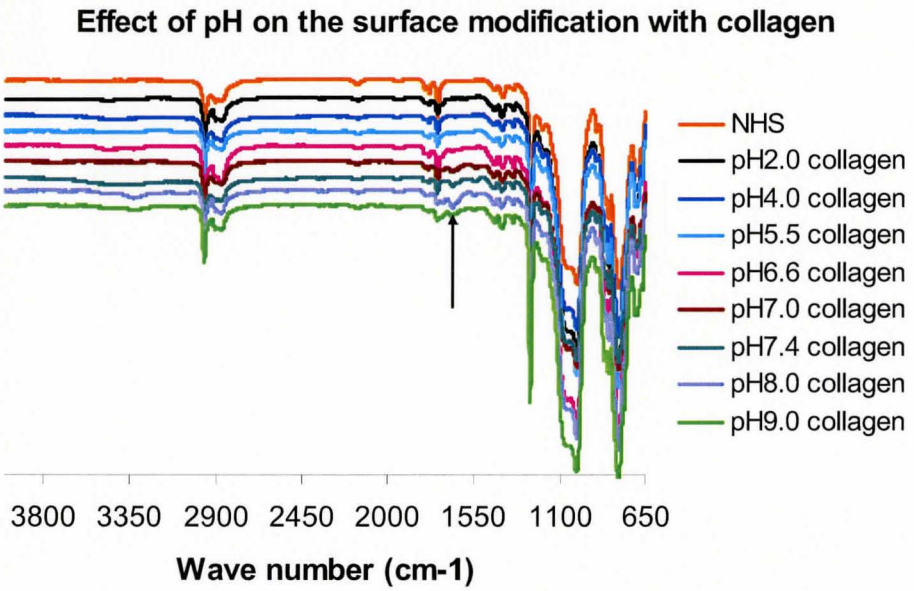

Figure 3.2 FTIR spectra of the surfaces before and after modification with collagen at different pH

From the ATR-FTIR spectra of the resulting surfaces in the range studied, as shown in Figure 3.2, the reaction to graft collagen to activated silicone took place only at pH7 and above. This reactivity matched our prediction that near neutrality nucleophilic amine groups start to form, and their concentration increases with an increase in the solution basicity. However, upon further increasing the pH, the desired reaction with the amine group increases, but so does undesired hydrolysis. The optimized reaction conditions involved pHs in the range of pH 7.4 and 8.0.

3.3.2.2. Ionic Strength

As shown above in Figure 3.2, the amide bands obtained at 50mM buffered collagen solution in FTIR were not very intense. Therefore, increasing the buffer capacity became another strategy to operate at a higher pH with higher concentration collagen solutions. PBS of ionic strength 50~200mM was used to adjust the pH by both dilution and dialysis of the collagen solution.

Table 3.1 Collagen solution variations on investigating its solubility

Solution No.	A1	A2	A3	A4
Ionic strength(mM)	50	50	100	100
PBS pH	8.0	8.0	8.0	8.0
Collagen concentration(mg/ml)	3.0	1.5	3.0	1.5
Solution No.	B1	B2	B3	B4
Ionic strength(mM)	50	50	100	100
PBS pH	7.4	7.4	7.4	7.4
Collagen concentration(mg/ml)	3.0	1.5	3.0	1.5

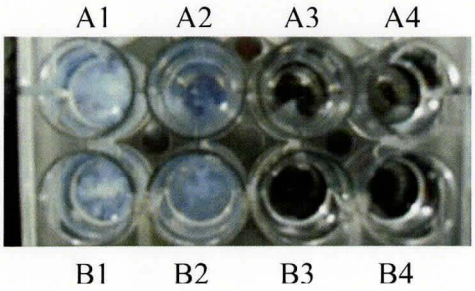

Figure 3.3 Pictures of collagen solutions adjusted using 50mM and 100mM PBS at pH 7.4 or 8.0 in a plastic cell plate (the number A1~A4, B1~B4 correspond to those in Table 3.1)

From Figure 3.3, it can be seen that collagen precipitation occurred when the collagen solutions were adjusted using 50mM PBS, but a clear collagen solution was obtained when 100mM PBS was used. The pictures for those solutions adjusted using 150mM and 200mM PBS are not shown here, but they all gave clear solutions. That is, salt facilitated collagen solubilization at concentrations up to 200mM, concentrations at which the collagen was soluble. Salt concentrations above 200mM were not studied. At pH7.4 as shown in Figure 3.4, collagen (1.5mg/ml) at all the ionic strength conditions investigated showed amide-formation, and it in 50mM and 100mM PBS displayed more intensive amide band, but again, the result from the solution (50mM PBS) with gel-like collagen was especially inconsistent when repeating the experiments.

At pH8.0 only the reaction in 100mM PBS showed product formation (Figure 3.5). As described above, the reproducibility of the amide formation in 50mM PBS was not high, especially at higher pH. The reason could be that the hydrolysis of NHS surface was facilitated at higher pH. Therefore, it is normal to get only a little reaction in 50mM

PBS (pH8.0) in these systematic ionic strength studies. The reasons for less intensive band formed from collagen in 150mM and 200mM PBS at pH8.0 especially were not quite understood yet.

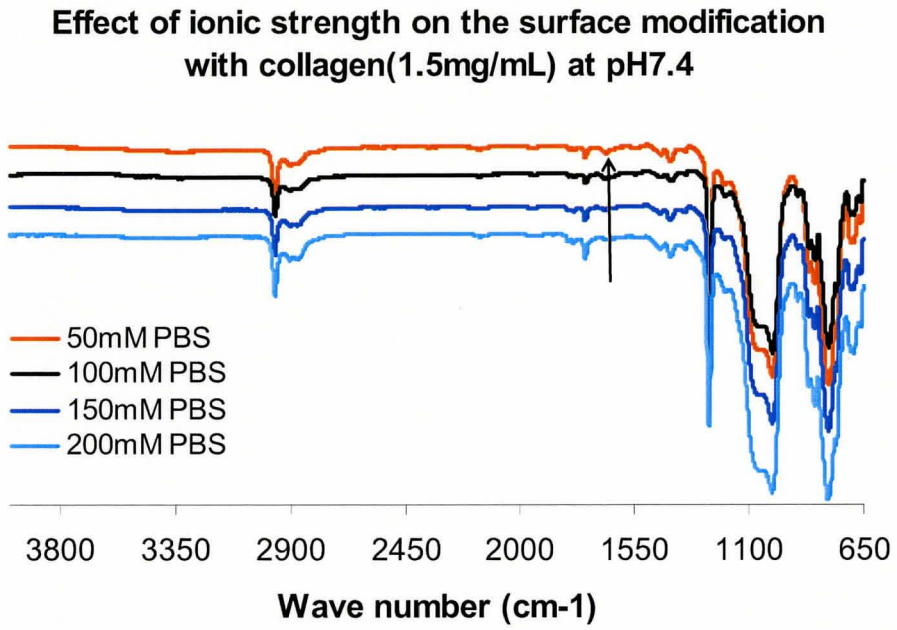

Figure 3.4 FTIR spectra of PDMS surfaces modified with collagen (1.5mg/ml) at pH 7.4 with ionic strength varying from 50mM to 200mM

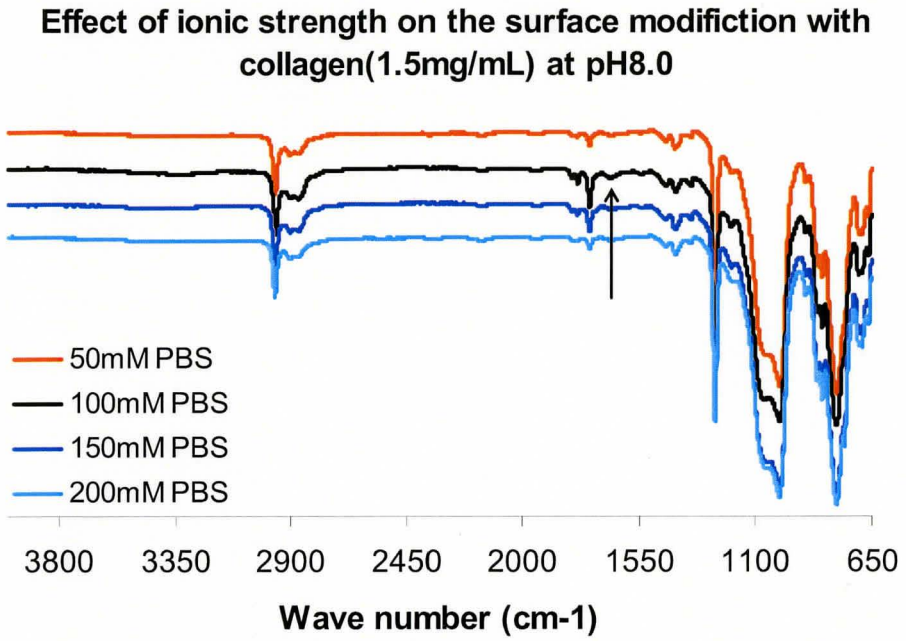

Figure 3.5 FTIR spectra of PDMS surfaces modified with collagen (1.5mg/ml) at pH 8 with ionic strength varying from 50mM to 200mM

3.3.2.3. Effect of Concentration of Collagen on the Amide Formation Reaction

To study how the concentration of collagen affects the acylation reaction, all the collagen solutions were dialyzed or diluted with 100mM PBS at pH7.4 or pH8.0 (the collagen was soluble at this ionic strength, therefore, they were homogeneous solutions). The concentrations varied from 1.5mg/mL to 3mg/mL. Figures 3.6 and 3.7 showed clearly that the more concentrated homogeneous collagen solution (1.8 and 3mg/mL) underwent more acylation reaction compared to the 1.5mg/mL one under the conditions investigated. The intensity of amides bands at 1668 cm^{-1} and 1556 cm^{-1} were dramatically

increased at higher collagen concentrations of 1.8mg/mL or above. The reproducibility was above 90% at both pH7.4 and pH8.0.

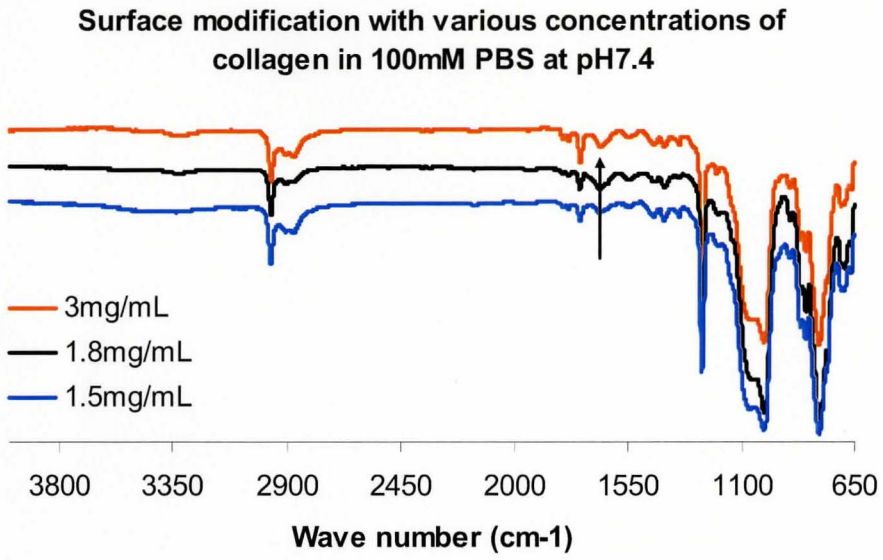

Figure 3.6 FTIR spectra of PDMS surfaces modified with collagen (concentration varied from 1.5 to 3mg/mL) at pH 7.4 with ionic strength 100mM

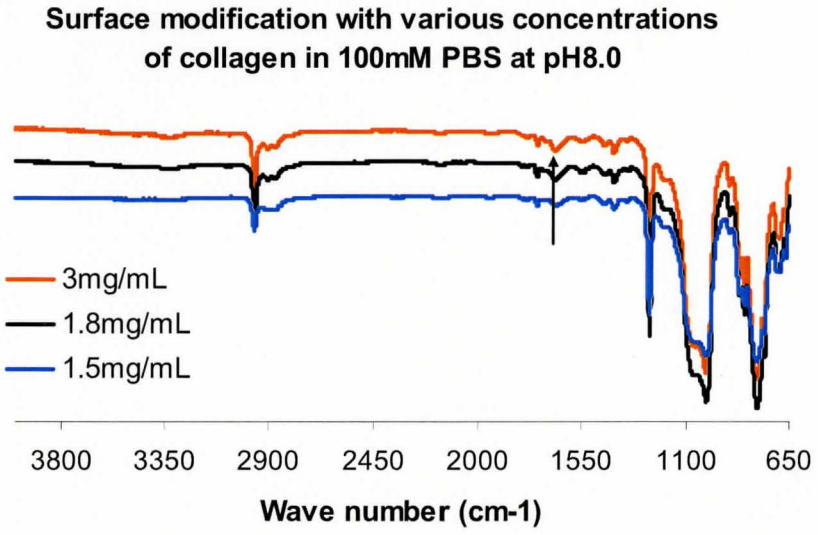

Figure 3.7 FTIR spectra of PDMS surfaces modified with collagen (concentration varied from 1.5 to 3mg/mL) at pH 7.4 with ionic strength 100mM

3.3.3. Water Contact Angle

The wettability of the PDMS surfaces before and after grafting with collagen was investigated with ambient humidity. Figure 3.8 showed a decrease tendency on water contact angle over time for all surfaces. For unmodified PDMS surfaces, the decrease may result from the octamethylcyclotetrasiloxane (D_4) and decamethylcyclopentasiloxane (D_5) leaching out and migrating to the surface of the PDMS. For other surfaces, the surface groups rearrangement, which presents collagen to the surface, may contribute to the contact angle decrease tendency. Obviously, the water contact angle of the surface after modification with collagen was dramatically decreased compared to the angle at any other modification step, which is another proof that the surface was modified with collagen, since it is well known that collagen is hydrophilic.

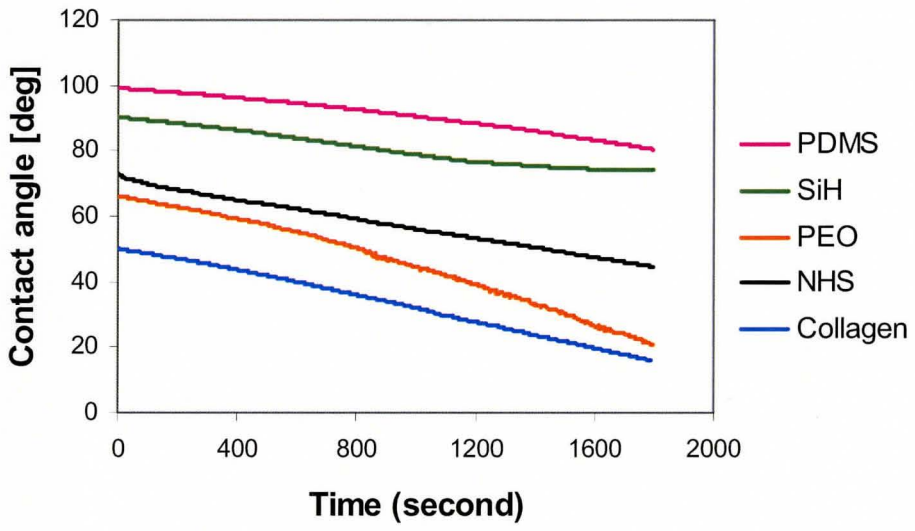

Figure 3.8 Water contact angles of the surfaces before and after modification as a function of time

Since collagen will normally be found in aqueous conditions in vivo, the captive bubble contact angle in water method was believed to more closely mimic real conditions. It can be seen from Figure 3.9 that the surfaces modified with collagen showed a lowest contact angle, of about 40°, on the investigated surfaces. The PEO-surfaces displayed higher contact angle (60°) than collagen-surfaces but lower than that of PDMS and NHS-surfaces. This is anticipated, as PEO is both hydrophilic and hydrophobic due to the OCH_2CH_2 groups. Both Figure 3.8 and 3.9 indicate that collagen was covalently bound to the PDMS surfaces.

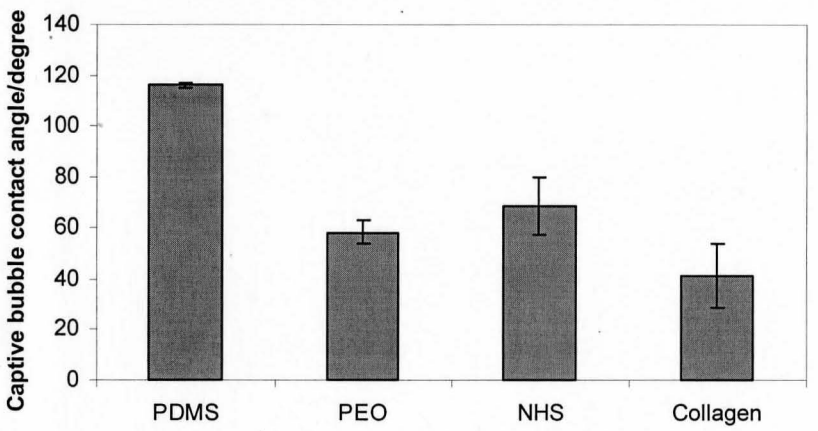

Figure 3.9 Captive bubble contact angles in water of the surfaces before and after each modification

3.3.4. Optical Profiling System

An optical profilometer system was used to study the surface roughness change before and after collagen modification. Figure 3.10 displays the subtle changes observed in roughness of the NHS-surface and collagen-surfaces. The pictures were taken at

different areas on the surfaces. It is difficult to determine whether the surface became rougher or less rough after modification with collagen. That is, the optical profiling system showed no obvious change when the surface was modified with collagen even though we expected that the collagen-modified surface should be rougher than the other surfaces because of collagen aggregation. This result may indicate either that the collagen grafted as an individual molecular layers, of that surface rearrangement occurred, migrating the collagen into the silicone layer.

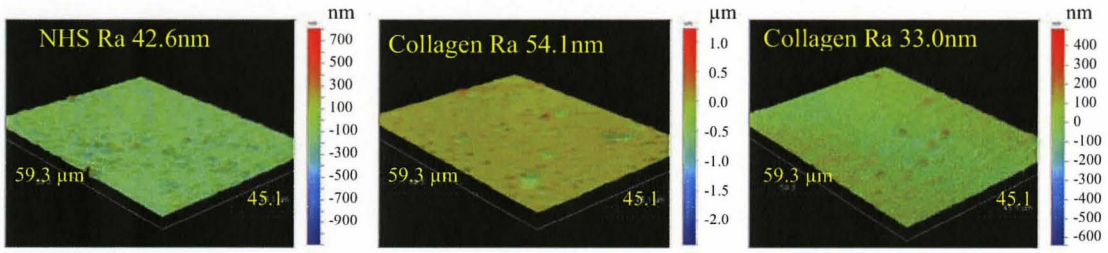

Figure 3.10 Pictures taken by optical profiling system of the surfaces before and after modification with collagen (Ra: roughness by average)

3.3.5. X -ray Photoelectron Spectroscopy (XPS)

XPS data indicated the elemental compositions of the top approximately 9 nm of the surfaces. Carbon, oxygen, silicon were present in XPS spectra of all the dry surfaces, but nitrogen was present only in the spectra of NHS and collagen surfaces (Figures 3.11 and 3.12). There was a sharp increase in the nitrogen content when NHS surface (1.6%) was compared to the collagen modified surface (5.1%) at ToA 90°, which suggested the presence of collagen molecules on this collagen modified surface.

When the upper layer of the collagen surface was examined, at ToA 20°, 2.1% nitrogen was observed on this surface, but only 0.6% for the NHS surface, which indicated that surface rearrangement occurred during the drying of the surfaces.[38] In air or vacuum, hydrophobic groups migrate to the surface to minimize the surface free energy at the interface.[39-41] Therefore, the comparatively hydrophilic NHS groups or long amino acid chains from collagen prefer inserting into the surface instead of being on the top when exposed to air or vacuum – silicone migrates to the exterior layer. That is why a higher nitrogen content was observed at ToA 90° than at ToA 20°. The control for this experiment was an NHS surface that had been incubated in the same buffer solution as was used for collagen (no collagen was in the solution). Under these conditions, the NHS groups were hydrolyzed and a PEO-OH surface was produced. Thus, no nitrogen was observed on the control surface as is shown in Figure 3.12. It can also be seen that the surfaces of PDMS, SiH and PEO showed no nitrogen as expected.

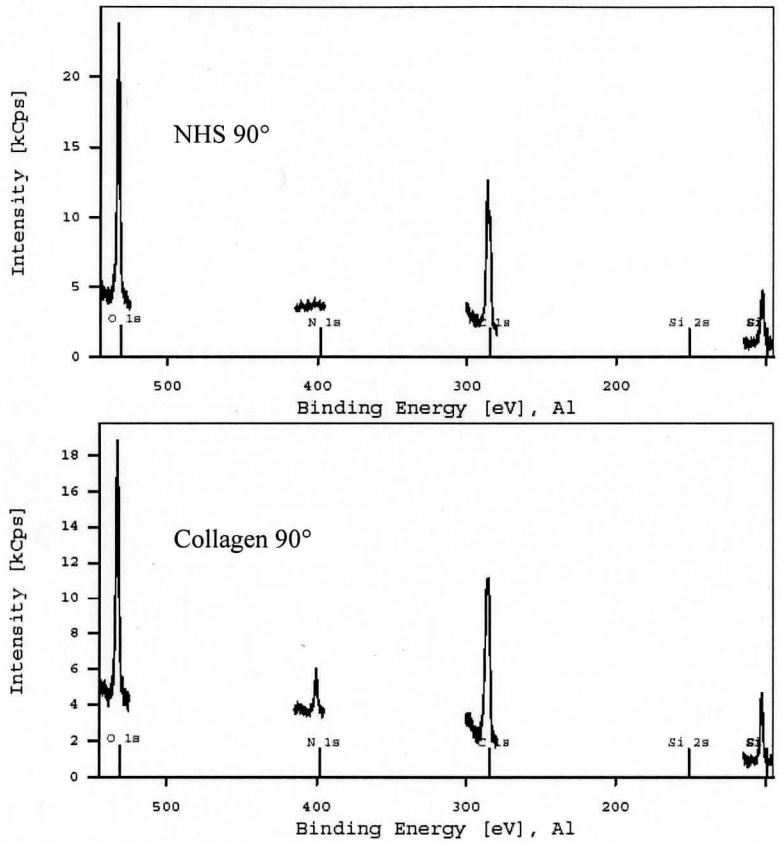

Figure 3.11 XPS spectra of dry modified PDMS surfaces (N content increased from 1.6% to 5.1% after chemical modification with collagen from the NHS surface)

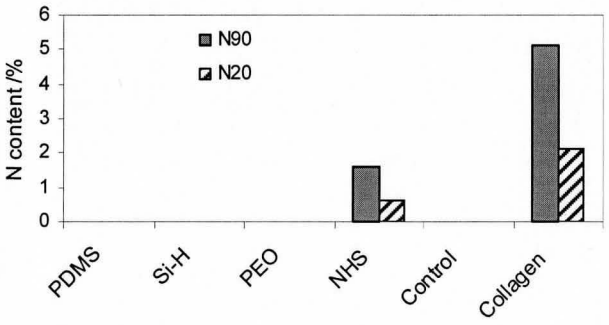

Figure 3.12 XPS data at take-off angles of 20° and 90° for nitrogen content of the PDMS surfaces before and after modifications (Control represents the NHS-modified surface incubated using a similar buffer solution as that used for collagen)

The high resolution C1s spectra of the surfaces (Figure 3.13) allowed us to assign the different carbons based on their binding energy. All the spectra displayed a huge peak at 284.5eV, which was assigned to the methyl carbons (C-H) attached to silicon atoms in PDMS (The bands with energies of 286.1 and 288.4eV might come from the filler in the raw material of silicone and/or some impurities).[42] No obvious difference can be seen from the spectra for the PDMS and SiH surfaces, but a dramatic peak at 286.2eV, corresponding to C-O species, appeared in all spectra of the PEO, NHS and collagen surfaces, which provided an evidence of PEO being grafted on the surface.[43,44] The carbons with binding energy of 287.8eV in the collagen surface spectrum were assigned to O=C-N.[28] For the NHS surface, the O=C-N species could not be differentiated from O-C=O due to their similar concentrations and close positions in the spectrum. The carbons with binding energy of 288.8eV (in the spectrum of the NHS and collagen surfaces) were assigned to those of carbons in O-C=O. It should be pointed out that there should be a band at 285.8eV for C-N in the collagen surface spectrum,[28] but it seemed to be overlapped by the huge C-O band, which can be indirectly proven by the very intensive band for O=C-N, which only appeared in the spectrum of the surface modified with collagen.

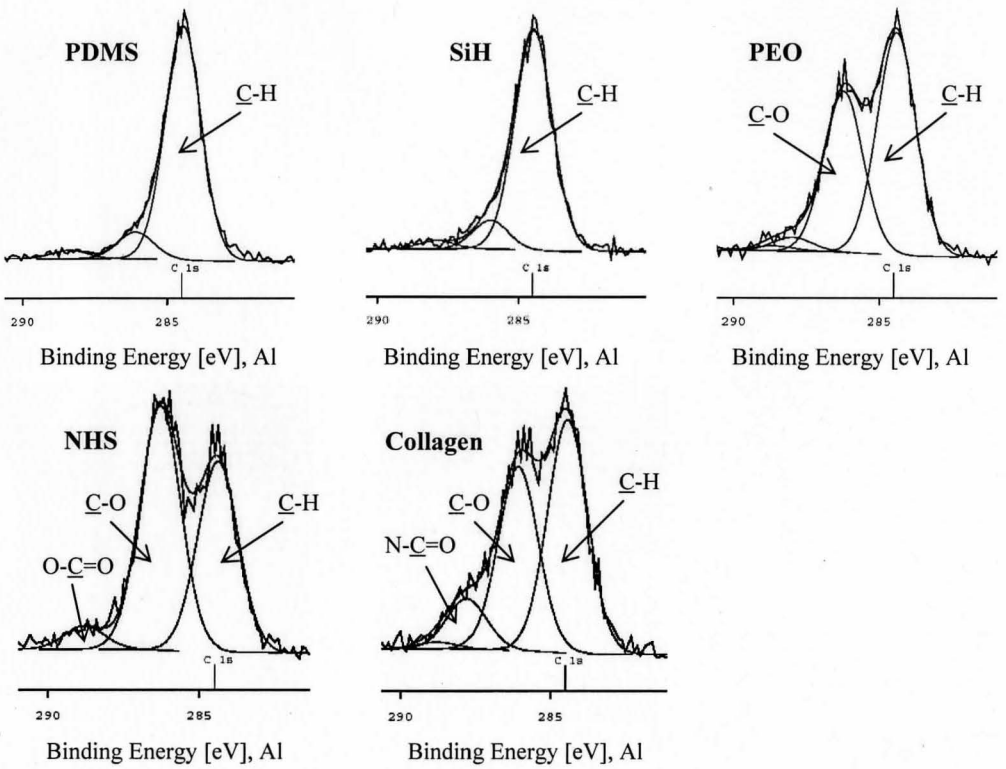

Figure 3.13 High resolution C1s XPS spectra of the PDMS surfaces (intact PDMS, modified with SiH, PEO, NHS and collagen, respectively)

3.3.6. Time-of-Flight Secondary Ion Mass Spectrometry (TOF-SIMS)

In the XPS section, the rearrangement of hydrophilic groups on the dry surfaces was described. ToF-SIMS experiments were performed using a 'deep freezing' technique to analyze the wet collagen surface. The surface was studied under progressive heating from -96 °C to room temperature. As shown in Figure 3.14, the positive ion spectrum of the surface modified with collagen showed increased $C_2H_6N^+$ (44.05m/z, alanine of collagen) and $C_2H_4O^+$ (44.03m/z, PEO segment)[38] when it was frozen to -96

°C compared to the result at room temperature, which further supports the suggestion that collagen is at the upper surface in water, but moves down into the silicone in a vacuum.

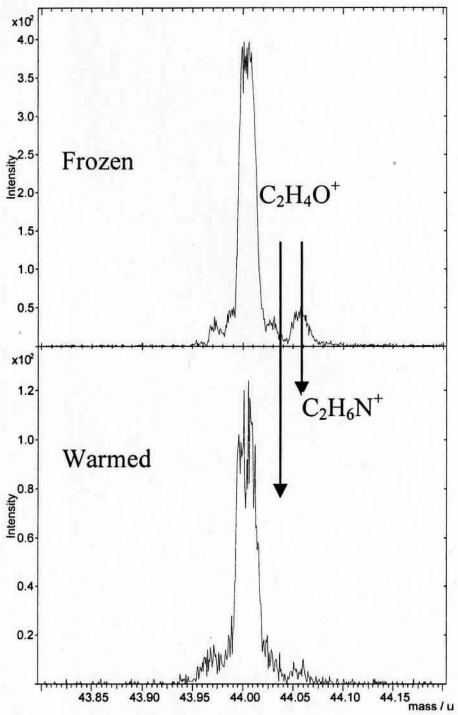

Figure 3.14 Positive ion spectra of collagen-modified surface by ToF-SIMS

3.3.7. Atomic Force Microscopy (AFM)

The tapping-mode AFM images for the surfaces were taken from three areas widely spaced apart. The images are of both height and phase. All images for a given type of surface had similar features, so the images of the surface shown are representative. The images in Figure 3.15 showed considerable variations on the surfaces topology. Comparatively, the PDMS surface was very flat, but it became rougher when the PEO-NHS chain was incorporated onto the surface as the image for NHS surfaces shows (lots

of little pearl-like bumps were seen). However, a very clear layer of collagen fibers on the surfaces modified with collagen was observed on both large scan (c: 2.5μm x 2.5μm) and smaller scan (d: 1μm x 1μm) images. Nodules (bright areas in the height image) were seen on the PDMS surface, NHS surface and collagen surface. Some of the nodules might come from the PDMS surface itself, some might be incorporated after modifications. Two 1 micron scans and one 2.5 micron scan were run on the collagen surface. The 2.5 micron scan showed nodules everywhere. The 1 micron scans were of a region between the nodules and directly a nodule directly. The phase allows the fine details to be revealed without the much larger objects obscuring them as occurred with the height data in this case. It seemed that fewer fibers displayed on the nodules than on other areas. Other than that, fibers were seen everywhere on the collagen surface.

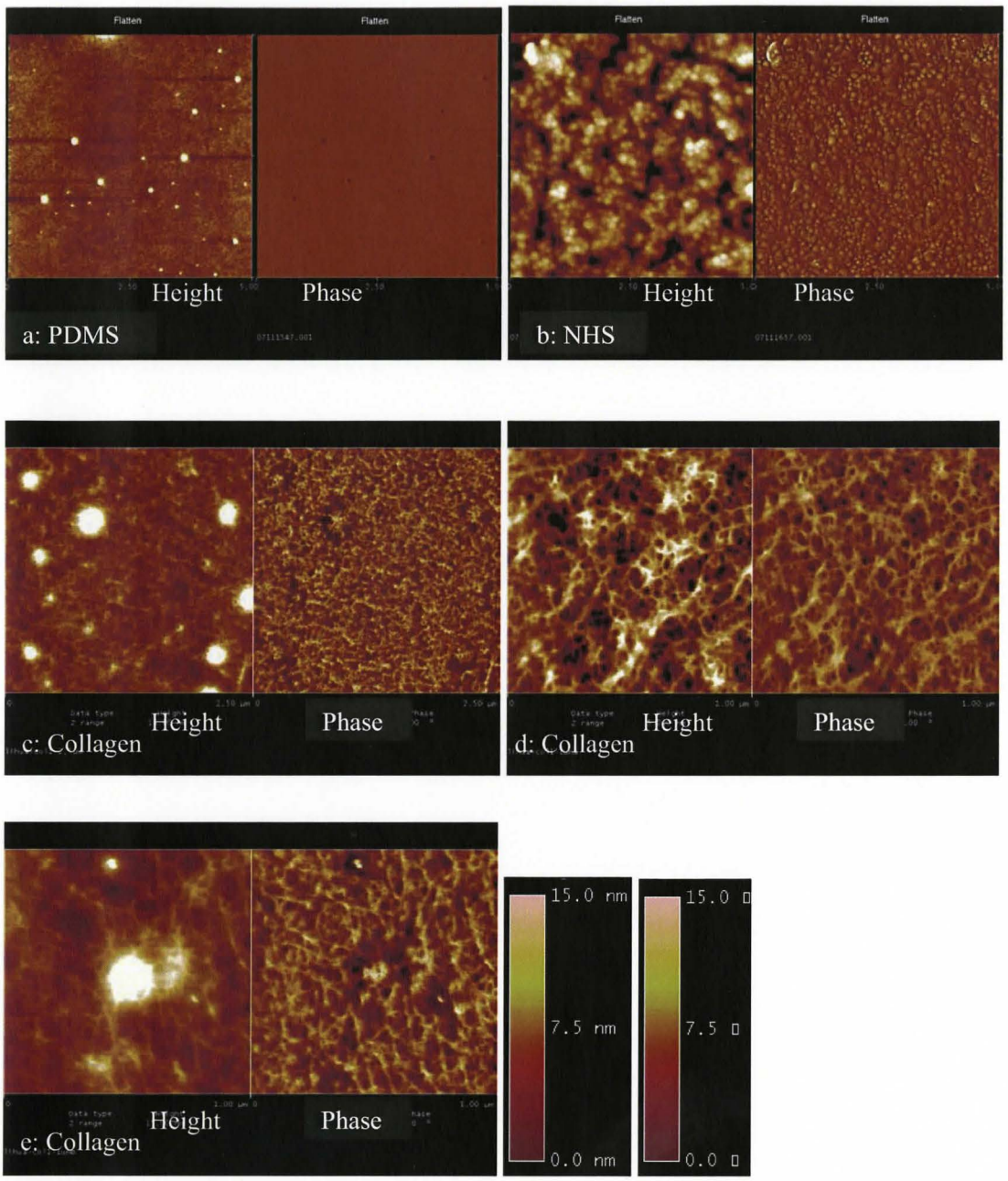

Figure 3.15 Tapping-mode AFM height and phase images of surfaces before and after modification with NHS and collagen; (a, b) 5μm x 5μm, (c) 2.5μm x 2.5μm, and (d, e) 1μm x 1μm (d: a region between the nodules; e: of a nodule directly)

3.3.8. Collagen Staining

The dye Sirius red F3B (Direct red 80) was used to stain the surface modified with collagen. The first picture is a positive control and the last 3 are negative controls. The red fibers on the 'surface modified with collagen' are the covalently bound collagen fibers on the surface. The elongated Sirius red molecule binds to triple helical collagen molecules in a parallel fashion and therefore will not bind to denatured or degraded collagen or to other proteins which do not possess the typical helical collagenous triple helical structure.[35] Thus, the collagen fibers being seen are only those in their natural state (see Figure 3.16).

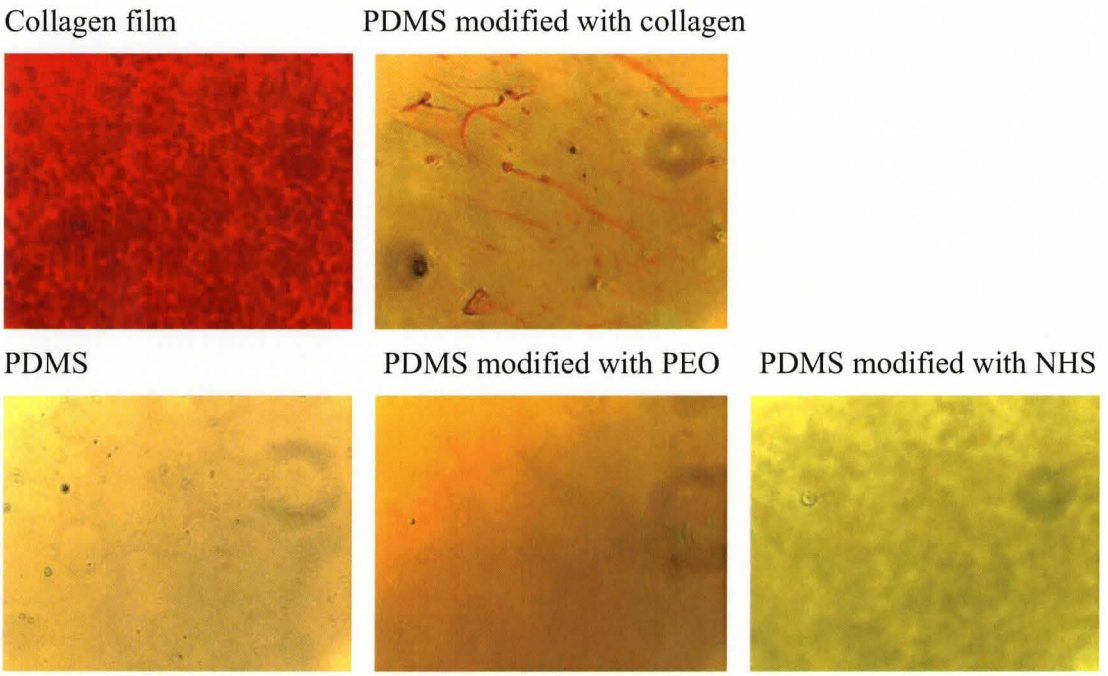

Figure 3.16 Pictures of the surfaces stained with Sirius red F3B ('Collagen film' is the positive control; PDMS, 'PDMS modified with PEO' and 'PDMS modified with NHS' are negative controls)

3.3.9. Corneal Epithelial Cell Culture

The surfaces were examined for their ability to support adhesion and proliferation of corneal epithelial cells. Not surprisingly, there were nearly no cells on PEO surfaces as shown in Figure 3.17, consistent with that PEO is a protein-repelling group.[43,44] On the NHS surface, a few cells grew in the first two days and more cells appeared at day 5, but most of them had died; this is consistent with the notion that upon linking to PEO, NHS, as a small group, does not change the properties of PEO surface, and thus poorly supports cell growth. The transient but poor cell growth on NHS surface may result from deposited medium on the surface. As expected, cells reached confluence at day 5 on both the collagen-modified and unmodified PDMS surfaces and it seems that more cells grew on the collagen surface than on the unmodified PDMS surface. Additionally, on PDMS surface, a number of cells were found in round shape, indicating poor adhesion of these cells to the surface. However, no cells on collagen surface were found to have this morphological change. Therefore, all these results suggest that collagen surfaces may provide the most supportive environment for cell adhesion and growth among all the surfaces investigated.

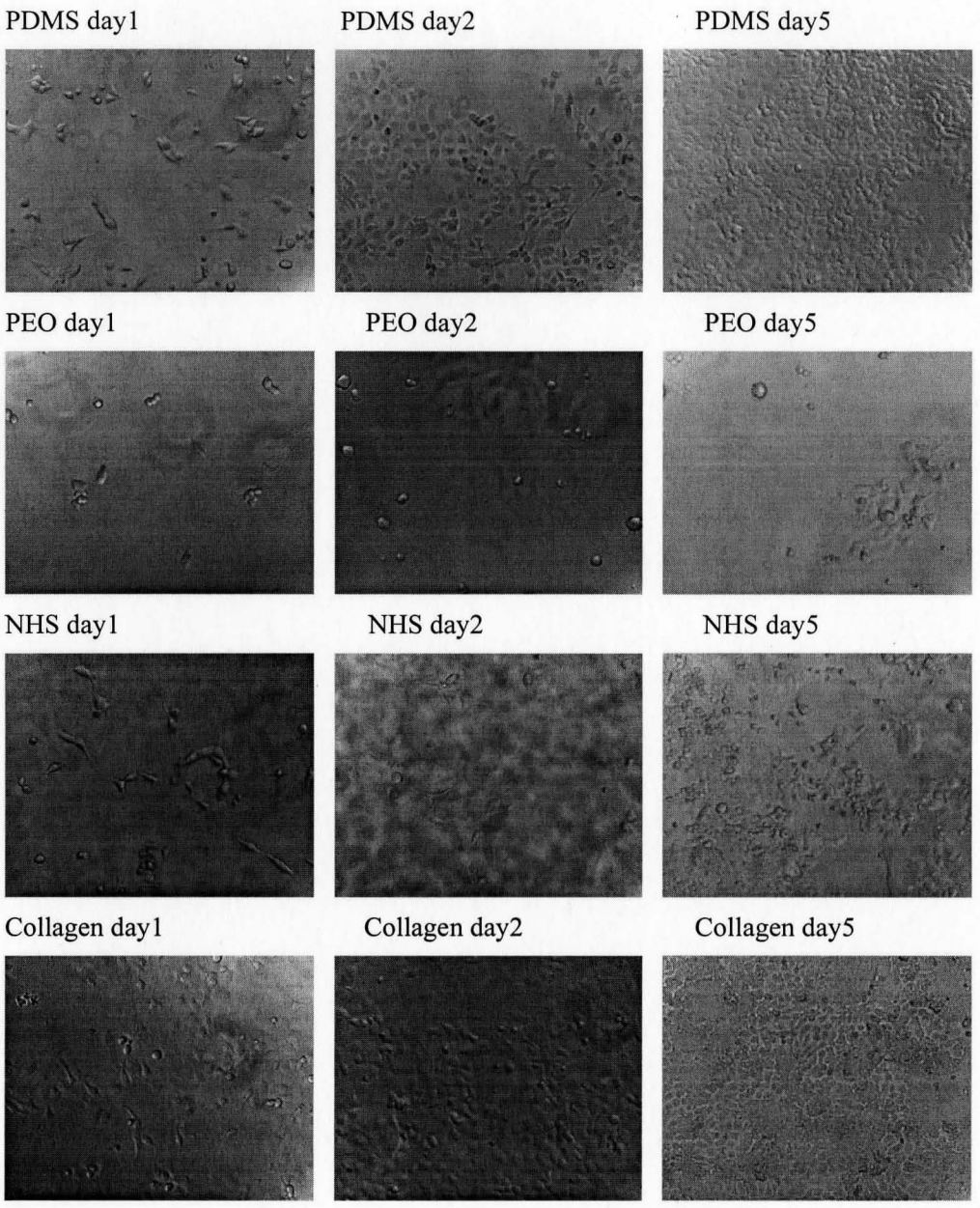

Figure 3.17 Cell culture pictures after 1day, 2day, and 5 days human epithelial cell seeding

3.4. DISCUSSION

The ability to covalently link collagen to PDMS surfaces was assessed by ATR-FTIR, XPS, ToF-SIMS, Tapping-mode AFM, cell culture, collagen stain and other measurements. The presence of collagen in FTIR analyses was evident from the spectral changes in the amide I carbonyl stretching region after surface modification with collagen. The C=O bands at 1789 and 1743cm^{-1} for NHS decreased and a new –NH-C=O vibration band at 1668cm^{-1} characteristic of collagen appeared. Furthermore, the appearance of the band in amide II region, NH bending in the vicinity of 1556cm^{-1} also indicated the presence of collagen.[34,45,46]

The reaction of activated NHS-esters with protein is well known and has been thoroughly studied since before the 1960s.[29-31,33,47-49] However, the optimal pH, reagent concentration, and reaction time course may have to be determined experimentally for each particular peptide or protein, especially for those with very high molecular weight and special tertiary structures.[1] An NHS-ester principally reacts with the epsilon amine groups on lysines and *N*-terminus amines if available, but it can also react with other functional groups, such as non cyclic secondary amines when incubated for a long period of time (i.e. overnight). It has been reported that NHS esters do not react with thioether of methionine or the cyclic secondary amine of tryptophan.[47] Some other amino acids containing nitrogen in their side chains, such as amides on asparagine and glutamine, guanidine of arginine, do not react with NHS esters.[47] For serine and tyrosine, the reactivity is limited because of transesterification of the hydroxyl group with the NHS

ester. Although the imidazole group in histidine reacts with NHS esters, it forms an unstable product that hydrolyzes rapidly.[50]

The NHS ester acylation reaction in aqueous solutions undergoes two competing reactions, one is the reaction with the primary amine, and the other is the hydrolysis of the NHS ester. The former reaction leads to a stable, covalent amide bond between the NHS ester and the primary amine by producing the by-product *N*-hydroxysuccinimide. The hydrolysis of the NHS ester results in the release of *N*-hydroxysuccinimide but without producing a crosslinked product, therefore, it inactivates the NHS ester and decreases the efficiency of the crosslinking reaction. Hydrolysis is favored in dilute protein solutions. To avoid or decrease the hydrolysis of the NHS ester, more concentrated protein solutions are usually used, under which conditions the acylation reaction is favored. By using the appropriate molar ratio of NHS ester to amine groups and reaction pH, the extent of crosslinking can be controlled. Both the hydrolysis and acylation reactions with the amine group increase with increasing pH. It has been reported that the half life of the hydrolysis decreased dramatically with the increase of pH from 7 to 9.[33,47,49]

Collagen is known to be a giant protein molecule, which leads to its low solubility in alkaline condition and therefore, low reactivity compared to other small proteins. Usually it is highly diluted into acidic solutions, which makes the NHS ester acylation less likely due to the weaker nucleophilicity of amine groups at lower pH, as they are protonated, and the hydrolysis of NHS ester in overly dilute solution is facilitated.

In our research, the parameters affecting the NHS ester reaction with collagen were investigated. The optimized pH for NHS ester acylation reactions with collagen was between 7.0 and 9.0. At the optimum pH and the collagen concentration of 1.5mg/mL or below with ionic strength of 50-200mM, the change on amide bands from FTIR was quite subtle. However, it was noted that the collagen became more soluble when the ionic strength was increased in the investigated range, even when the concentration of collagen was increased to the original concentration of 3mg/mL by dialysis. At concentrations above 1.8mg/mL (up to 3mg/mL) in 100mM PBS, much more reaction of collagen was observed in FTIR spectra. Therefore, the salt facilitated collagen solubilization in our study range. This can be explained by 'salting-in' and 'salting-out' theory. The solubility of proteins depends, among other things, on the salt concentration in the solution. At low concentrations, the presence of salt can stabilize the various charged groups on a protein molecule, so attracting protein into the solution and enhancing the solubility of protein. This is commonly known as *salting-in*. However, as the salt concentration is increased, a maximum protein solubility point will be usually reached. A further increase in salt concentration implies that there is less and less water available to solubilize the protein. Finally, protein starts precipitating when there are insufficient water molecules to interact with protein molecules. This phenomenon of protein precipitation in the presence of excess salt is known as *salting-out*.[51,52] By adding the appropriate amount of salt, the poor solubility of collagen in base was improved, which allowed for higher collagen concentrations to be achieved and, therefore, more efficient NHS acylation with collagen obtained.

The reactions in our studies were performed overnight but there were always little unreacted NHS present. Increasing the reaction duration didn't increase the reaction extent based on FTIR spectra. This is possible since the giant covalently bound collagen molecules can form domains in which the residual amine group are shielded from NHS groups. There is also an issue of geometric accessibility. Once tethered to the surface, many amines will not be in the proximity of the tethered NHS groups. When the collagen-bound surface was quenched in pH8 Tris buffer, which supplies abundant amine groups on small molecules, all the NHS groups disappeared.

Water contact angle (or captive bubble contact angle 40° in water) of collagen-modified surfaces also demonstrated the presence of collagen on the surface, due to its higher water affinity than that before modification.[27] XPS data and ToF-SIMS further proved that the collagen molecules were attached onto the PDMS surface by higher nitrogen content (5.1%) in XPS and appearance of collagen fragments in ToF-SIMS data.

Epithelial cell growth seemed to be more promoted on the surface modified with collagen than on all the other surfaces. The unmodified PDMS surface also gave large scale cell coverage, which was regarded as our positive control.[53,54] Cells reached confluence after 4 to 5 days in both cases. The surface modified with collagen gave almost full cell coverage. Because the modified surface was not quite smooth, there was the development of multiple cell layers which be the reason why the cells seemed to be smaller than those on the unmodified PDMS surface. The PEO surface showed nearly no cells even by day 5; only a few cells were observed on the NHS surface. The PEO surface was used as our negative control, since such surfaces are well recognized as resisting

protein biofouling and had been proved possible to demonstrate a high degree of H_2O/PEG structural organization.[55] Underlying this effect is the chain orientation dependence of the H_2O interaction,[56] not only at the anisotropic PEG surface, but also the length of its chain repeat units. A certain prevailing view on the effects of this peculiar surface structure was pictorially described as 'molecular cilia' on adhesive interactions in aqueous environments.[57,58] McGurk has suggested, as the reason behind the protein resistant behavior, 'the formation of a steric barrier from the PEO polymer brush' is based on their PEO–polypropylene oxide copolymers.[59] The scattered cells on the NHS surface may due to direct grafting and immobilization on the surface, or tethering of EGF (a cell adhesion promoting peptide that was added to the cell culture assay), to which the cells adhere. Sheardown's group has compared the enhancement of the adhered cells on the EGF-grafted PDMS surface with that on the unmodified PDMS.[54] The abundant cells observed on the surface modified with collagen but only a few on the NHS surface indicated that collagen was bound on the surface, since collagen is known to be cell adhesive.[60]

The cellular response induced by collagen is mainly mediated through the amino acid sequence arginine-glycine-asparagine (RGD), which is recognized by the integrin receptors located at the cell membrane.[61,62] The images for collagen staining with Sirius red also provided the presence of collagen molecules on the surface. However, only some red collagen fibers can be seen clearly. Sirius red is known to bind to the [Gly-X-Y] helical structure found in all collagens and it was thought that the interaction between collagen and Sirius Red was due mainly to the reaction of its sulfonic acid groups with

the basic groups of collagen.[63,64] The elongated Sirius red molecules bind to only triple helical collagen molecules in a parallel fashion but not to the denatured or degraded ones.[35] The AFM images assisted in revealing that there were many more collagen molecules on the surface modified with collagen. The above results suggested that the tertiary structure of collagen may not be necessary for supporting cell adhesion and proliferation on this artificial surface.

3.5. CONCLUSION

The PDMS surface was successfully modified with collagen by covalent immobilization. The crosslinking reaction between collagen and NHS ester only occurred at pH7 and above. The full solubilization of collagen in basic solution was achieved by increasing the ionic strength in the solution but no decreasing on the concentration of collagen. The presence of fibrillar collagen on the PDMS surface enhanced cell adhesion and proliferation, and the cell culture results suggested that the tertiary structure of collagen may not be necessary for supporting cell adhesion and proliferation on this collagen-immobilized PDMS surface.

3.6. REFERENCES

(1) Kadler, K. E.; Holmes, D. F.; Trotter, J. A.; Chapman, J. A. *Biochem J* **1996**, *316*, 1-11.

(2) Lee, C. H.; Singla, A.; Lee, Y. *Int J Pharm* **2001**, *221*, 1-22.

(3) Salchert, K.; Streller, U.; Pompe, T.; Herold, N.; Grimmer, M.; Werner, C. *Biomacromolecules* **2004**, *5*, 1340-50.

(4) Aprahamian, M.; Lambert, A.; Balboni, G.; Lefebvre, F.; Schmitthaeusler, R.; Damge, C.; Rabaud, M. *J Biomed Mater Res* **1987**, *21*, 965-77.

(5) Giusti, P.; Lazzeri, L.; De Petris, S.; Palla, M.; Cascone, M. G. *Biomaterials* **1994**, *15*, 1229-33.

(6) Stol, M.; Tolar, M.; Adam, M. *Biomaterials* **1985**, *6*, 193-7.

(7) Dufrene, Y. F.; Marchal, T. G.; Rouxhet, P. G. *Langmuir* **1999**, *15*, 2871-2878.

(8) Shimizu, Y.; Abe, R.; Teramatsu, T.; Okamura, S.; Hino, T. *Biomater Med Devices Artif Organs* **1977**, *5*, 49-66.

(9) Shi, Y.; Ma, L.; Zhou, J.; Mao, Z.; Gao, C. *Polym Adv Tech* **2006**, *16*, 789-794.

(10) Harada, O.; Kadota, K.; Yamamoto, T. *J Appl Poly Sci* **2001**, *81*, 2433-2438.

(11) Amudeswari, S.; Nagarajan, B.; Reddy, C. R.; Joseph, K. T. *J Biomed Mater Res* **1986**, *20*, 1103-9.

(12) Sherman, M. A.; Kennedy, J. P.; Ely, D. L.; Smith, D. *J Biomater Sci Polym Ed* **1999**, *10*, 259-69.

(13) Park, J. H.; Park, K. D.; Bae, Y. H. *Biomaterials* **1999**, *20*, 943-53.

(14) Bordenave, L.; Bareille, R.; Lefebvre, F.; Caix, J.; Baquey, C. *J Biomater Sci Polym Ed* **1992**, *3*, 509-16.

(15) van Kooten, T. G.; Whitesides, J. F.; von Recum, A. *J Biomed Mater Res* **1998**, *43*, 1-14.

(16) Ertel, S. I.; Ratner, B. D.; Kaul, A.; Schway, M. B.; Horbett, T. A. *J Biomed Mater Res* **1994**, *28*, 667-75.

(17) Interrante, L. V.; Shen, Q.; Li, J. *Macromolecules* **2001**, *34*, 1545-1547.

(18) Dahrouch, M.; Schmidt, A.; Leemans, L.; Linssen, H.; Goetz, H. *Macromo Symp* **2003**, *199*, 147-162.

(19) Ng, J. M.; Gitlin, I.; Stroock, A. D.; Whitesides, G. M. *Electrophoresis* **2002**, *23*, 3461-73.

(20) McDonald, J. C.; Whitesides, G. M. *Acc Chem Res* **2002**, *35*, 491-9.

(21) Xia, Y.; Whitesides, G. M. *Ann Rev Mater Sci* **1998**, *28*, 153-184.

(22) Sia, S. K.; Whitesides, G. M. *Electrophoresis* **2003**, *24*, 3563-76.

(23) Ostuni, E.; Kane, R.; Chen, C. S.; Ingber, D. E.; Whitesides, G. M. *Langmuir* **2000**, *16*, 7811-7819.

(24) Ostuni, E.; Chen, C. S.; Ingber, D. E.; Whitesides, G. M. *Langmuir* **2001**, *17*, 2828-2834.

(25) Müller, R.; Abke, J.; Schnell, E.; Macionczyk, F.; Gbureck, U.; Mehrl, R.; Ruszczak, Z.; Kujat, R.; Englert, C.; Nerlich, M.; Angele, P. *Biomaterials* **2005**, *26*, 6962-6972.

(26) Okada, T.; Ikada, Y. *J Biomed Mate Res* **1992**, *26*, 1569-81.

(27) Wallace, D. G.; Rosenblatt, J.; Ksander, G. A. *J Biomed Mater Res* **1992**, *26*, 1517-34.

(28) Cheng, Z.; Teoh, S. H. *Biomaterials* **2004**, *25*, 1991-2001.

(29) Chen, H.; Chen, Y.; Sheardown, H.; Brook, M. A. *Biomaterials* **2005**, *26*, 7418-24.

(30) Gong, P.; Grainger, D. W. *Surf Sci* **2004**, *570*, 67-77.

(31) Xia, N.; Hu, Y.; Grainger, D. W.; Castner, D. G. *Langmuir* **2002**, *18*, 3255-3262.

(32) Elbert, D. L.; Hubbell, J. A. *Ann Rev Mater Sci* **1996**, *26*, 365-394.

(33) Staros, J. V. *Acc Chem Res* **1988**, *21*, 435-41.

(34) Camacho, N. P.; West, P.; Torzilli, P. A.; Mendelsohn, R. *Biopolymers* **2001**, *62*, 1-8.

(35) Lee, D. A.; Assoku, E.; Doyle, V. *J Mater Sci Mater Med* **1998**, *9*, 47-51.

(36) Chen, H.; Brook, M. A.; Sheardown, H. D.; Chen, Y.; Klenkler, B. *Bioconjug Chem* **2006**, *17*, 21-8.

(37) Kirk, G. J. D.; Singh, R. *Atmospheric Environment, Part A: General Topics* **1992**, *26A*, 1651-60.

(38) Sosnik, A.; Sodhi, R. N. S.; Brodersen, P. M.; Sefton, M. V. *Biomaterials* **2006**, *27*, 2340-2348.

(39) Zhang, D.; Ward, R. S.; Shen, Y. R.; Somorjai, G. A. *J Phys Chem B* **1997**, *101*, 9060-9064.

(40) Wen, J.; Somorjai, G.; Lim, F.; Ward, R. *Macromolecules* **1997**, *30*, 7206-7213.

(41) Chen, Q.; Zhang, D.; Somorjai, G.; Bertozzi, C. R. *J Am Chem Soc* **1999**, *121*, 446-447.

(42) Beamson, G.; Briggs, D. *High resolution XPS of organic polymers: the Scienta ESCA300 database*; Wiley: Chichester, 1992.

(43) Chen, H.; Brook, M. A.; Sheardown, H. *Biomaterials* **2004**, *25*, 2273-82.

(44) Chen, H.; Zhang, Z.; Chen, Y.; Brook, M. A.; Sheardown, H. *Biomaterials* **2005**, *26*, 2391-9.

(45) Vyavahare, N.; Ogle, M.; Schoen, F. J.; Zand, R.; Gloeckner, D. C.; Sacks, M.; Levy, R. J. *J Biomed Mater Res* **1999**, *46*, 44-50.

(46) Andrade, A. L.; Ferreira, J. M. F.; Domingues, R. Z. *Mater Res* **2004**, *7*, 631-634.

(47) Cuatrecasas, P.; Parikh, I. *Biochemistry* **1972**, *11*, 2291-9.

(48) Gong, P.; Grainger, D. W. *Biomed Sci Inst* **2004**, *40*, 18-23.

(49) Lomant, A. J.; Fairbanks, G. *J Mol Biol* **1976**, *104*, 243-61.

(50) Wong, S. S. *Chemistry of protein conjugation and cross-linking*; CRC-Press: Boca Raton, **1993**.

(51) Jakoby, W. B. *Methods in enzymol* 1971; Vol. 22, p 248-252.

(52) Tanford, C. *Physical chemistry of macromolecules*; Wiley: New York, **1961**.

(53) Lee, J. N.; Jiang, X.; Ryan, D.; Whitesides, G. M. *Langmuir* **2004**, *20*, 11684-11691.

(54) Klenkler, B. J.; Griffith, M.; Becerril, C.; West-Mays, J. A.; Sheardown, H. *Biomaterials* **2005**, *26*, 7286-96.

(55) Heuberger, M.; Drobek, T.; Voros, J. *Langmuir* **2004**, *20*, 9445-8.

(56) Morra, M. *J Biomater Sci Polym Ed* **2000**, *11*, 547-69.

(57) Lee, J. H.; Ju, Y. M.; Lee, W. K.; Park, K. D.; Kim, Y. H. *J Biomed Mater Res* **1998**, *40*, 314-23.

(58) Kim, Y. H.; Han, D. K.; Park, K. D.; Kim, S. H. *Biomaterials* **2003**, *24*, 2213-23.

(59) McGurk, S. L.; Green, R. J.; Sanders, G. H. W.; Davies, M. C.; Roberts, C. J.; Tendler, S. J. B.; Williams, P. M. *Langmuir* **1999**, *15*, 5136-5140.

(60) Kleinman, H. K.; Klebe, R. J.; Martin, G. R. *J Cell Biol* **1981**, *88*, 473-85.

(61) Anselme, K. *Biomaterials* **2000**, *21*, 667-81.

(62) Ruoslahti, E.; Pierschbacher, M. D. *Science* **1987**, *238*, 491-7.

(63) Junqueira, L. C.; Bignolas, G.; Brentani, R. R. *Histochem J* **1979**, *11*, 447-55.

(64) Junqueira, L. C.; Bignolas, G.; Brentani, R. R. *Anal Biochem* **1979**, *94*, 96-9.

SUPPLEMENTAL MATERIALS

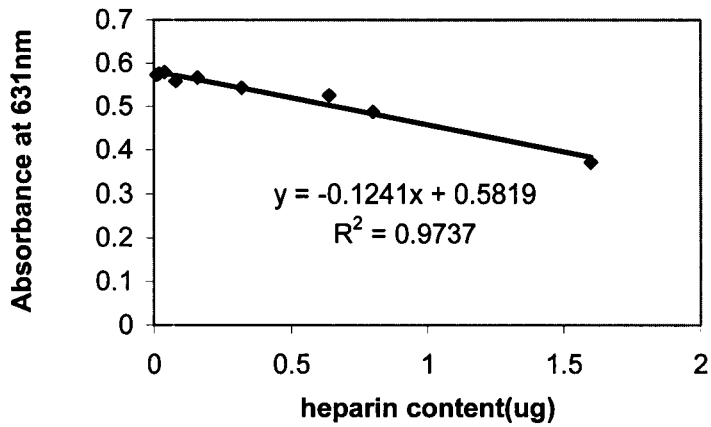

Figure S1 Calibration curve for measuring total heparin density

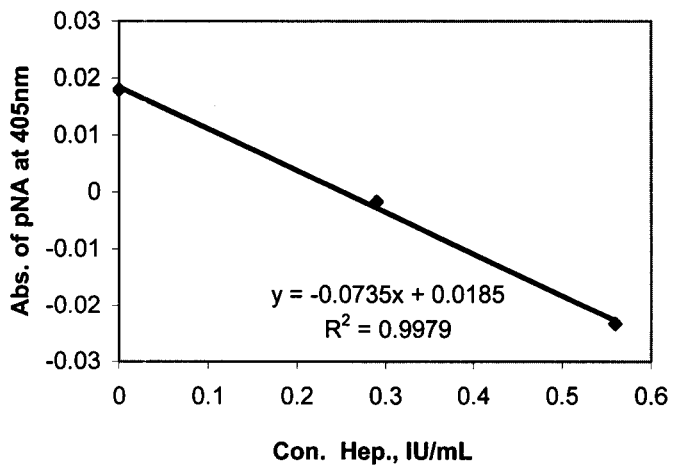

Figure S2 Calibration curve of heparin activity

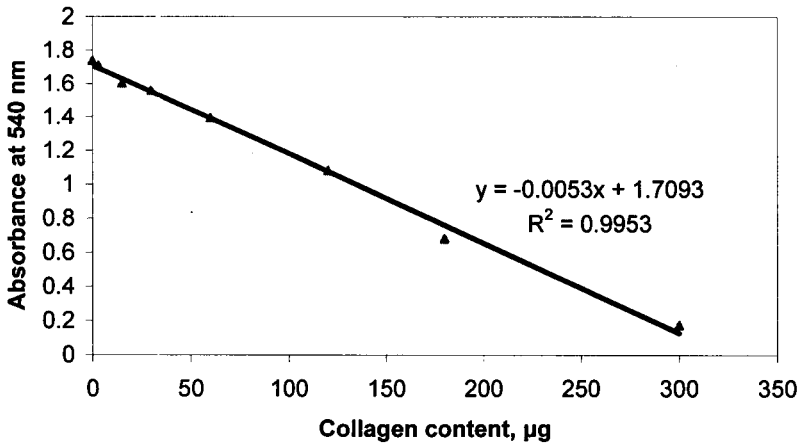

Figure S3 Calibration Curve of Collagen Stained with Sirius Red F3B

PDMS

Surface Stats:

Ra: 17.21 nm

Rq: 22.04 nm

Rt: 521.34 nm

Measurement Info:

Magnification: 104.19

Measurement Mode: VSI

Sampling: 161.24 nm

Array Size: 368 X 240

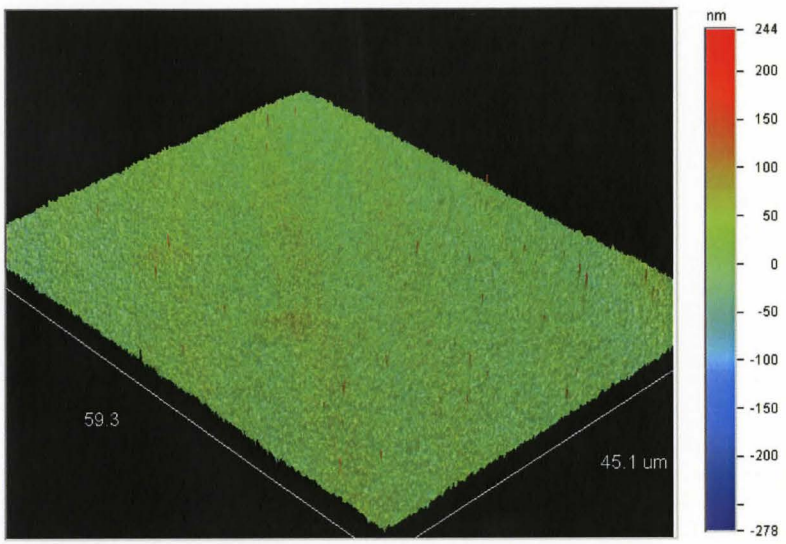

Title: PDMS

SiH

Surface Stats:

Ra: 25.42 nm

Rq: 32.76 nm

Rt: 794.07 nm

Measurement Info:

Magnification: 104.19

Measurement Mode: VSI

Sampling: 161.24 nm

Array Size: 368 X 240

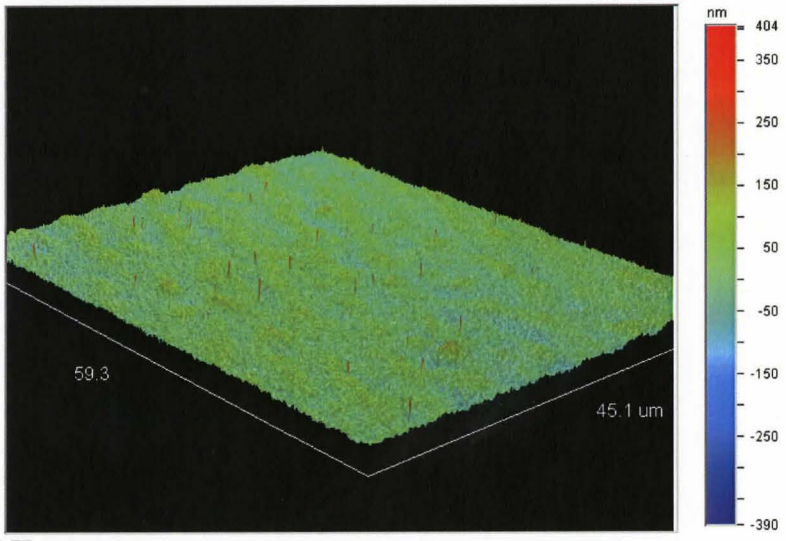

Title: SiH-6%TfOH

PEO

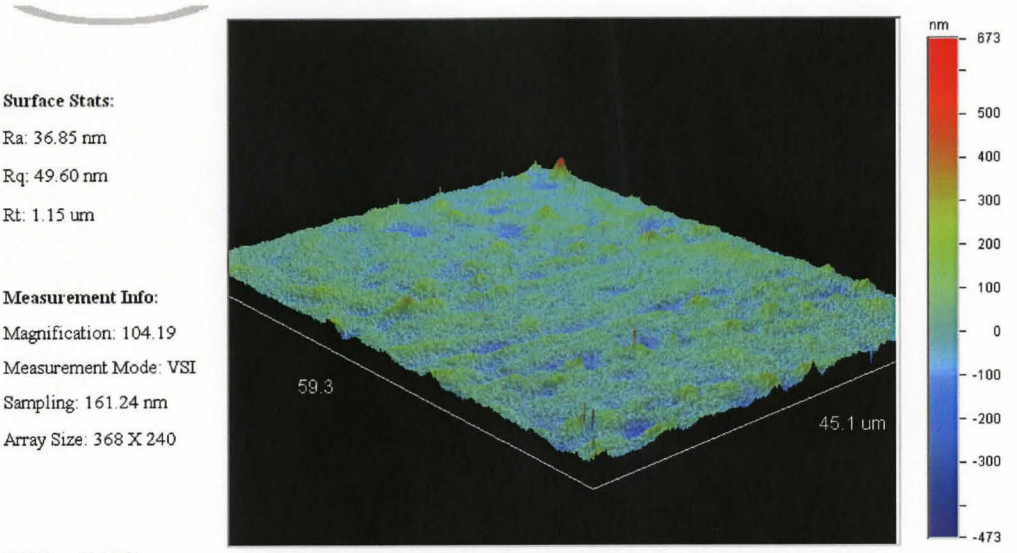

NHS

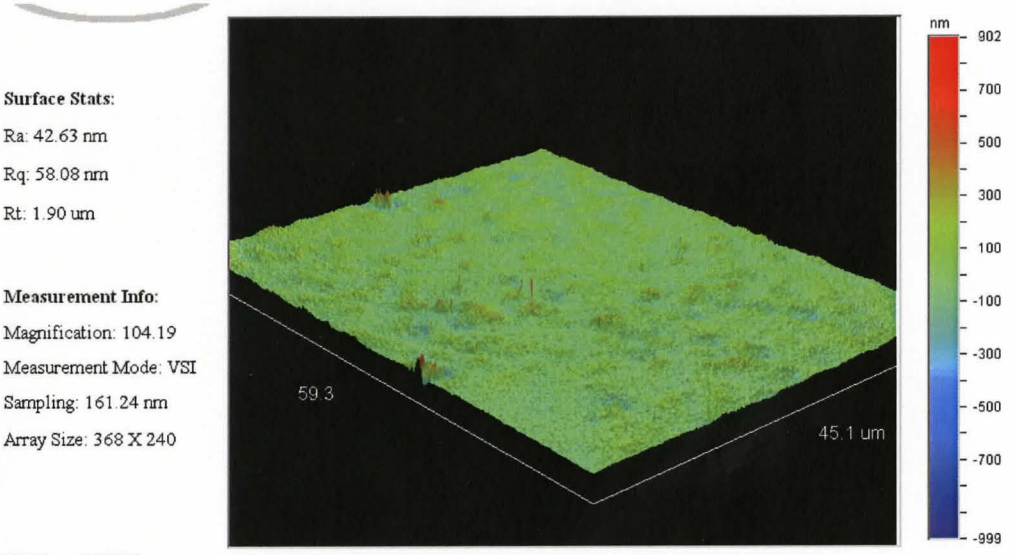

Figure S4 Full pictures of Figure 2.13

PDMS height image, 5μm x 5μm

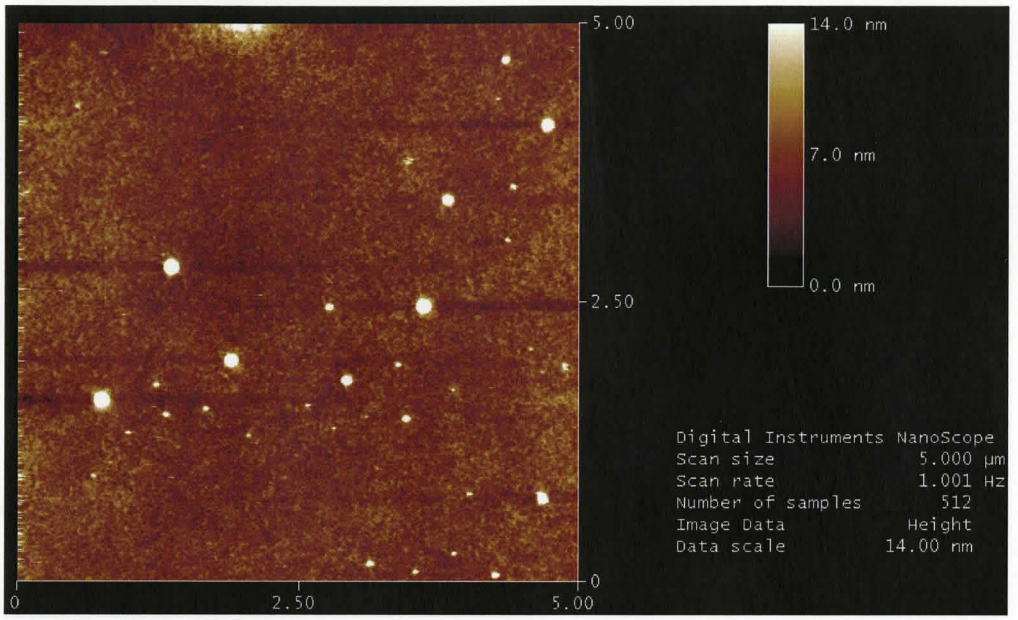

PDMS phase image, 5μm x 5μm

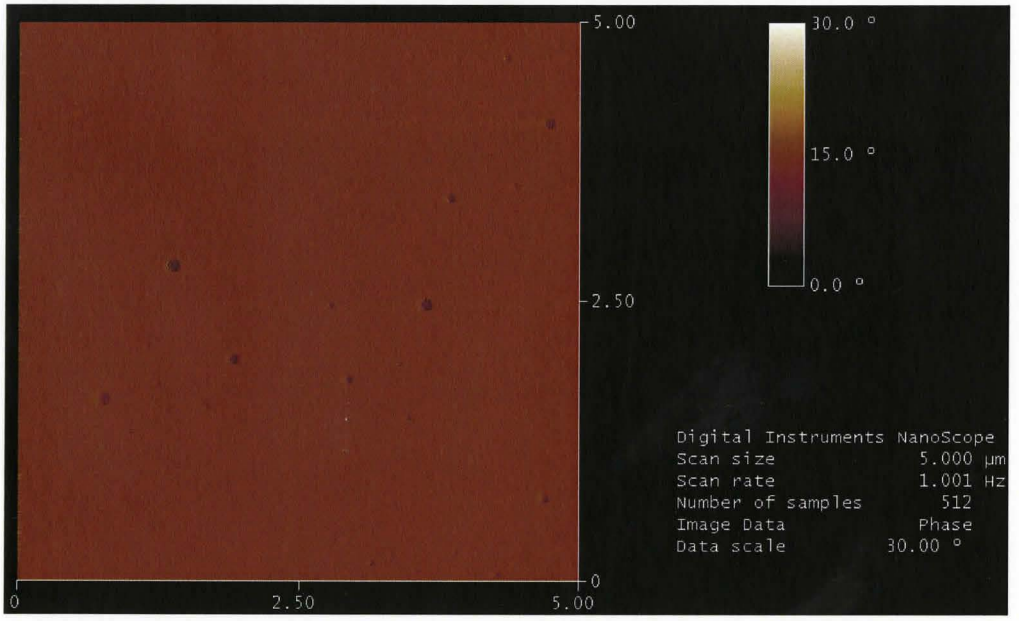

SiH height image, 5μm x 5μm

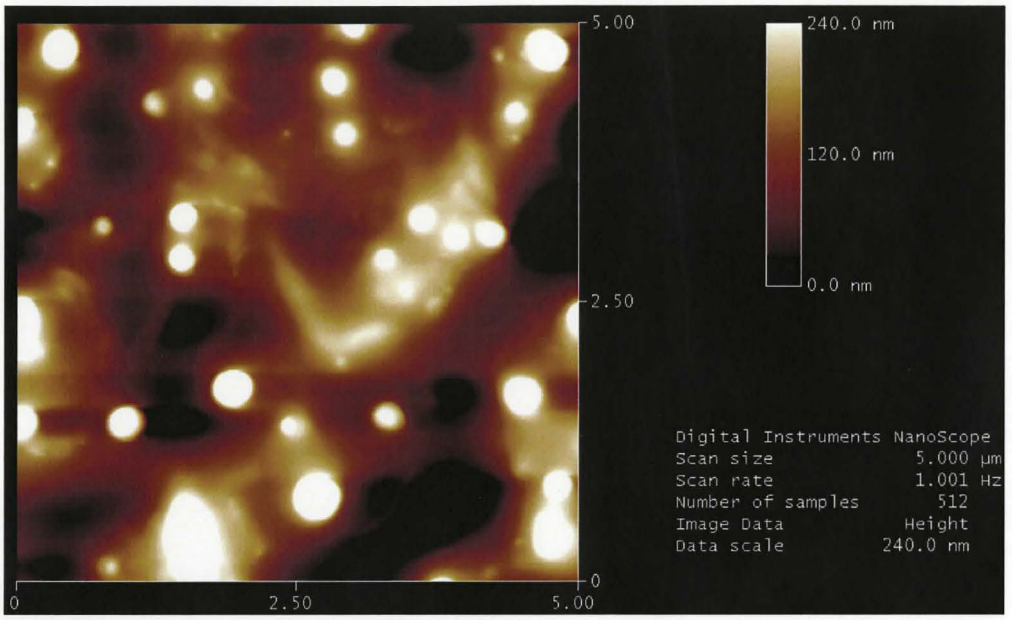

SiH phase image, 5μm x 5μm

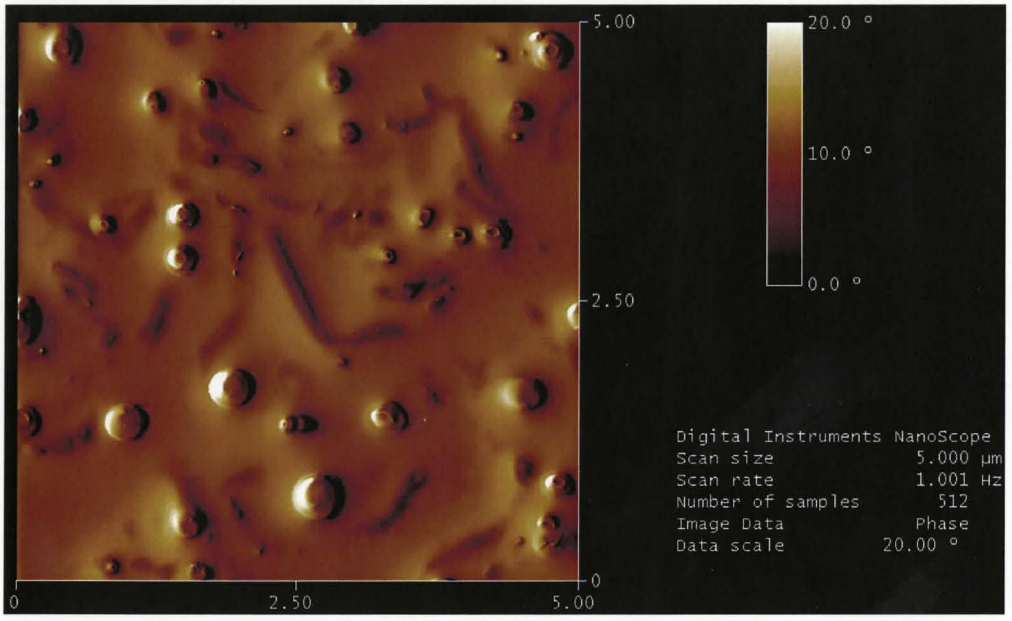

NHS height image, 5μm x 5μm

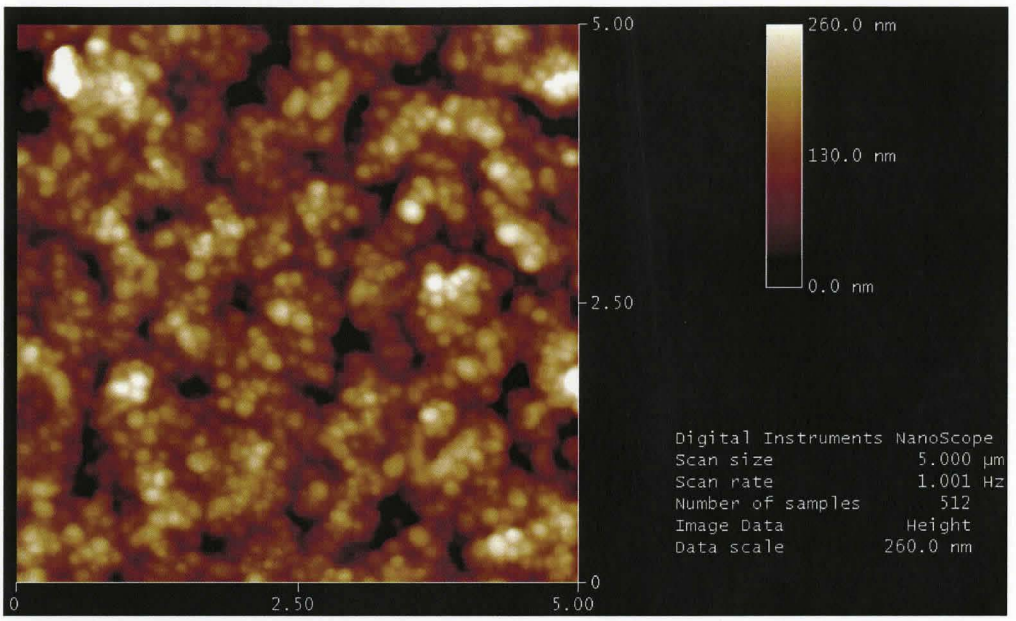

NHS phase image, 5μm x 5μm

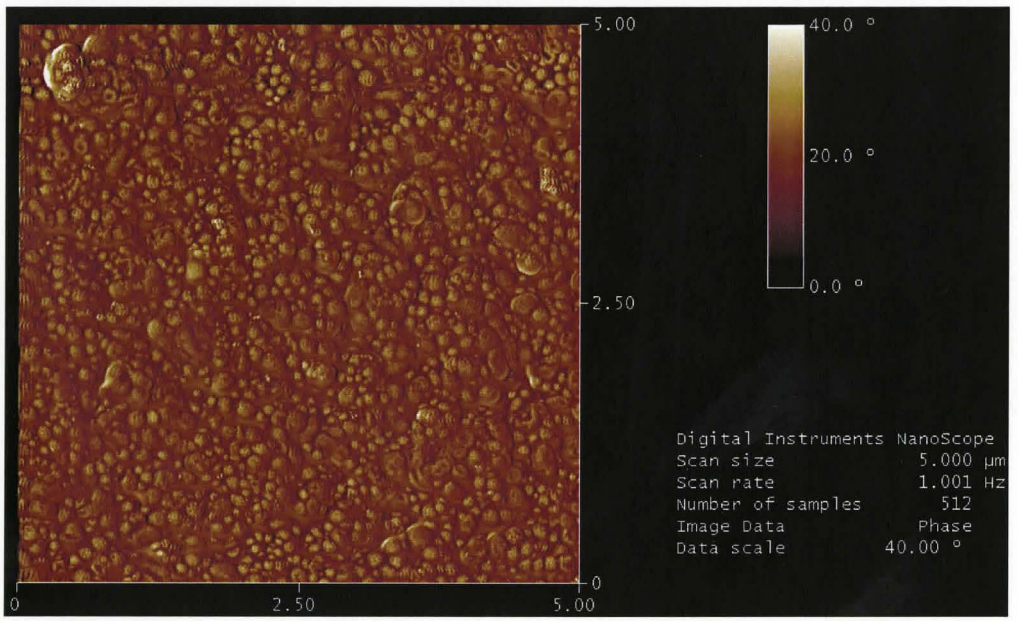

Figure S5 Full images of Figure 2.14

NHS (See NHS in Figure S4)

Collagen

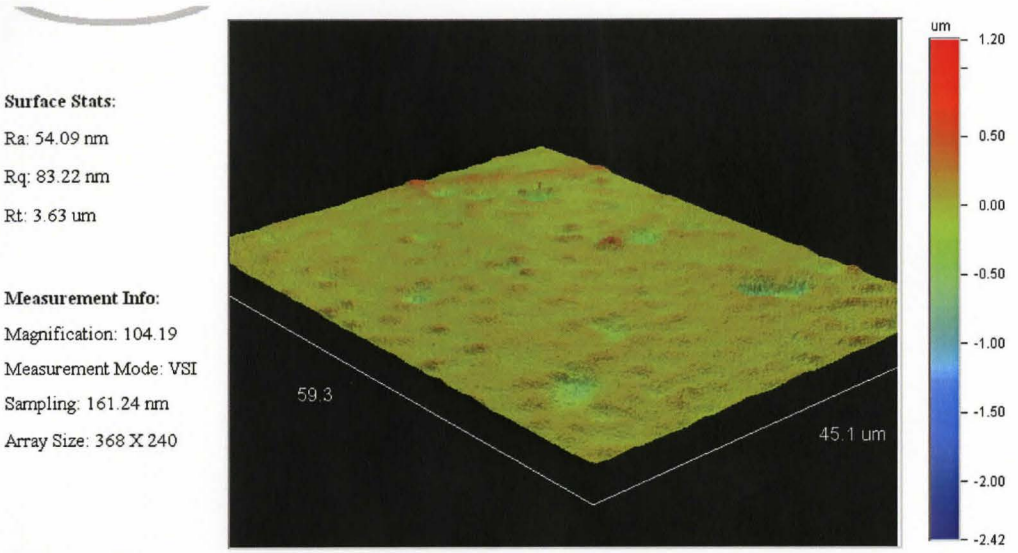

Collagen

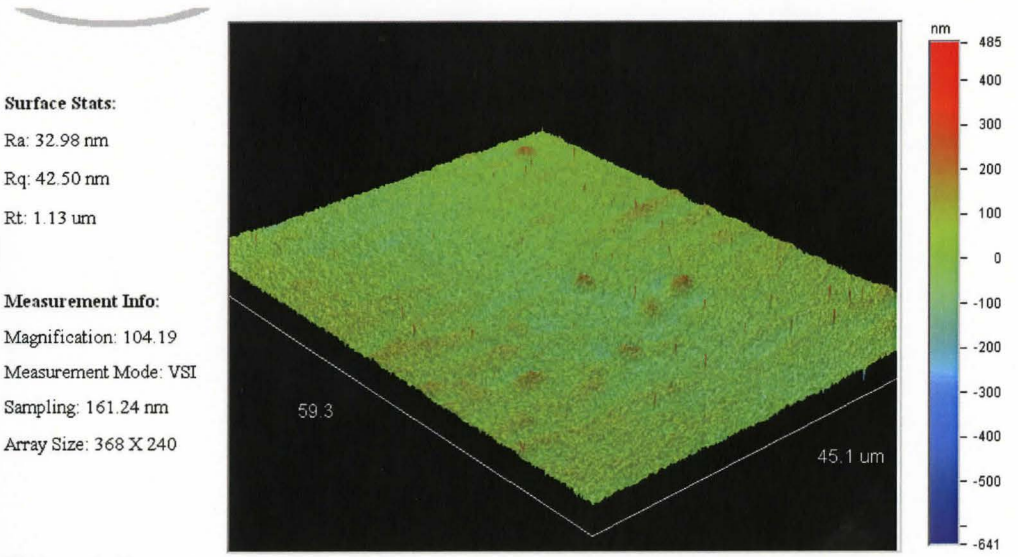

Figure S6 Full pictures of Figure 3.10

A (PDMS) and B (NHS) (see PDMS and NHS in Figure S5)

C (Collagen height image, 2.5μm x 2.5μm)

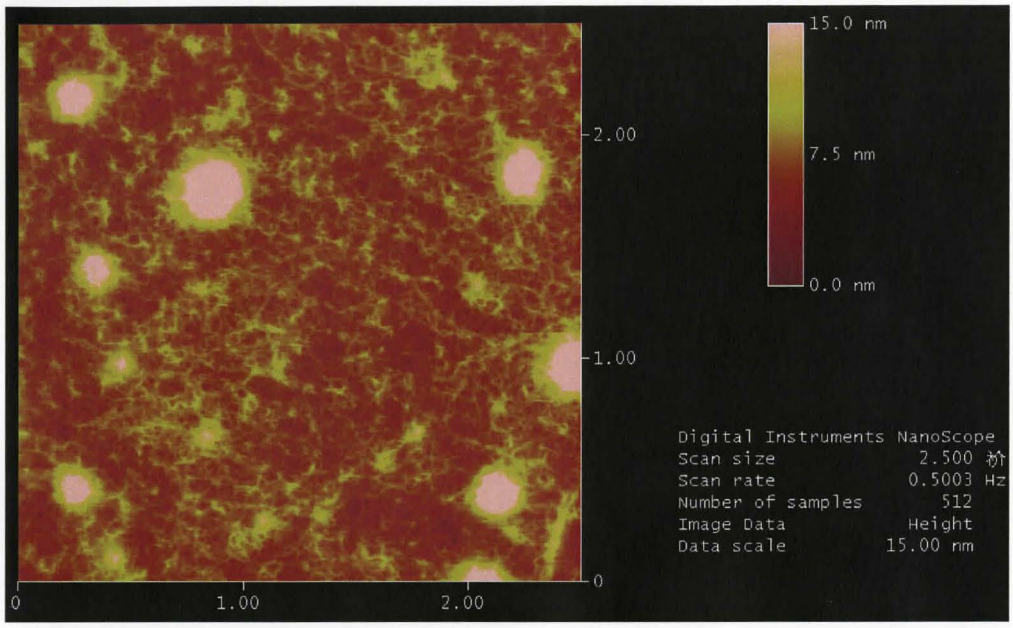

C (Collagen phase image, 2.5μm x 2.5μm)

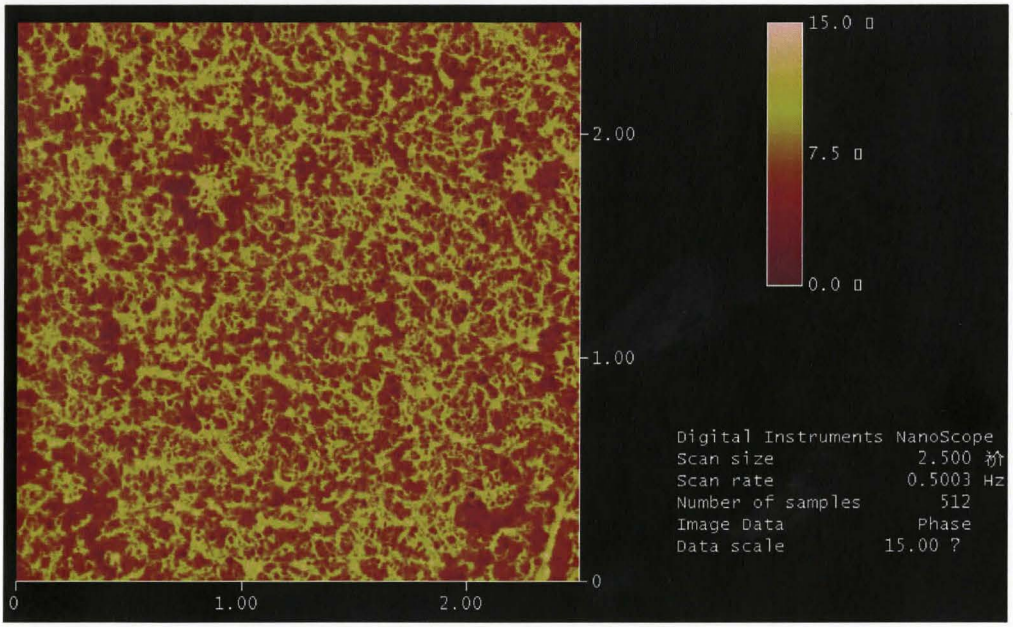

D (Collagen height image, a region between nodules, 1μm x 1μm)

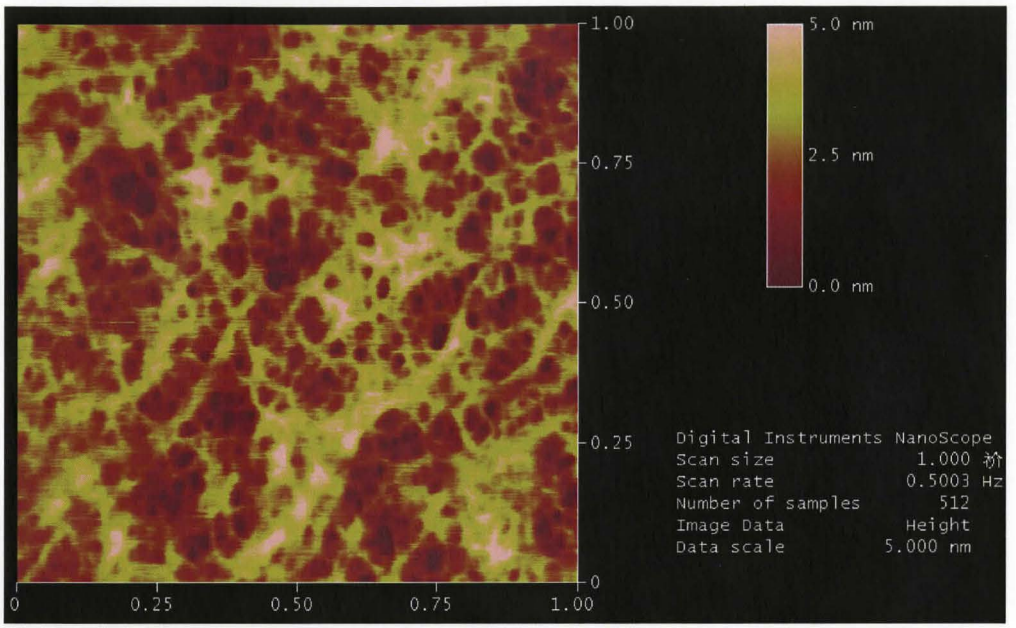

D (Collagen phase image, a region between nodules, 1μm x 1μm)

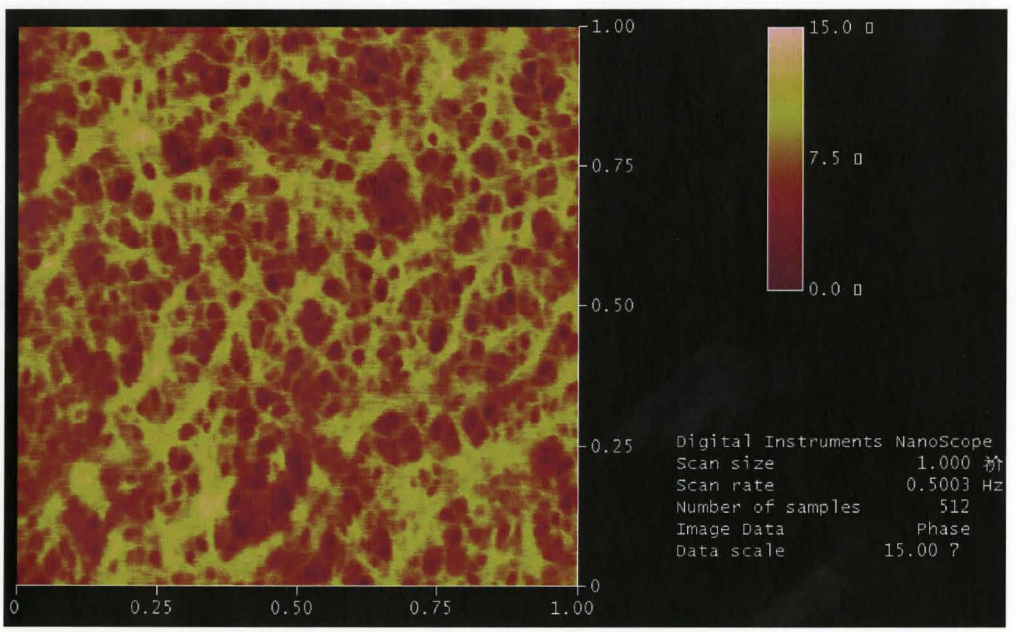

E (Collagen height image, of a nodule directly, 1μm x 1μm)

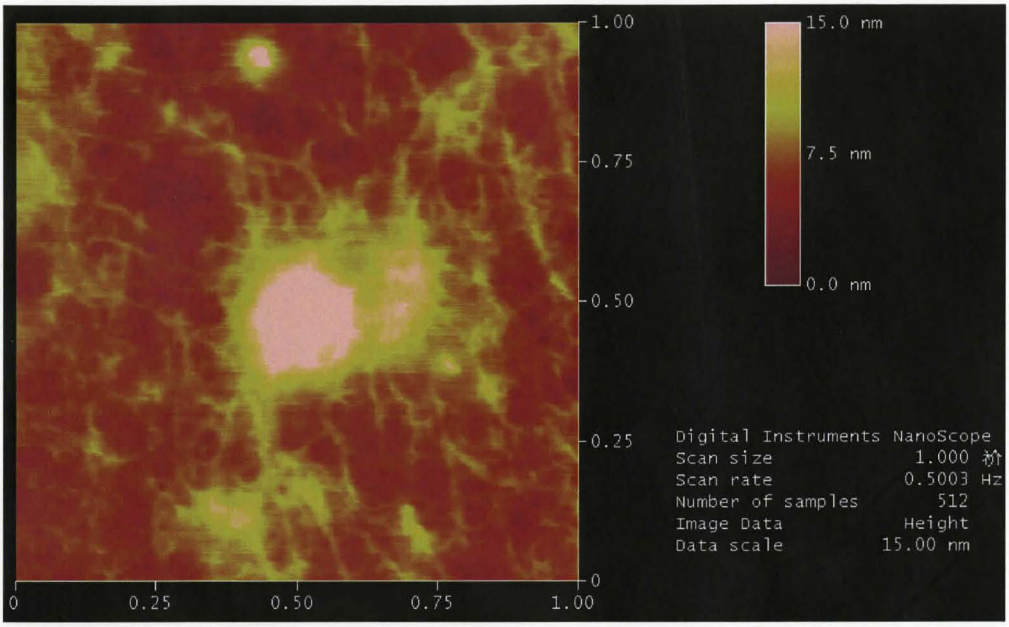

E (Collagen phase image, of a nodule directly, 1μm x 1μm)

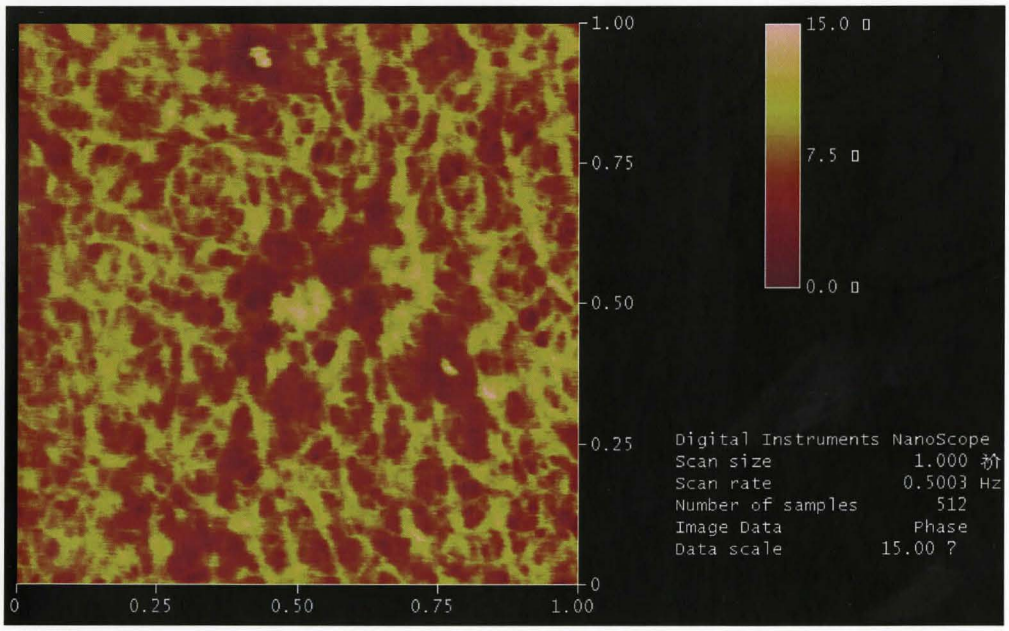

Figure S7 Full images of Figure 3.15